IOWA STATE UNIVERSITY
Digital Repository

Graduate Theses and Dissertations

Iowa State University Capstones, Theses and Dissertations

2009

Development of ion mobility mass spectrometry coupled with ion/ion reactions:

Qin Zhao
Iowa State University

Follow this and additional works at: https://lib.dr.iastate.edu/etd

 Part of the Chemistry Commons

Recommended Citation
Zhao, Qin, "Development of ion mobility mass spectrometry coupled with ion/ion reactions:" (2009). *Graduate Theses and Dissertations*. 10478.
https://lib.dr.iastate.edu/etd/10478

This Dissertation is brought to you for free and open access by the Iowa State University Capstones, Theses and Dissertations at Iowa State University Digital Repository. It has been accepted for inclusion in Graduate Theses and Dissertations by an authorized administrator of Iowa State University Digital Repository. For more information, please contact digirep@iastate.edu.

www.manaraa.com

Development of ion mobility mass spectrometry coupled with ion/ion reactions: instrumentation and applications for protein analysis

by

Qin Zhao

A dissertation submitted to the graduate faculty

in partial fulfillment of the requirements for the degree of

DOCTOR OF PHILOSOPHY

Major: Analytical Chemistry

Program of Study Committee:
R.S. Houk, Major Professor
Mei Hong
Victor Shang-yi Lin
Emily Smith
Hans Stauffer

Iowa State University

Ames, Iowa

2009

Copyright © Qin Zhao, 2009. All rights reserved.

www.manaraa.com

TABLE OF CONTENTS

www.manaraa.com

www.manaraa.com

www.manaraa.com

ABSTRACT

As the widespread use of mass spectrometry (MS) for biological analyses, particularly in areas like proteomics and characterization of large macromolecular complexes, further improvements in MS instrumentation provide analytical capabilities that enable these new biological studies.

An ion trap ion trap - ion mobility – time of flight mass spectrometer with three ion sources was built which combines the capabilities of ion/ion reactions with ion mobility**.** The characterization of the instrument was demonstrated with ubiquitin. Ubiquitin ions from either of two electrospray ionization (ESI) sources are stored in a 3D ion trap (IT) and reacted with negative ions from atmospheric sampling glow discharge ionization (ASGDI). The proton transfer reaction products are then separated by IM and analyzed via a TOF mass analyzer. In this way, ubiquitin +7 ions are converted to lower charge states down to +1; the ions in lower charge states tend to be in compact conformations with cross sections down to ~ 880 $Å^2$. The duration and magnitude of the ion ejection pulse on the IT and the entrance voltage on the IM drift tube can affect the measured distribution of conformers for ubiquitin +7 and +6. Alternatively, protein ions are fragmented by collision-induced dissociation (CID) in the IT, followed by ion/ion reactions to reduce the charge states of the CID product ions, thus simplifying assignment of charge states and fragments using the mobility-resolved tandem mass spectrum. Instrument characteristics and the use of a new ion trap controller and software modifications to control the entire instrument are described.

www.manaraa.com

Effects of ion/ion reactions on conformation of gas-phase cytochrome *c* were also studied on this instrument. Positive ions from cytochrome *c* are studied in a 3-D ion trap/ion mobility (IM)/quadrupole-time-of-flight (TOF) instrument with three independent ion sources. The IM separation allows measurement of the cross section of the ions. Ion/ion reactions in the 3-D ion trap that remove protons cause the cytochrome c ions to refold gently without other degradation of protein structure. The conformation(s) of the product ions generated by ion/ion reactions in a given charge state are independent of the original charge state of the cytochrome c ions. In the lower charge states (+1 to +5) cytochrome *c* ions made by the ion/ion reaction have a single conformation with cross section of ~ 1110 to 1180 $Å^2$, even if the original +8 ion started with two conformations. These cross section values are close to those of the "most folded" conformation found previously. In a given charge state, ions created by ion/ion reaction prefer to produce the more compact conformation in somewhat higher abundances, compared to those produced by the electrospray ionization (ESI) source alone. A variety of related studies that employ ion/ion reactions and IM to probe conformations of biomolecular ions should be possible by these methods.

A mass-selective ejection method from the ion trap was also developed. Instead of the applying a high voltage pulse to eject simultaneously, the ion trap mass-selective instability scan was used. Ions are ejected from the ion trap in a time dependent manner (sequentially): scanning the RF from 1 to 5 kV while a fixed frequency (47 kHz) sine wave was applied to the front cap of the ion trap with ramping amplitude from 4 V to 41 V. This ion trap ejection method provides another option for the separation of protein mixture ions, which have similar mobility but

www.manaraa.com

different mass to charge ratio. This capability has the potential to expand the ability of the ion mobility labeling parallel experiments to handle complex mixtures.

To improve the ion storage capacity and sensitivity of the ion trap instrument, a linear ion trap (LIT) with electrospray ionization (ESI) has been constructed for ion/ion reactions. To reduce the instrument's complexity and make it available for wide dissemination, only a few simple electronics components were custom built. The instrument functions as both a reaction vessel for gas-phase ion/ion reactions, and a mass spectrometer using mass-selective axial ejection. Initial results demonstrate trapping efficiency of 70 to 90% and the ability to perform proton transfer reactions on intact protein ions, including dual polarity storage reactions, transmission mode reactions, and ion parking.

www.manaraa.com

CHAPTER 1

INTRODUCTION TO ION MOBILITY MASS SPECTROMETRY AND ION/ION REACTION FOR PROTEIN ANALYSIS

Background

From the point view of life science or biology, proteins are large molecules in the life system that serve crucial functions, such as acting as enzyme that catalyze biochemical reactions, transporting molecules, and providing immune protection. The amino acid sequences of proteins also express the gene code in the cell, in other words, they provide the link between function and genetics [1]. So discovering the secret of the proteins (their sequence and structure) bridges biology to chemistry, and has become one of the central parts of the related chemistry area.

In the past 30 years, with the revolution of the analytical chemistry and instruments, mass spectrometry and related techniques are replacing the old method and fundamentally change the way proteins are analyzed [2]. Mass spectrometry offers many advantages over other methods, which are the most accuracy measurement of molecular mass, high resolution, rapid analysis times, and the ability to determine structure information. But before 1990's, the conventional mass spectrometric ionization methods were mainly electron ionization (EI), chemical ionization (CI) and photoionization (PI), only suitable for the lower mass volatile molecules. This brought mass spectrometrists a question: can we use mass spectrometry for non-volatile molecules? The answer is yes.

www.manaraa.com

The development of some desorption methods, for example, secondary ion (SIMS) [3], fast atom bombundant (FAB) [4], matrix assisted laser desorption ionization (MALDI) [5]), and spray ionization methods, such like electrospray ionization (ESI) [6, 7], nano-ESI [8], ion spray [9], thermospray [10], sonic spray [11], provide a breakthrough for ionization of high mass, non-volatile biomolecules so that mass spectrometry can be used in biomolecule analysis. In all these methods, MALDI and ESI have become the two most significant ones [2] and won the Nobel Prize in Chemistry in 2002 for the contributions for soft desorption ionization methods for mass spectrometric analyses of biological macromolecules.

The principle of MALDI [12] can be simply described. The analyte compound is mixed with organic molecules that have strong absorption at the laser wavelength. The mixture is then dried to remove all the liquid and form a "solid solution" with the matrix, in which the analyte molecules are diluted by the matrix molecules and isolated from each other. The matrix molecules absorb a large amount of energy during laser irradiation and eject the matrix plume (a gas-jet of matrix neutral molecules) into the gas phase which entrains the analyte molecule. Since little energy is transferred to the analyte molecules so they stay intact during the ionization process. Ions generated by MALDI are predominantly singly charged and easy to interpret. After the problem of production of bimolecular ions was solved, how to analyze such high-mass singly charged ions become another topic to study. The most frequently used mass spectrometer coupled with MALDI source is a Time-Of-Flight (TOF) instrument [13].

www.manaraa.com

ESI is another choice for the ionization method for biomacro-molecules [14]. A dilute solution of analyte is pumped at a very low flow rate (0.1–1 mL/min) through a capillary, to which high voltage (2–5 kV) is applied [14]. This voltage can be either negative or positive depending on the analyte ion property and solution conditions. The applied voltage provides the electric field gradient required to produce charge separation at the surface of the liquid. As a result, the liquid protrudes from the capillary tip and forms a ‘‘Taylor cone’’ with excess charges on the surface. Spraying mode [15] can be adjusted by changing the potential so that the ESI ion yields can be optimized. The large droplets generated from the elctrospray will desorb from the surface as the Coulomb repulsion exceeds the surface tension of the solution. As the droplet moves through the atmosphere towards the entrance to the mass spectrometer by the electric field, the solvent evaporates, large droplets shrink and split repeatedly into small droplets. This process continues until small charged gas-phase analyte ions are left. Gas-phase ions could also be generated from gas-phase reaction [16] or electrochemical oxidation and reduction [17].

Both ESI and MALDI are very “soft” ionization methods and have become very popular in protein analysis. ESI has been chosen in this work because it can produce multiply charged ions which allow it to be coupled with a lower mass range mass analyzer such as quadrupole mass filter and ion trap. Another advantage is that the multiple-charging phenomenon associated with electrospray also makes it possible to reduce the charge states and study the ion/ion reaction chemistry in gas-phase. The third advantage is that it is ideally compatible with chromatographic separation techniques such as high performance liquid chromatography (HPLC) and capillary electrophoresis (CE).

www.manaraa.com

An easy electrospray technique will be used for this work, named nano-ESI. It was first developed in 1996 by Wilm and coworkers [18]. Nano-ESI has some unique features including: low flow rate 20 nL/min (less sample is needed), easy operation without solvent pump, small droplets (easy to desolvate). The most important advantage is the buffer solution and even 100% water can be used for nano-ESI, which makes the study of biomolecules in the native conditions possible.

Protein Analysis by Mass Spectrometry

There are some questions that are of interest to the studies on proteins analysis: accurate molecular weight, primary structure of a protein (amino acid sequence), proteomics (function and interaction of a large scale of proteins), and the higher order protein structures (conformation or how protein folds). Mass spectrometry provides a rapid and sensitive way for these studies.

Protein mass measurement is the first benefit from the establishment of ESI and MALDI. The molecular mass of very large polypeptides (for example, mass above 100,000 Da) can be easily measured by ESI-MS speedily with accuracy [19, 20].

Mass spectrometry also become common in protein identification and the methodology has evolved from “bottom-up” mass analysis to “top-down” analysis [21-25]. For the “bottom-up” method, large proteins of interest are digested into smaller polypeptides with molecular mass usually lower than 3 kDa. The mixtures of polypeptides are then analyzed by MS or MS/MS often with on-line LC separation to yield molecular mass and fragment information. The protein is identified by peptide mass mapping. This strategy is

www.manaraa.com

very successful and still being used, but it has some limitations. One practical limitation is the peptides generated from the protein digestion have similar mass, so a high resolution mass spectrometer is needed for mass analysis. Also low abundance peptides from the digestion may be lost in the following separation process. Because the mass of the intact protein is not directly measured, some important information for protein identification like post translational modification (PTM) is often not accessible [25].

For "top-down" approach [22, 25], the protein mixtures are introduced into the mass spectrometer usually by ESI. Each molecular protein ion can be mass selected and dissociated inside the mass spectrometer by MS/MS. In this way, both the molecular weight information and the sequence of the each protein ion can be obtained from MS and MS/MS spectra. In contrast with "bottom-up" method, the two main advantages for the "top-down" protein analysis are: 1) it can study the intact protein to measure the molecular weight information, which can indicate the specific PTM, and 2) the primary structure can be obtained by the dissociation of the whole protein ion in the gas-phase with sequence coverage as high as 100%.

Mass spectrometry is also an essential method to study protein structure and function, and provide complementary data to classical methods, nuclear magnetic resonance, X-ray crystallography, circular dichroism. The above "top-down" method in proteomics is mostly for primary structure (amino acids sequence of protein). MS can be also applied to study protein secondary structure (regular polypeptide structure unit, such as α helix, β sheet, and loops and turns), tertiary structure (three-dimensional folding structure) and even quaternary structure (assembling of protein molecules or subunits into a protein complex). The structure

www.manaraa.com

can be probed through chemical and physical ways [26]. Chemical ways make some chemical changes to the interest molecules before observations, for example, H/D exchange [27-31], ion-molecule reaction [32], or proton transfer reaction [33]. Physical methods evaluate other properties of the molecule interest not chemical changes, such as cross-section measurement by ion mobility spectrometry [34-36] or fragmentation by electron capture dissociation (ECD) [37-39].

The combination of chemical and physical methods for protein conformation studies gives more interesting results. There are two techniques we will mainly use with mass spectrometry in protein analysis: ion mobility MS and ion/ion reaction MS. The principles of the two techniques and their instrumentation and applications in protein analysis will be introduced in the following pages.

Ion Mobility Principles

Ion mobility spectrometry (IMS) is a technology which is based on the slow motion of ions in gas phase in a uniform external electric field. Association between experimental ion mobility measurements and ion structures provides a low-cost and convenient way for gas-phase ion identification, characterization and separation.

The Motion of Ions in Low-Field Electric Field

As ions move through a neutral buffer gas under the influence of electric field (Figure 1), the electrostatic forces from the electric field (depend on the charge of the ions) drove ions forward against the resistance from the buffer gas molecules. In micro view, the motion

www.manaraa.com

of ions in the electric field is spasmodic motion: an ion is accelerated by the electric field until it collides with a buffer gas molecule and loses the acquired momentum [40]. This process is repeated throughout the transit of the ion packet through the electric field and leads to a particular velocity for the ion packet based on the charge and the size of the ion.

Ion Mobility Coefficient

Ion mobility coefficient (K) describes how fast the ions move in an electric field in gas phase under the effect of a buffer gas [34]. It can be determined by measuring the time it takes for ions to travel through a uniform electric field in the presence of buffer gas.

$$v_D = KE = L/t_D \quad (1)$$

The physical property of the buffer gas (pressure, temperature) affects each ion mobility measurement. So the ion mobility coefficient K measured from each individual experiment is usually scaled to standard pressure and temperature, and reported in the literature for comparison.

$$K_0 = \frac{L^2}{t_D V} \times \frac{273.2}{T} \times \frac{p}{760} \quad (2)$$

Parameters in equation (1) and (2) represent: K: ion mobility, K_0 : reduced ion mobility, E- Electric field (V/cm), v_D -velocity in the electric field (cm/s), L- length of the electric field, t_D- drift time , p: pressure, T: temperature (K).

www.manaraa.com

Effect of Electric Field and Buffer Gas Number Density on Mobility

As described above, increasing the electric field will increase the velocity, but increasing the pressure will diminish the effect, so the mobility of an ion is governed by both factors. The ratio of the electric field to the number density of the buffer gas (E/N) is used as a parameter to determine the effect on the ion mobility. At low E/N ratio, the electric field does not heat the ions because the energy gained is removed by the collisions with the neutral gas molecules in the regime; the mobility coefficient is independent of the electric field, this regime is the so called low-field limit [34, 41]. At high field limit, the mobility depends on E/N ratio and the ions may align to some extent in the drift tube [42].

Resolution in Ion Mobility Spectrometry

The theory of ion mobility was systematized and reviewed by Revercomb and Mason in 1975 [43]. The resolving power of ion mobility is given approximately by [34, 43]:

$$\frac{t_D}{\Delta t} = \left(\frac{LEze}{16k_B T \ln 2}\right)^{1/2} \tag{3}$$

From this equation, the resolution can be improved by use of higher electric field (practically, higher pressure is needed in operation), longer drift tube and lower temperature for a specific ion.

There are two experimental configurations for ion mobility measurement. One is low resolution configuration [41]; the pressure of the buffer gas is less than 10 torr, and drift field is also low (~10V/cm), the resolution is around 20. Another is high resolution ion mobility

www.manaraa.com

spectrometry [44]; the pressure for the buffer gas is ~100 Torrs and the electric field is also as high as ~200 V/cm, the resolution can be 200-400.

The Correlation of Ion Mobility and Ions Collision Cross-Section

In the low- field limit, the ion mobility is independent of the electric field, and the dependence of ion mobility on the average cross-section can be expressed by this equation [34, 43]:

$$K = \frac{(18\pi)^{1/2}}{16}\left[\frac{1}{m}+\frac{1}{m_b}\right]^{1/2}\frac{ze}{(k_B T)^{1/2}\Omega_{avg}^{(1,1)}}\frac{1}{N} \quad (3)$$

m: mass of the ion, m_b: mass of the buffer gas, k_B: Boltzmann constant, N: number density of the buffer gas, Ω is the average collisional cross-section of the ion. An ion with large average cross-section will undergo more collisions with buffer gas and therefore travel more slowly than an ion with a small average collision cross-section (as shown in Figure 1).

The Device for Cross-Section Measurement

The device to measure the ion mobility is usually called drift tube (or drift cell). A schematic representation is shown in Figure 1. The body of the drift tube consists of alternating ring electrodes and ring insulating spacers to provide a uniform electric field. Both ends are also sealed with small apertures to contain neutral buffer gas. A short ion packet is injected into the drift tube, and the time to travel through the drift tube can be recorded by detecting the ions at the exit.

www.manaraa.com

Another type of ion mobility technique is called field asymmetric waveform ion mobility spectrometry (FAIMS), which separates ions by both high and low electric field [45]. A new travelling-waveform ion mobility technique is recently developed and commercial instrument is available, called Synapt HDMS and manufactured by Waters [46, 47]. It is a hybrid quadrupole- IMS- orthogonal time-of-flight mass spectrometer.

The Evolution of the Instrumentation for Ion Mobility /Mass Spectrometry

IM not only provides direct information about molecular structure and geometries, but also is a separation method based on the collision cross-section. Ion mobility based instruments can be used as an analytical tool for chemical composition, and can also be hyphenated with mass spectrometry on the back or with other techniques like chromatographic separation in the front to add more selectivity. The development of ESI/IMS/MS instrumentation is briefly described in the following pages.

Figure 2 shows an early injected drift tube instrument built by Clemmer's group in 1997 [48]. This instrument is equipped with an ESI source and a chamber so that neutral reagent gas can be added to the source region. Ions are injected into the drift tube and then mass analyzed by a quadrupole mass spectrometer. This instrument has the chemical reactivity/ion mobility measurement feature, and can be used to do reduce the charge states of the protein ion mode by ESI [48, 49] and also can do H/D exchange [50].

To improve the sensitivity of ion mobility measurement of ions generated from the source, an ion trap was interfaced between the source and drift tube, as shown in Figure 3 [51]. The ions from ESI can be accumulated in the ion trap for a selected time (10 ms to 1000

www.manaraa.com

ms), and then injected into the drift tube by pulsing the ion trap end plate with a high voltage (40-400V). After the ions pass through the drift tube, they are mass analyzed by a qudrupole mass analyzer.

A big step in IMS/MS instrument development is the combination of TOF instrument with ion mobility measurement [52, 53] as shown in Figure 4. The two separations at different pressure conditions occure in the substantial different time scales: ~10 ms in the high pressure (~2 torr) ion mobility drift tube and ~ 100 μs in the high vacuum ($\leq 10^{-6}$ torr) time of flight drift region. Because the TOF flight time is much faster than the ion mobility drift time, entire mass spectra can be measured repeatedly for each individual IMS peak. The fight time can be nested in the drift time and three dimensional mass spectra can be obtained which include the cross-section, mass-to-charge rate, and abundance information.

Another improvement is an octopole collision cell is inserted between the drift tube and time of flight mass analyzer, as shown in Figure 5 [54]. After ions exit from the drift tube, they can be fragmented by collision induced dissociation (CID) in an octopole collision cell. The fragment ions and remaining parent ions are mass analyzed by a reflectron TOF mass spectrometer. Because the fragment ions have the same IM drift time as their precursor ions, parent ions with similar m/z can sometimes be pre-separated by ion mobility and then fragmented by CID to generate sequence information. This approach helps to simplify the CID spectra. Another advantage is the ions from the mixture can be first labeled with ion mobility drift time and then sequence analyzed in parallel [55].

Multi-dimensional ion mobility mass spectrometry was developed in 2006 [56, 57]. Figure 6 shows a three-stage IMS/IMS/IMS/MS spectrometer [57]. Ions from ESI can be

www.manaraa.com

separated in the first drift tube D1 and a certain ion can be selected by ion mobility by gate G2 and then fragmented in IA2. The fragments are further separated by ion mobility and then a certain fragment ion can be selected by G3 and fragmented in IA3. The second generation fragment ions are separated by mobility and mass analyzed by the TOF mass analyzer. Figure 7 is a demonstration of the whole analysis [57]. Sixty-four ions out of 76 were identified from the fragments. This method is very efficient in generating fragments and is very valuable for peptide or protein identification.

To analyze complex real biological mixtures, liquid chromatography is an essential technique, so coupling IMS with LC has a lot of advantages [58-60]. Figure 8 shows nano-flow LC coupled to an IMS/MS instrument. Protein mixtures are separated prior to introduction into the drift tube, and the ions are labeled with retention time first, then separated by ion mobility in ~10 ms scale, and finally mass analyzed by TOF in ~100 μs. LC is well suited to IMS/MS: it adds one more dimension of separation and is a very efficient and highly parallel way for protein mixture analysis or proteomics. LC may also improve the performance of ESI as some very complex mixtures sometime are hard to spray directly. Because of the IMS/MS on the back, the analysis could be done in a faster way and less extensive LC optimization is needed.

Ion/Ion Reaction

The establishment of ESI opens a lot of new areas for mass spectrometry research based on the high-mass multiply charged ions, and the study of ion/ion reaction chemistry in the gas phase is one of them. Gas-phase ion/ion reaction [61, 62] within an ion trap at room

www.manaraa.com

temperature is another interesting technique for this thesis. Since the ion trap can trap both positive and negative ions, the oppositely charged ion clouds could overlap in the same space that makes the study of ion/ion reactions at a reduced pressure environment (~1 mtorr) possible. The charged products from ion/ion reaction can be studied with mass spectrometric methods, providing very useful information.

Gas-phase ion/ion reactions fall into four categories by the phenomenology observed: proton transfer reaction, electron transfer reaction, ion exchange reaction, and complex formation reaction. The application of these reactions in protein analysis will be discussed in detail.

Proton transfer reaction (PTR) is mainly observed between multiply charged protein or peptide ions with singly charged even-electron negative ions. The transfer of a proton forms charge reduced products [61]:

$$(M + n\,H)^{n+} + Y^- \rightarrow (M + (n\text{-}1)\,H)^{(n-1)+} + HY$$

This reaction can be used to reduce the charge state of the ions from ESI and generate ions not directly formed from ESI, or to reduce the product ion charge states to simplify identification of product ions.

Compared with proton transfer reaction, electron transfer reaction occures between the multiply charged analyte ions and a radical negative ion [63, 64]. When both reagents are trapped in the same space, the electron from the radical negative ion is transferred to the positively charged ion. This is an exothermic reaction, and the energy can trigger the release of H· and induce subsequent dissociation [65-68]. Since electron transfer reaction is generally accompanied by the dissociation, it is called electron transfer dissociation (ETD).

www.manaraa.com

When ETD occurs with multiply charged protein ions, it makes c and z ions providing complementary information to that predominantly b and y ions coming from traditional CID method. ETD fragments often keeps some very labile post translational modifications (PTM) [64], like phosphorylation, glycosylation. ETD is also very efficient on large mass protein molecules and has become a main method for top-down protein analysis.

The ion exchange reaction results from the reaction of multiply charged positive peptide/protein ions with metal containing negative ions; the metal ion inserts into the peptide/protein [69-72]. Complex formation reaction involves two ions of opposite polarity that associate into one ion [73, 74]. They are very interesting reactions that macromolecules can be assembled in the gas-phase and also provide a potential way for the gas-phase synthesis

Instrumentation for Ion/Ion Reaction:

Early ion/ion reaction studies were performed in quadrupole ion trap, which is used both as a reaction vessel and as a mass analyzer (Figure 9) [73]. The three independent sources are mounted in the three faces of a cube attached to the main chamber that contains the ion trap. The three sources can be ESI in either positive mode or negative mode or atmospheric sampling glow discharge ionization (ASGDI). The ions are transmitted into the ion trap by a turning quadrupole. Another source is orthogonal to the main instrument axis and ions are focused into the ion trap through a hole in the ring electrode. Three types of ion/ion reaction were demonstrated on this type of instrument [73]. One is complex formation reaction: cytochrome c positive and negative ions were made from positive and

www.manaraa.com

negative ESI, and reacted in the ion trap for ~100 ms to form cytochrome c dimer. Another example is the charge state of the ions from ESI can be manipulated by reaction with perfluoro-1,3-dimethylcyclohexane (PDCH) negative ions from ASGDI source. Since the ion trap can fragment the ions, the product ions from MS^n can be reduced to low charge state (+1, +2) to make it easier to assign the fragments.

The linear ion trap (2-D) trap [75, 76] provides a new, higher capacity and more efficient vessel to trap ions compared with the 3-D quadrupole ion trap [77, 78]. As seen from the name "2-D" trap, their design are based on the linear quadrupole (same as quadrupole mass filter) the ions are trapped in the radial direction (x and y directions in Figure 10) by applying RF waveforms 180 degree out of phase on each pair of rods, and the trapping in axial direction (z direction in Figure 10) are from the DC voltage applied to the entrance and exit lenses.

Two types of linear ion traps are shown in Figure 10 and Figure 11. The difference between the two is that the way the ions are ejected for mass analysis. As described by Schwartz [75] in Figure 10, there is a slot cut into one of the rod and a detector is set on the side. Mass analysis was performed by ejection of ions through the slot using the mass selective instability mode of operation. For the other type of linear ion trap in Figure 11 [76], ions are ejected by mass selective axial ejection [79], that utilizes the fringe field coupling of the RF voltage applied to the LIT rods with the DC voltage applied to the exit lens of the LIT.

To perform ion/ion reaction, the linear ion trap should have the ability for dual polarity ion storage. There are two ways reported to trap positive and negative ions

www.manaraa.com

simultaneously in the linear ion trap. In the method developed by Hunt's group [63], a Finnigan LTQ mass spectrometer was modified for ETD reaction with a chemical ionization (CI) source coupled to the rear part of the instrument. It takes advantage of the tri-filter quadrupole configuration (Figure12): positive ions from electrospray are injected from the front and trapped in the left filter; negative ions from CI source are injected from the right, then the DC voltages applied to the entrance and exit lenses are replace with a low frequency RF, so both polarity ions are trapped and reacted.

An alternative method developed by McLuckey's group is to unbalance the RF voltage on the two pair of rods to generate a RF waveform in the z direction (shown in Figure 13) [80]. The QTRAP mass spectrometer has Q-q-$Q_{\text{linear ion trap}}$ configuration, so each of the quadupole section can be used as linear ion trap for mutual trapping by unbalancing the RF voltage applied to the rods array.

Recently, the mass analysis process is separated from the ion/ion reaction by coupling a mass spectrometer on the back, for example, the modified QqTOF instrument from Applied Biosystem/MDS Sciex QSTAR by McLuckey's group [81-83] (Figure 14), and another QLT-orbitrap instruments by Coon's group [84] (Figure 15). Both instruments have high mass resolution and accuracy, and they are especially useful for analysis of ETD products for top-down proteomic applications, large protein mixtures and post translational modification analysis.

www.manaraa.com

Thesis Overview

From the background discussion, ion mobility provides one more dimension of separation by the size of ions to the mass separation and also gives the direct conformation about protein gas-phase structure. Ion/ion reactions (PCR and ETD) can simplify the MS/MS spectrum or generate fragments to identify the sequence from the fragmentation patterns. So, the combination of ion mobility and ion/ion reaction must be a very powerful technique, and will provide a high throughput way to conduct protein top-down analysis and give a whole picture of protein in a single run. This is why we come up this idea to build a very complicate instrument that including all these capabilities.

In Chapter 2, how the instrument was built is described in detailed. The characterization of the instrument was demonstrated with ubiquitin. The work in Chapter 3 is the study on the effect of ion/ion reaction on the conformation change. Cytochrome c ions are used as a test protein, the folding of protein and effect of solution conditions was also studied. Chapter 4 described a mass-selective ejection method from the ion trap which gives an improved separation for the ions with similar ion mobilities. In the last chapter, future directions of this technology will be described and discussed.

The appendix is about a second instrument we built which uses a LIT modified from primarily commercially available components. It has versatile functions and high capacity storage, and could be combined with the IMS/TOF instrument described in earlier chapter.

www.manaraa.com

Reference

1. Domon, B., and Aebersold, R. Review - Mass Spectrometry and Protein Analysis *Science* **2006**, *312*, 212-217
2. Aebersold, R., and Goodlett, D. R. Mass Spectrometry in Proteomics *Chemical Reviews* **2001**, *101*, 269-295
3. Odom, R. W. Secondary-Ion Mass-Spectrometry Imaging *Applied Spectroscopy Reviews* **1994**, *29*, 67-116
4. Barber, M., Bordoli, R. S., Sedgwick, R. D., and Tyler, A. N. Fast Atom Bombardment of Solids (FAB) - a New Ion-Source for Mass-Spectrometry *Journal of the Chemical Society-Chemical Communications* **1981**, 325-327
5. Fenselau, C. MALDI MS and Strategies for Protein Analysis *Analytical Chemistry* **1997**, *69*, A661-A665
6. Fenn, J. B., Mann, M., Meng, C. K., Wong, S. F., and Whitehouse, C. M. Electrospray Ionization for Mass-Spectrometry of Large Biomolecules *Science* **1989**, *246*, 64-71
7. Fenn, J. B., Mann, M., Meng, C. K., Wong, S. F., and Whitehouse, C. M. Electrospray Ionization-Principles and Practice *Mass Spectrometry Reviews* **1990**, *9*, 37-70
8. Karas, M.; Bahr, U.; Dulcks, T. Nano-Electrospray Ionization Mass Spectrometry: Addressing Analytical Problems Beyond Routine *Fresenius Journal of Analytical Chemistry* **2000**, *366*, 669-676
9. Von Brocke, A., Nicholson, G., and Bayer, E. Recent Advances in Capillary Electrophoresis/Electrospray-Mass Spectrometry *Electrophoresis* **2001**, *22*, 1251-1266
10. Yamane, M. High-Performance Liquid Chromatography-Thermo Spray Ionization-Mass Spectrometry of the Oxidation Products of Polyunsaturated-Fatty Acids *Analytica Chimica Acta* **2002**, *465*, 227-236
11. Xia, Y., Liang, X. R., and McLuckey, S. A. Sonic Spray as a Dual Polarity Ion Source for Ion/Ion Reactions *Analytical Chemistry* **2005**, *77*, 3683-3689
12. Karas, M., Gluckmann, M. and Schafer, J. Ionization in Matrix-Assisted Laser Desorption/Ionization: Singly Charged Molecular Ions Are the Lucky Survivors *Journal of Mass Spectrometry* **2000**, *35*, 1-12
13. Lay, J. O. MALDI-TOF Mass Spectrometry of Bacteria *Mass Spectrometry Reviews* **2001**, *20*, 172-194
14. Cech, N. B., and Enke, C. G. Practical Implications of Some Recent Studies in Electrospray Ionization Fundamentals *Mass Spectrometry Reviews* **2001**, *20*, 362-387
15. Nemes, P., Marginean, I., and Vertes, A. Spraying Mode Effect on Droplet Formation and Ion Chemistry in Electrosprays *Analytical Chemistry* **2007**, *79*, 3105-3116
16. Amad, M. H., Cech, N. B., Jackson, G. S. and Enke, C. G. Importance of Gas-Phase Proton Affinities in Determining the Electrospray Ionization Response for Analytes and Solvents *Journal of Mass Spectrometry* **2000**, *35*, 784-789

www.manaraa.com

17. Van Berkel, G. J., McLuckey, S. A. and Glish, G. L. Electrochemical Origin of Radical Cations Observed in Electrospray Ionization Mass Spectra *Analytical Chemistry* **1992**, *64*, 1586-1593
18. Wilm, M., and Mann, M. Analytical Properties of the Nanoelectrospray Ion Source *Analytical Chemistry* **1996**, *68*, 1-8
19. Loo, J. A., Edmonds, C. G., and Smith, R. D. Tandem Mass-Spectrometry of Very Large Molecules - Serum- Albumin Sequence Information from Multiply Charged Ions Formed by Electrospray Ionization *Analytical Chemistry* **1991**, *63*, 2488-2499
20. Loo, J. A., Edmonds, C. G., and Smith, R. D. Tandem Mass-Spectrometry of Very Large Molecules 2. Dissociation of Multiply Charged Proline-Containing Proteins from Electrospray Ionization *Analytical Chemistry* **1993**, *65*, 425-438
21. McLafferty, F. W., Breuker, K., Jin, M., Han, X. M., Infusini, G., Jiang, H., Kong, X. L., and Begley, T. P. Top-Down MS, a Powerful Complement to the High Capabilities of Proteolysis Proteomics *Febs Journal* **2007**, *274*, 6256-6268
22. Breuker, K., Jin, M., Han, X. M., Jiang, H. H., and McLafferty, F. W. Top-Down Identification and Characterization of Biomolecules by Mass Spectrometry *Journal of the American Society for Mass Spectrometry* **2008**, *19*, 1045-1053
23. Kelleher, N. L.; Lin, H. Y.; Valaskovic, G. A.; Aaserud, D. J.; Fridriksson, E. K.; McLafferty, F. W. Top Down Versus Bottom up Protein Characterization by Tandem High-Resolution Mass Spectrometry *Journal of the American Chemical Society* **1999**, *121*, 806-812
24. Kelleher, N. L. Top-Down Proteomics *Analytical Chemistry* **2004**, *76*, 196A-203A
25. Reid, G. E.; McLuckey, S. A. 'Top Down' Protein Characterization Via Tandem Mass Spectrometry *Journal of Mass Spectrometry* **2002**, *37*, 663-675
26. Hoaglund-Hyzer, C. S., Counterman, A. E., and Clemmer, D. E. Anhydrous Protein Ions *Chemical Reviews* **1999**, *99*, 3037-3079
27. Englander, J. J., Del Mar, C., Li, W., Englander, S. W., Kim, J. S., Stranz, D. D., Hamuro, Y., and Woods, V. L. Protein Structure Change Studied by Hydrogen-Deuterium Exchange, Functional Labeling, and Mass Spectrometry *Proceedings of the National Academy of Sciences of the United States of America* **2003**, *100*, 7057-7062
28. Cassady, C. J., and Carr, S. R. Elucidation of Isomeric Structures for Ubiquitin $[M+12H]^{(12+)}$ Ions Produced by Electrospray Ionization Mass Spectrometry *Journal of Mass Spectrometry* **1996**, *31*, 247-254
29. McLafferty, F. W., Guan, Z. Q., Haupts, U., Wood, T. D., Kelleher, N. L. Gaseous Conformational Structures of Cytochrome C *Journal of the American Chemical Society* **1998**, *120*, 4732-4740
30. Freitas, M. A., Hendrickson, C. L., Emmett, M. R., Marshall, A. G. Gas-Phase Bovine Ubiquitin Cation Conformations Resolved by Gas-Phase Hydrogen/Deuterium Exchange Rate and Extent *International Journal of Mass Spectrometry* **1999**, *187*, 565-575
31. Freitas, M. A., Hendrickson, C. L., Marshall, A. G. Correlation between Solution and Gas-Phase Protein Conformation: H/D Exchange, IRMPD, and ESI FT-ICR MS *Proc. SPIE-Int. Soc. Opt. Eng.* **2000**, *3926*, 61-68

www.manaraa.com

32. Green, M. K.; Lebrilla, C. B. Ion-Molecule Reactions as Probes of Gas-Phase Structures of Peptides and Proteins *Mass Spectrometry Reviews* **1997**, *16*, 53-71
33. Valentine, S. J., Counterman, A. E., Clemmer, D. E. Conformer-Dependent Proton-Transfer Reactions of Ubiquitin Ions *Journal of the American Society for Mass Spectrometry* **1997**, *8*, 954-961
34. Clemmer, D. E., Jarrold, M. F. Ion Mobility Measurements and Their Applications to Clusters and Biomolecules *Journal of Mass Spectrometry* **1997**, *32*, 577-592
35. Jarrold, M. F. Unfolding, Refolding, and Hydration of Proteins in the Gas Phase *Accounts of Chemical Research* **1999**, *32*, 360-367
36. Segev, E., Wyttenbach, T., Bowers, M. T., and Gerber, R. B. Conformational Evolution of Ubiquitin Ions in Electrospray Mass Spectrometry: Molecular Dynamics Simulations at Gradually Increasing Temperatures *Physical Chemistry Chemical Physics* **2008**, *10*, 3077-3082
37. Breuker, K., Oh, H. B., Horn, D. M., Cerda, B. A. and McLafferty, F. W. Detailed Unfolding and Folding of Gaseous Ubiquitin Ions Characterized by Electron Capture Dissociation *Journal of the American Chemical Society* **2002**, *124*, 6407-6420
38. Breuker, K., and McLafferty, F. W. The Thermal Unfolding of Native Cytochrome c in the Transition from Sollution to Gas Phase Probed by Native Electron Capture Dissociation *Angrew Chem. Int. Ed.* **2005**, *44*, 4911-4914
39. Breuker, K., and McLafferty, F. W. Native Electron Capture Dissociation for the Structural Characterization of Noncovalent Interactions in Native Cytochrome c *Angewandte Chemie-International Edition* **2003**, *42*, 4900-4904
40. G.A Eiceman, Z. K. *Ion Mobility Spectrometry, 2nd Ediition,* **2005**
41. Wyttenbach, T.; Kemper, P. R.; Bowers, M. T. Design of a New Electrospray Ion Mobility Mass Spectrometer *International Journal of Mass Spectrometry* **2001**, *212*, 13-23
42. Dressler, R. A., Meyer, H., and Leone, S. R. Laser Probing of the Rotational Alignment of N_2^+ Drifted in Helium *Journal of Chemical Physics* **1987**, *87*, 6029-6039
43. Revercomb, H. E., and Mason, E. A. Theory of Plasma Chromatography Gaseous Electrophoresis - Review *Analytical Chemistry* **1975**, *47*, 970-983
44. Dugourd, P., Hudgins, R. R., Clemmer, D. E., and Jarrold, M. F. High-Resolution Ion Mobility Measurements *Review of Scientific Instruments* **1997**, *68*, 1122-1129
45. Shvartsburg, A. A., Tang, K., and Smith, R. D. Optimization of the Design and Operation of Faims Analyzers *Journal of the American Society for Mass Spectrometry* **2005**, *16*, 2-12
46. Scarff, C. A., Thalassinos, K., Hilton, G. R., and Scrivens, J. H. Travelling Wave Ion Mobility Mass Spectrometry Studies of Protein Structure: Biological Significance and Comparison with X-Ray Crystallography and Nuclear Magnetic Resonance Spectroscopy Measurements *Rapid Communications in Mass Spectrometry* **2008**, *22*, 3297-3304
47. Pringle, S. D., Giles, K., Wildgoose, J. L., Williams, J. P., Slade, S. E., Thalassinos, K., Bateman, R. H., Bowers, M. T. and Scrivens, J. H. An Investigation of the Mobility Separation of Some Peptide and Protein Ions Using a New Hybrid

www.manaraa.com

Quadrupole/Travelling Wave Ims/Oa-Tof Instrument *International Journal of Mass Spectrometry* **2007**, *261*, 1-12

48. Valentine, S. J., Counterman, A. E., and Clemmer, D. E. Conformer-Dependent Proton Transfer Reactions of Ubiquitin Ions *Journal of American Society for Mass Spectrometry* **1997**, *8*, 954-961
49. Valentine, S. J., Anderson, J. G., Ellington, A. D., and Clemmer, D. E. Disulfide-Intact and -Reduced Lysozyme in the Gas Phase: Conformations and Pathways of Folding and Unfolding *Journal of Physical Chemestry B* **1997**, *101*, 3891-3900
50. Valentine, S. J.; Clemmer, D. E. H/D Exchange Levels of Shape-Resolved Cytochrome C Conformers in the Gas Phase *Journal of the American Chemical Society* **1997**, *119*, 3558-3566
51. Hoaglund, C. S., Valentine, S. J., and Clemmer, D. E. An Ion Trap Interface for Esi-Ion Mobility Experiments *Analytical Chemistry* **1997**, *69*, 4156-4161
52. Hoaglund, C. S., Valentine, S. J., Sporleder, C. R., Reilly, J. P., and Clemmer, D. E. Three-Dimensional Ion Mobility Tofms Analysis of Electrosprayed Biomolecules *Analytical Chemistry* **1998**, *70*, 2236-2242
53. Henderson, S. C., Valentine, S. J., Counterman, A. E., and Clemmer, D. E. Esi/Ion Trap/Ion Mobility/Time-of-Flight Mass Spectrometry for Rapid and Sensitive Analysis of Biomolecular Mixtures *Analytical Chemistry* **1999**, *71*, 291-301
54. Hoaglund-Hyzer, C. S.; Clemmer, D. E. Ion Trap/Ion Mobility/Quadrupole/Time of Flight Mass Spectrometry for Peptide Mixture Analysis *Analytical Chemistry* **2001**, *73*, 177-184
55. Hoaglund-Hyzer, C. S., Lee, Y. J., Counterman, A. E., and Clemmer, D. E. Coupling Ion Mobility Separations, Collisional Activation Techniques, and Multiple Stages of Ms for Analysis of Complex Peptide Mixtures *Analytical Chemistry* **2002**, *74*, 992-1006
56. Koeniger, S. L., Merenbloom, S. I., Valentine, S. J., Jarrold, M. F., Udseth, H. R., Smith, R. D., and Clemmer, D. E. An Ims-Ims Analogue of Ms-Ms *Analytical Chemistry* **2006**, *78*, 4161-4174
57. Merenbloom, S. I., Koeniger, S. L., Valentine, S. J., Plasencia, M. D., and Clemmer, D. E. IMS-IMS and IMS-IMS-IMS/MS for Separating Peptide and Protein Fragment Ions *Analytical Chemistry* **2006**, *78*, 2802-2809
58. Clemmer, D. E., Valentine, S., and Sowell, R. Developing LC-IMS-(CID)n -TOF for Proteome Characterization *Faseb Journal* **2005**, *19*, A767-A767
59. Sowell, R. A., Koeniger, S. L., Valentine, S. J., Moon, M. H., and Clemmer, D. E. Nanoflow LC/IMS-MS and LC/IMS-CID/MS of Protein Mixtures *Journal of the American Society for Mass Spectrometry* **2004**, *15*, 1341-1353
60. Lee, Y. J., Hoaglund-Hyzera, C. S., Barnes, C. A. S., Hilderbrand, A. E., Valentine, S. J., and Clemmer, D. E. Development of High-Throughput Liquid Chromatography Injected Ion Mobility Quadrupole Time-of-Flight Techniques for Analysis of Complex Peptide Mixtures *Journal of Chromatography B-Analytical Technologies in the Biomedical and Life Sciences* **2002**, *782*, 343-351
61. McLuckey, S. A., and Stephenson, J. L. Ion Ion Chemistry of High-Mass Multiply Charged Ions *Mass Spectrometry Reviews* **1998**, *17*, 369-407

www.manaraa.com

62. Pitteri, S. J., and McLuckey, S. A. Recent Developments in the Ion/Ion Chemistry of High-Mass Multiply Charged Ions *Mass Spectrometry Reviews* **2005**, *24*, 931-958
63. Syka, J. E. P., Coon, J. J., Schroeder, M. J., Shabanowitz, J., and Hunt, D. F. Peptide and Protein Sequence Analysis by Electron Transfer Dissociation Mass Spectrometry *Proceedings of the National Academy of Sciences of the United States of America* **2004**, *101*, 9528-9533
64. Mikesh, L. M., Ueberheide, B., Chi, A., Coon, J. J., Syka, J. E. P., Shabanowitz, J., and Hunt, D. F. The Utility of Etd Mass Spectrometry in Proteomic Analysis *Biochimica Et Biophysica Acta-Proteins and Proteomics* **2006**, *1764*, 1811-1822
65. Zubarev, R. A.; Kelleher, N. L.; McLafferty, F. W. Electron Capture Dissociation of Multiply Charged Protein Cations. A Nonergodic Process *Journal of the American Chemical Society* **1998**, *120*, 3265-3266
66. Zubarev, R. A., Kruger, N. A., Fridriksson, E. K., Lewis, M. A., Horn, D. M., Carpenter, B. K., and McLafferty, F. W. Electron Capture Dissociation of Gaseous Multiply-Charged Proteins Is Favored at Disulfide Bonds and Other Sites of High Hydrogen Atom Affinity *Journal of the American Chemical Society* **1999**, *121*, 2857-2862
67. McLafferty, F. W., Horn, D. M., Breuker, K., Ge, Y., Lewis, M. A., Cerda, B., Zubarev, R. A., and Carpenter, B. K. Electron Capture Dissociation of Gaseous Multiply Charged Ions by Fourier-Transform Ion Cyclotron Resonance *Journal of the American Society for Mass Spectrometry* **2001**, *12*, 245-249
68. Zubarev, R. A., Horn, D. M., Fridriksson, E. K., Kelleher, N. L., Kruger, N. A., Lewis, M. A., Carpenter, B. K., and McLafferty, F. W. Electron Capture Dissociation for Structural Characterization of Multiply Charged Protein Cations *Analytical Chemistry* **2000**, *72*, 563-573
69. Newton, K. A., and McLuckey, S. A. Generation and Manipulation of Sodium Cationized Peptides in the Gas Phase *Journal of the American Society for Mass Spectrometry* **2004**, *15*, 607-615
70. Newton, K. A., and McLuckey, S. A. Gas-Phase Peptide/Protein Cationizing Agent Switching Via Ion/Ion Reactions *Journal of the American Chemical Society* **2003**, *125*, 12404-12405
71. Newton, K. A., He, M., Amunugama, R., and McLuckey, S. A. Selective Cation Removal from Gaseous Polypeptide Ions: Proton Vs. Sodium Ion Abstraction Via Ion/Ion Reactions *Physical Chemistry Chemical Physics* **2004**, *6*, 2710-2717
72. Newton, K. A., Amunugama, R., and McLuckey, S. A. Gas-Phase Ion/Ion Reactions of Multiply Protonated Polypeptides with Metal Containing Anions *Journal of Physical Chemistry A* **2005**, *109*, 3608-3616
73. Badman, E. R., Chrisman, P. A., and McLuckey, S. A. A Quadrupole Ion Trap Mass Spectrometer with Three Independent Ion Sources for the Study of Gas-Phase Ion/Ion Reactions *Analytical Chemistry* **2002**, *74*, 6237-6243
74. Wells, J. M., Chrisman, P. A., and McLuckey, S. A. Formation of Protein-Protein Complexes in Vacuo *Journal of the American Chemical Society* **2001**, *123*, 12428-12429

www.manaraa.com

75. Schwartz, J. C., Senko, M. W., and Syka, J. E. P. A Two-Dimensional Quadrupole Ion Trap Mass Spectrometer *Journal of the American Society for Mass Spectrometry* **2002**, *13*, 659-669
76. Hager, J. W. A New Linear Ion Trap Mass Spectrometer *Rapid Communications in Mass Spectrometry* **2002**, *16*, 512-526
77. March, R. E. An Introduction to Quadrupole Ion Trap Mass Spectrometry *Journal of Mass Spectrometry* **1997**, *32*, 351-369
78. Jonscher, K. R., and Yates, J. R. The Quadrupole Ion Trap Mass Spectrometer - a Small Solution to a Big Challenge *Analytical Biochemistry* **1997**, *244*, 1-15
79. Londry, F. A., and Hager, J. W. Mass Selective Axial Ion Ejection from a Linear Quadrupole Ion Trap *Journal of the American Society for Mass Spectrometry* **2003**, *14*, 1130-1147
80. Xia, Y., Jin, W., McLuckey, S. A., Londry, F. A., and Hager, J. W. Mutual Storage Mode Ion/Ion Reactions in a Hybrid Linear Ion Trap *Journal of the American Society for Mass Spectrometry* **2005**, *16*, 71-81
81. Han, H., Xia, Y., Yang, M., and McLuckey, S. A. Rapidly Alternating Transmission Mode Electron-Transfer Dissociation and Collisional Activation for the Characterization of Polypeptide Ions *Analytical Chemistry* **2008**, *80*, 3492-3497
82. Liang, X. R., Hager, J. W., and McLuckey, S. A. Transmission Mode Ion/Ion Electron-Transfer Dissociation in a Linear Ion Trap *Analytical Chemistry* **2007**, *79*, 3363-3370
83. Liang, X. R., and McLuckey, S. A. Transmission Mode Ion/Ion Proton Transfer Reactions in a Linear Ion Trap *Journal of the American Society for Mass Spectrometry* **2007**, *18*, 882-890
84. McAlister, G. C., Berggren, W. T., Griep-Raming, J., Horning, S., Makarov, A., Phanstiel, D., Stafford, G., Swaney, D. L., Syka, J. E. P., Zabrouskov, V., and Coon, J. J. A Proteomics Grade Electron Transfer Dissociation-Enabled Hybrid Linear Ion Trap-Orbitrap Mass Spectrometer *Journal of Proteome Research* **2008**, *7*, 3127-3136

www.manaraa.com

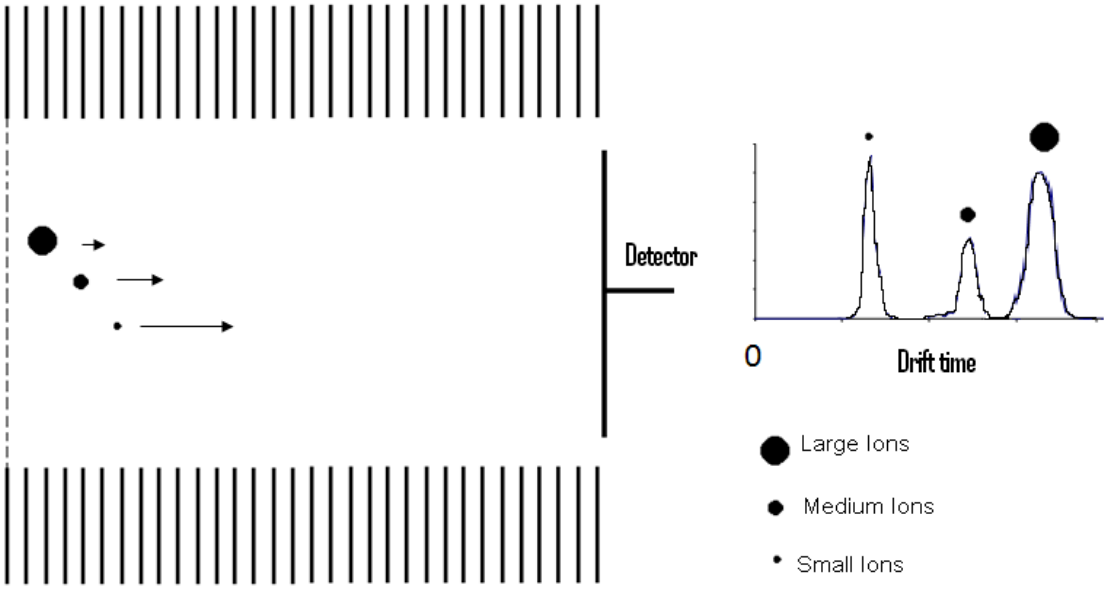

Figure1. Schematic representation of the ion motion in the drift region for ion mobility spectrometry. Ions with three different sizes are injected into the drift tube simultaneously and separated according to ion mobility. Smallest ions have the fastest speed and hit the detector first.

www.manaraa.com

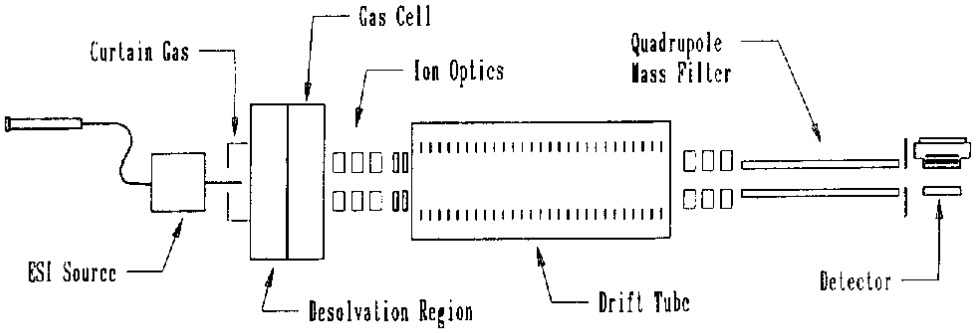

Figure 2. Schematic diagram of the ESI-ion mobility quadrupole instrument. Drift tube length: 32.4 cm, electric field: 13.9 V/cm, Drift tube pressure: He, ~2 Torr. [48]

www.manaraa.com

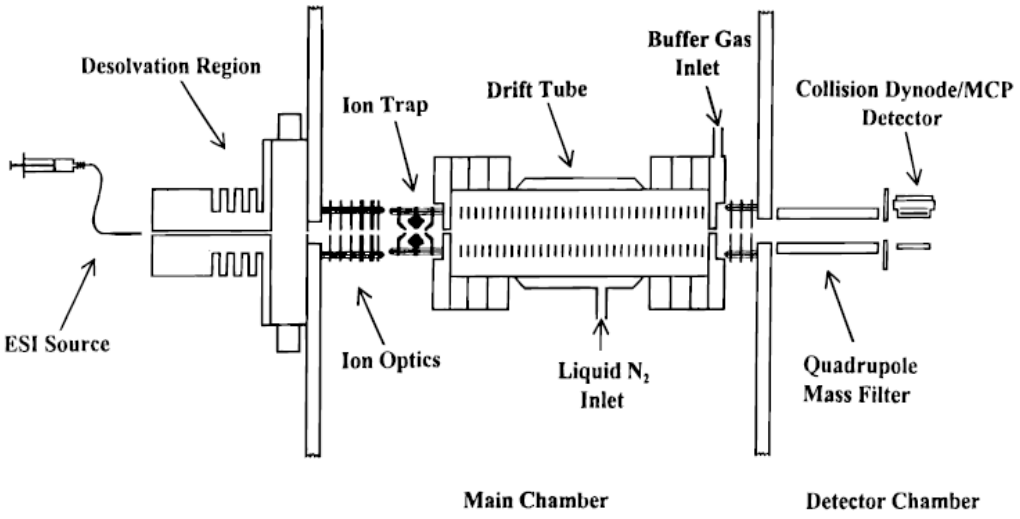

Figure 3. Schematic diagram of an ion trap/ion mobility quadrupole instrument. [51]

www.manaraa.com

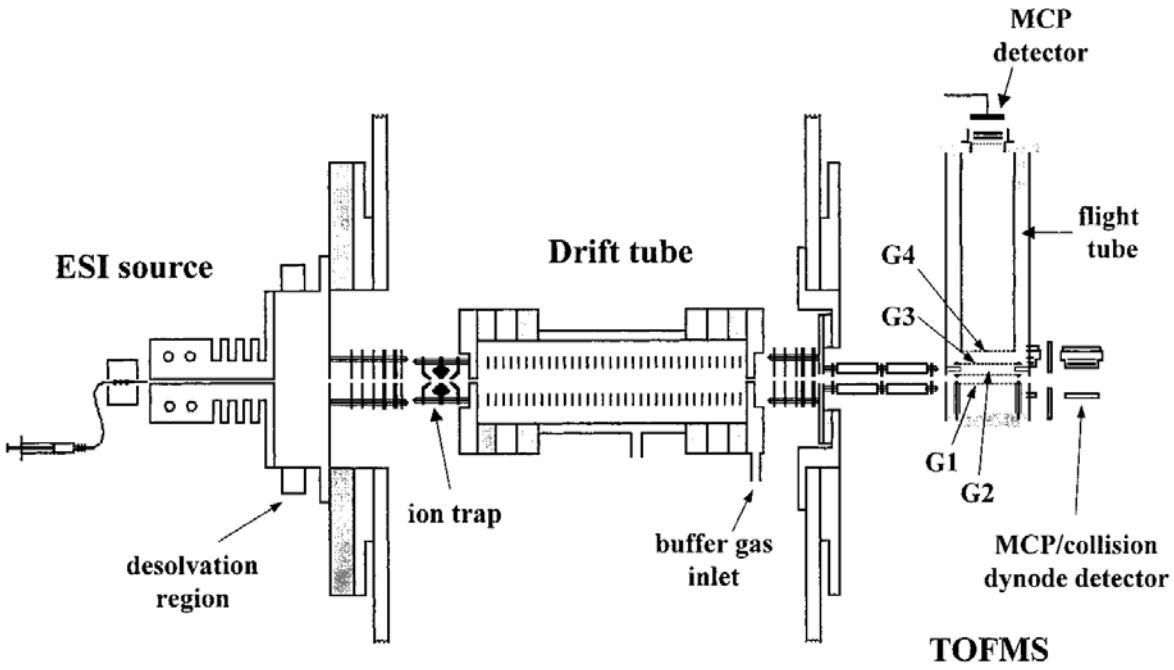

Figure 4. Schematic diagram of the experimental ion trap/ ion mobility/TOFMS instrument. [53]

www.manaraa.com

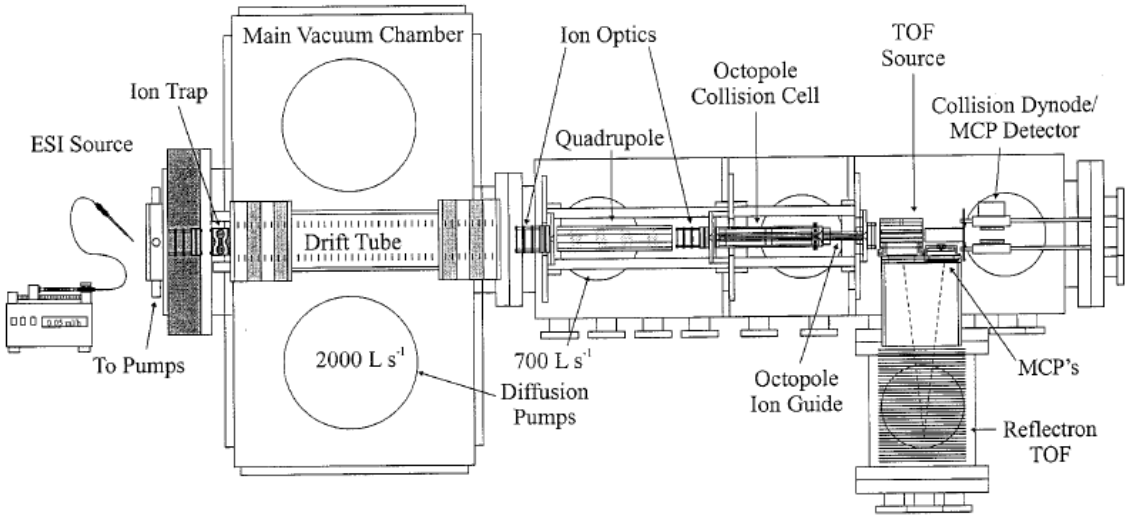

Figure 5. Schematic diagram of the ESI/ion trap/drift tube/quadrupole/collision cell/reflection time-of-flight mass spectrometer. Ion trap pressure: 10^{-4} to 10^{-3} Torr of He, ions are ejected from the trap by applying a short (0.6 μs) DC pulse (60 to 150 V) on the end cap, drift tube length: ~53 cm, pressure: 2 to 3 Torr, electric field: 12 V/cm. [54]

www.manaraa.com

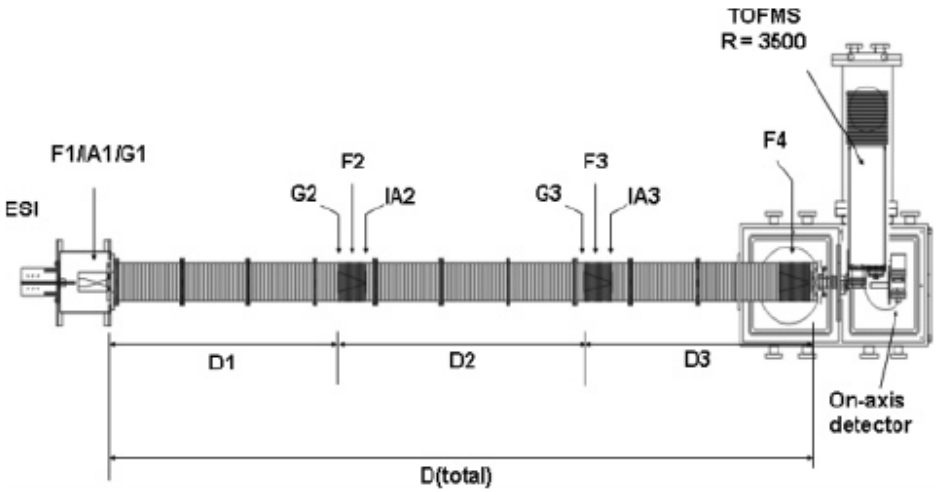

Figure 6. Schematic of the IMS-IMS-IMS-TOF instrument. Ions can be gated (G1-G3) and activated (IA1-IA3) in three regions of the instrument. The entire drift tube is ~290 cm long, electric field in drift region: 9 V/cm, pressure in the drift tube: ~3Torr He [57]

www.manaraa.com

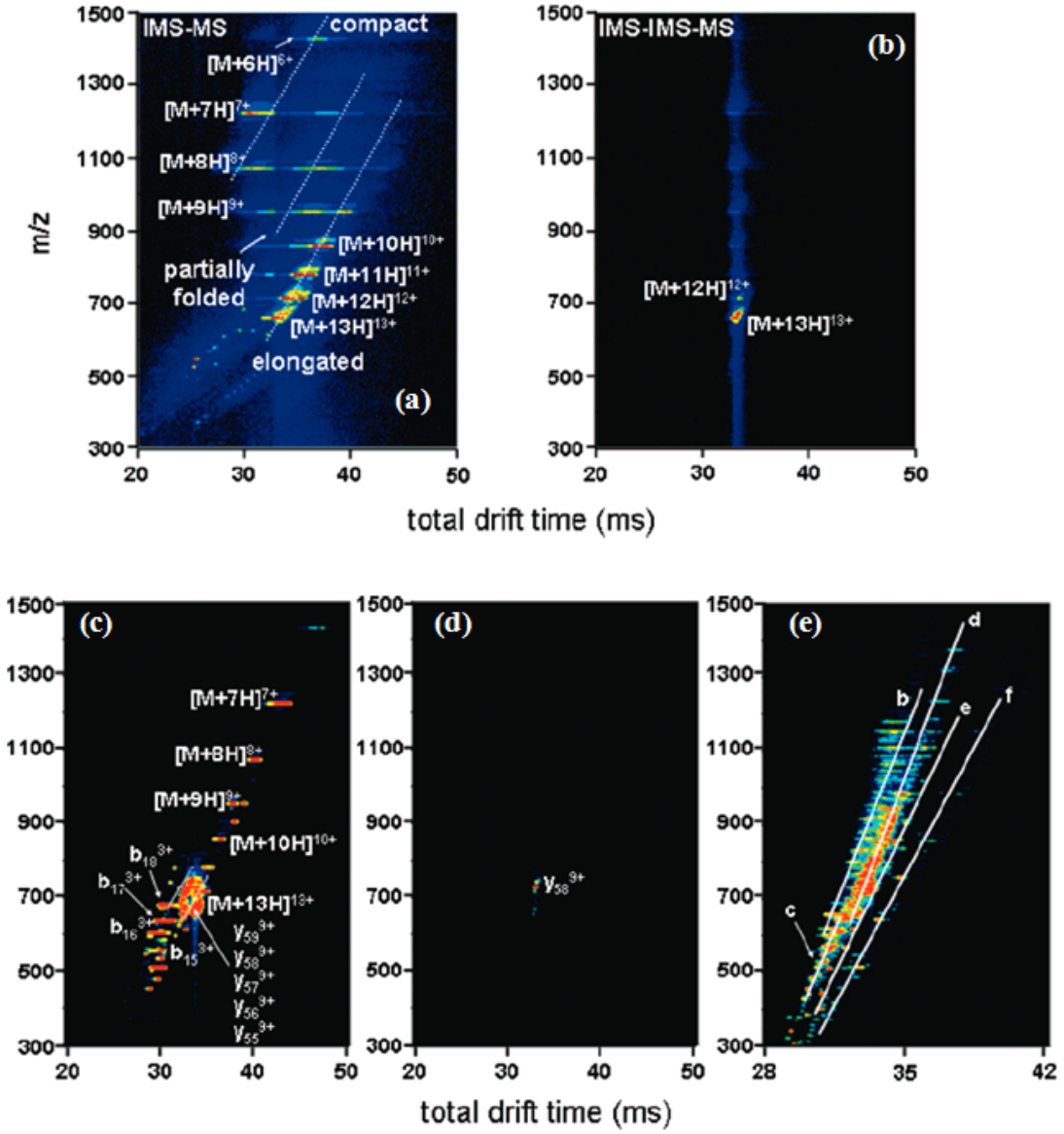

Figure 7. Two-dimensional t_D (m/z) plot of electrosprayed ubiquitin ions, (a) distribution of ions without gating and excitation, (b) $[M + 13H]^{13+}$ ions are gated in G2 (c) $[M + 13H]^{13+}$ ions are gated in G2 and then activated at IA2 and fragments travel through D2 and D3 (d) $y_{58}{}^{9+}$ fragment ions are gated by G3 (e) $y_{58}{}^{9+}$ fragment ions are gated in G3 and then fragmented by IA3. [57]

www.manaraa.com

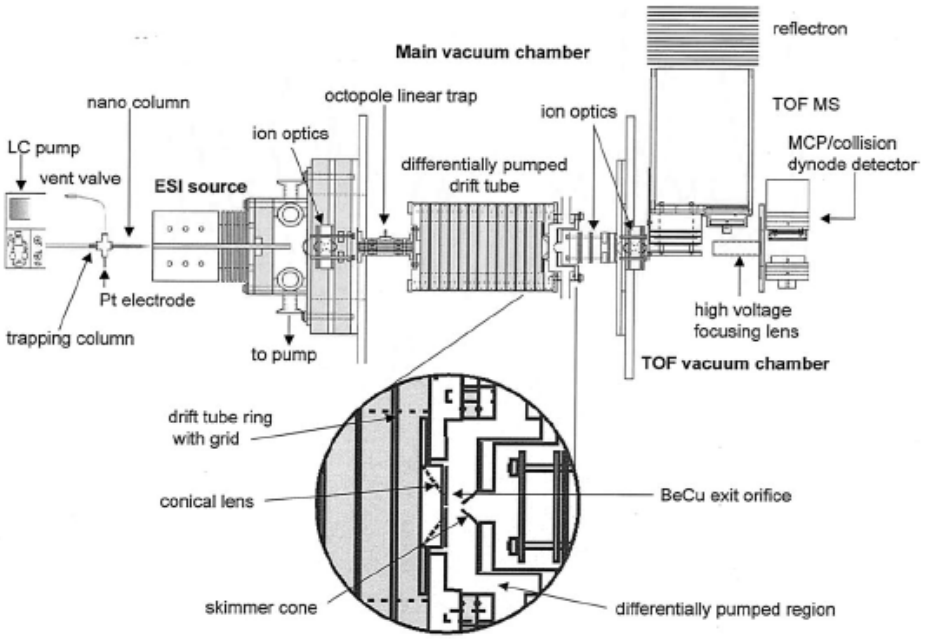

Figure 8. A schematic diagram of the nanoflow LC apparatus coupled to the split-field drift tube instrument. The insert shows the split-field region at the back of the drift tube. CID can be done in the split-field region [59].

www.manaraa.com

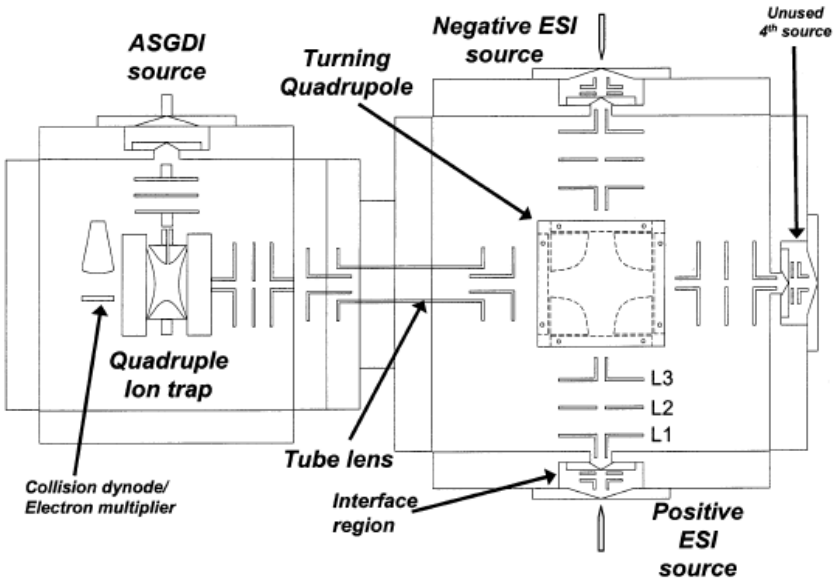

Figure 9. Schematic diagram of the three-source quadrupole ion trap instrument showing two electrospray ionization (ESI) sources and one atmospheric sampling glow discharge ionization (ASGDI) source interfaced to a quadrupole ion trap mass spectrometer. The turning quadrupole allows the ion beams generated by ESI to be deflected 90° to the axis of the ion trap. [73]

www.manaraa.com

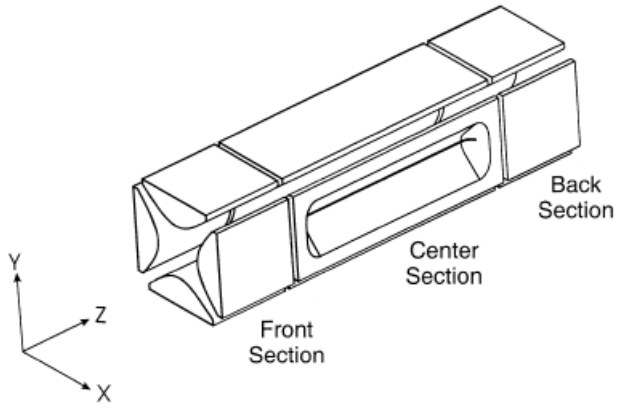

Figure 10. Basic design of the two-dimensional linear ion trap [75].

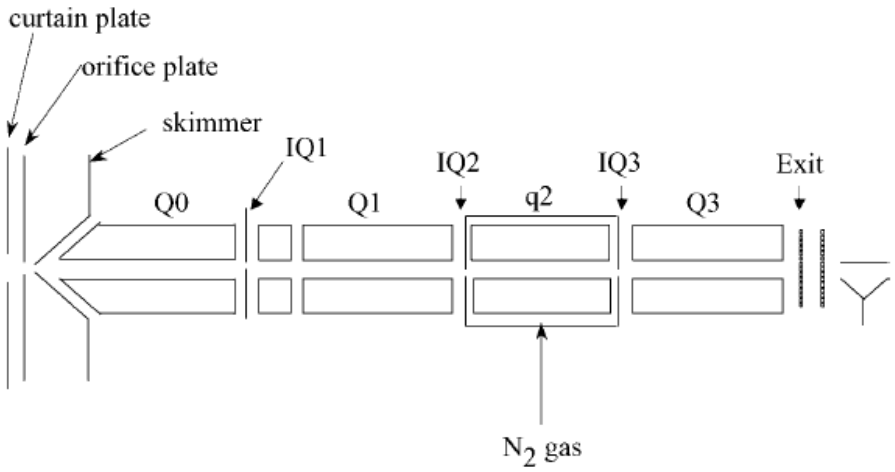

Figure 11. Schematic portrayal of the experimental apparatus based on the ion path of a triple quadrupole mass spectrometer. The linear ion trap mass spectrometer was created using either q2 or Q3 [76].

www.manaraa.com

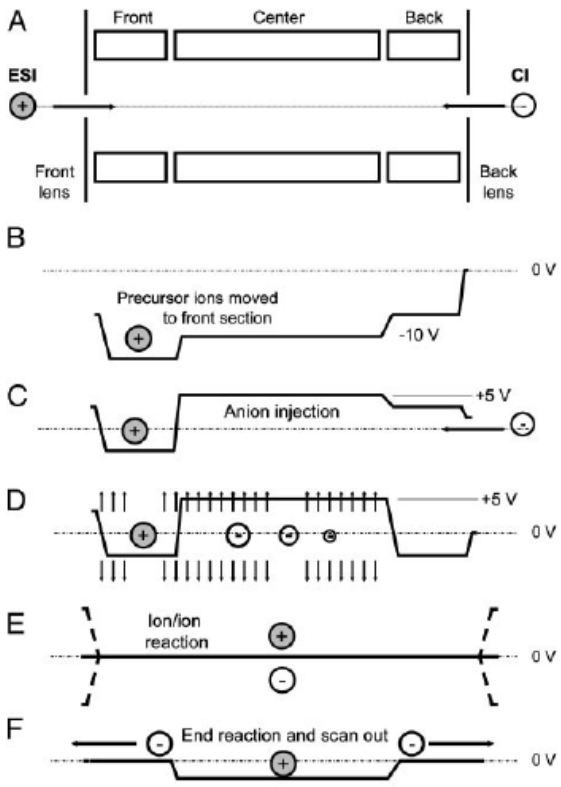

Figure 12. Schematic of steps involved in the operation of the LTQ mass spectrometer for peptide sequence analysis by ETD. (*A*) Injection of multiply protonated peptide molecules (precursor ions) generated by ESI. (*B*) Application of a dc offset to move the precursor ions to the front section of the linear trap. (*C*) Injection of negatively charged reagent ions from the CI source into the center section of the linear trap. (*D*) Application of a supplementary dipolar broadband ac field to eject all ions except those within 3 mass-unit windows centered around the positively charged precursor ions and the negatively charged electron-donor reagent ions. (*E*) Removal of the dc potential well and application of a secondary RF voltage (100 V zero to peak, 600 kHz) to the end lens plates of the linear trap to allow positive and negative ion populations to mix and react. (F) Termination of ion_ion reactions by axial ejection of negatively charged reagent ions while retaining positive ions in the center section of the trap. This is followed by mass-selective, radial ejection of positively charged fragment ions to record the resulting MS_MS spectrum [63].

www.manaraa.com

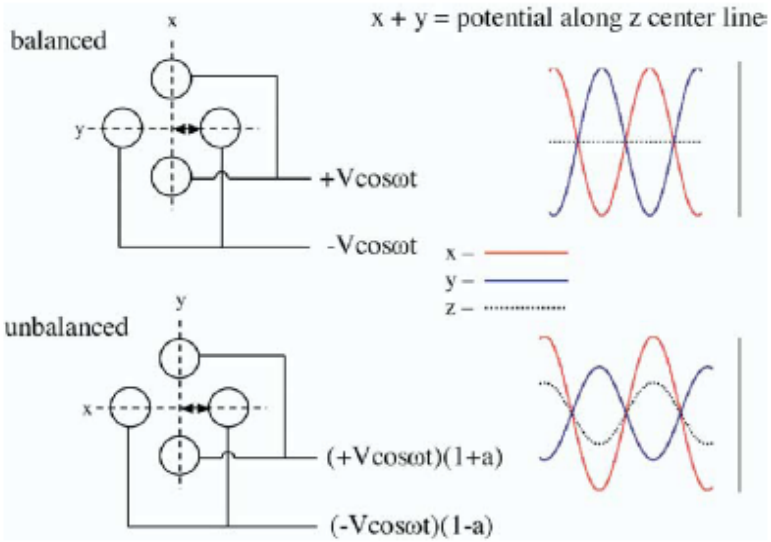

Figure 13. Conceptual depiction of unbalancing the RF amplitudes on the two sets of opposing poles of a quadrupole rod array. V is the RF amplitude applied on the rods, a is the degree of unbalance, and x, y, z represent the three dimensions [80].

www.manaraa.com

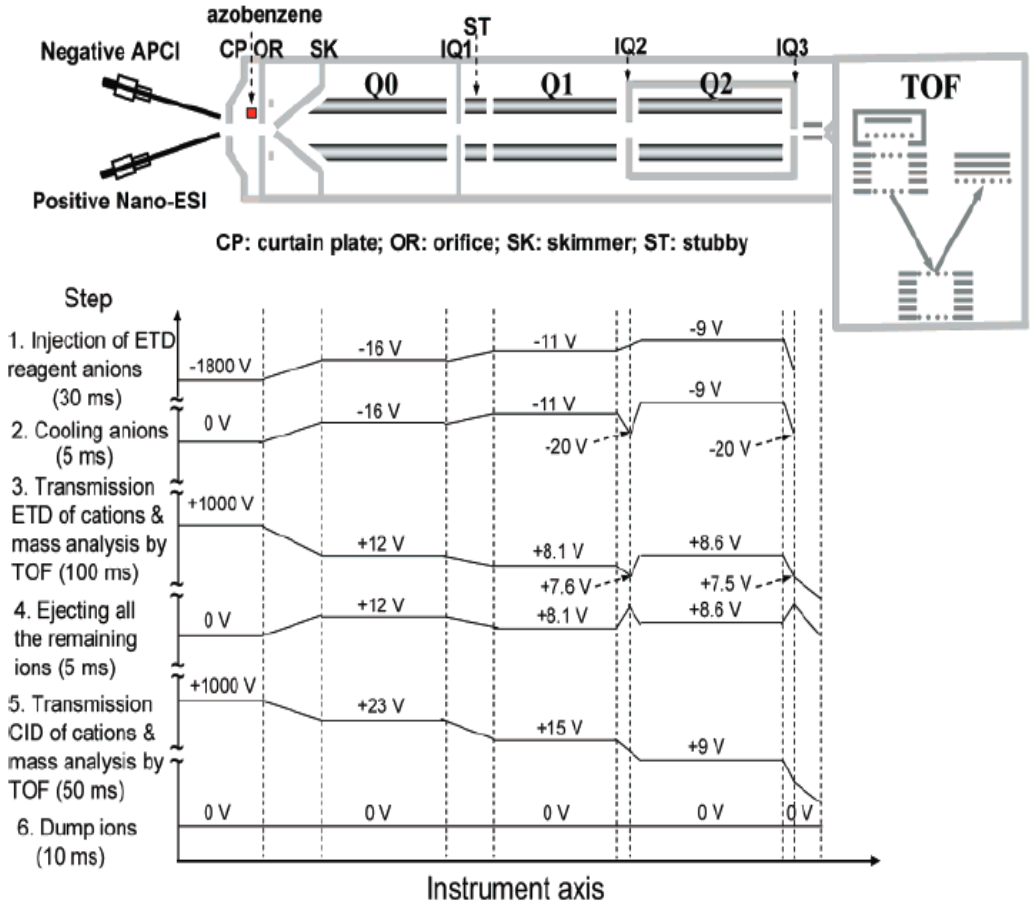

Figure 14. Schematic of the QSTAR mass spectrometer equipped with a home-built pulsed dual nano-ESI/APCI source [81].

www.manaraa.com

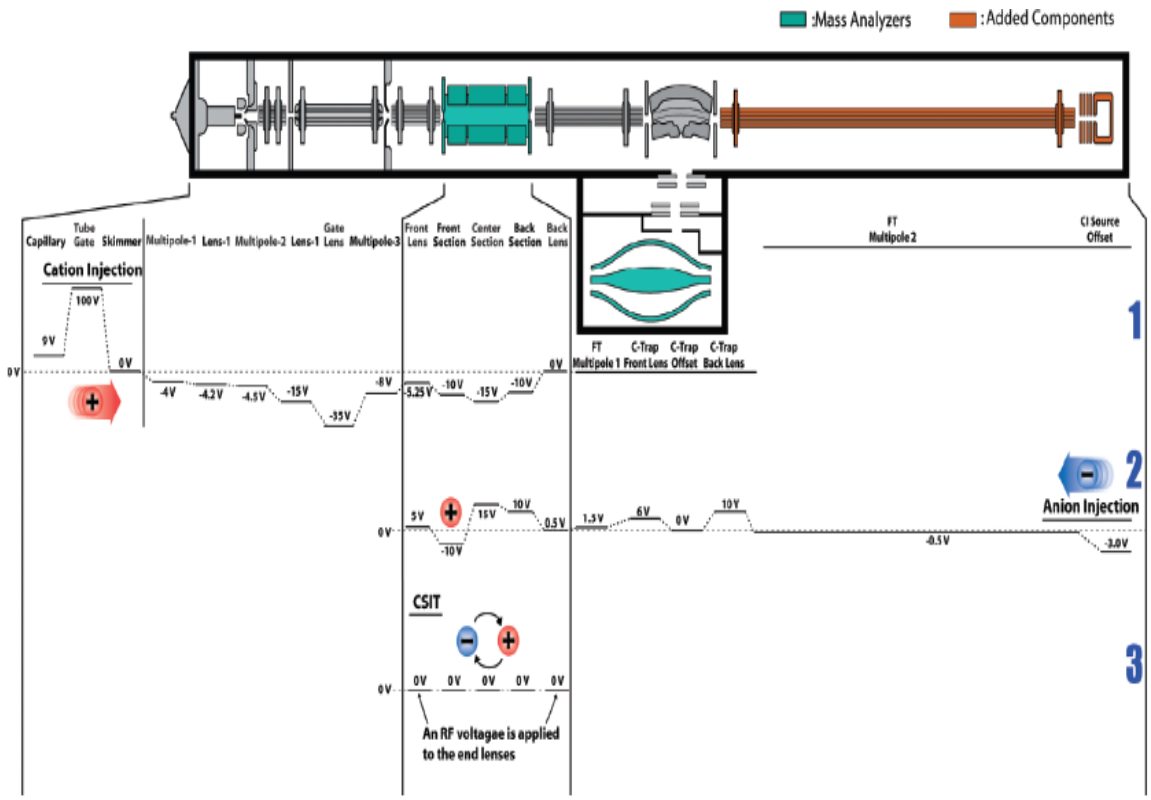

Figure 15. Schematic of the ETD-enabled QLT-orbitrap hybrid mass spectrometer. The mass analyzers are highlighted in green, while the added components, for ETD, are highlighted in orange. The lift-out information below the figure details the voltages used during (1) cation injection, (2) anion injection, and (3) ion/ion reaction [84]

www.manaraa.com

CHAPTER 2

AN ION TRAP - ION MOBILITY – TIME OF FLIGHT MASS SPECTROMETER WITH THREE ION SOURCES FOR ION-ION REACTIONS

Qin Zhao, Matthew W. Soyk, Gregg M. Schieffer, R.S. Houk,[†] Ethan R. Badman[‡]

Iowa State University, Department of Chemistry, Ames, IA, 50011 USA

Katrin Fuhrer, Marc Gonin

TOFWerk AG, Feuerwerkerstrasse 39, CH-3602 Thune, Switzerland

[†]Ames Laboratory U. S. Dept. of Energy, Iowa State University, Ames IA 50011 USA

[‡]Author for correspondence. Current Address: Hoffmann-La Roche Inc.,

Non-Clinical Safety, 340 Kingsland St., Nutley, NJ, 07110 USA

E-mail: ethan.badman@roche.com

Address reviews, revisions and other pre-publication matters to:

R. S. Houk

Department of Chemistry

Iowa State University

Ames IA 50011 USA

515-294-9462 fax -5233 rshouk@iastate.edu

J. Amer. Soc. Mass Spectrom., to be submitted November 2008

www.manaraa.com

Abstract: This instrument combines the capabilities of ion/ion reactions with ion mobility (IM) and time-of-flight (TOF) measurements for conformation studies and top-down analysis of large biomolecules. Ubiquitin ions from either of two electrospray ionization (ESI) sources are stored in a 3D ion trap (IT) and reacted with negative ions from atmospheric sampling glow discharge ionization (ASGDI). The proton transfer reaction products are then separated by IM and analyzed via a TOF mass analyzer. In this way, ubiquitin +7 ions are converted to lower charge states down to +1; the ions in lower charge states tend to be in compact conformations with cross sections down to ~ 880 $Å^2$. The duration and magnitude of the ion ejection pulse on the IT and the entrance voltage on the IM drift tube can affect the measured distribution of conformers for ubiquitin +7 and +6. Alternatively, protein ions are fragmented by collision-induced dissociation (CID) in the IT, followed by ion/ion reactions to reduce the charge states of the CID product ions, thus simplifying assignment of charge states and fragments using the mobility-resolved tandem mass spectrum. Instrument characteristics and the use of a new ion trap controller and software modifications to control the entire instrument are described.

Keywords: ion trap, ion mobility, time-of-flight mass spectrometry, protein conformation, ubiquitin

www.manaraa.com

Introduction

Despite the widespread use of mass spectrometry (MS) for biological analyses, further improvements in MS instrumentation are desirable, particularly in areas like proteomics [1] and characterization of large macromolecular complexes [2, 3]. These instrumentation improvements provide analytical capabilities that enable new biological studies not envisioned previously.

Ion mobility (IM) [4, 5] has become a very useful technique for analysis of biological ions in the gas phase [6]. IM provides information about ion size and structure [7], as it rapidly separates ions based on collision cross-section, rather than just m/z ratio. The use of IM to disperse a mixture of ions in time prior to analysis via a time-of-flight (TOF) MS, i.e, nested drift (flight) time measurements, is an important recent advance. These experiments were pioneered by Clemmer and coworkers in the mid-1990's [8] and have now been used by several other groups [9-13]. The recent Synapt ESI-IMS-MS by Waters Corp. provides a commercially available instrument for gas-phase ion conformation study by IM using a novel travelling wave approach [13].

In a series of instrumental designs, the Clemmer group has made various modifications to the initial ESI-IM-TOF, including the insertion of a collision cell between the IM drift tube and the TOF for mobility labeling experiments [14, 15], and the addition of an IT prior to the mobility drift tube to improve the duty cycle from the continuous ESI source [16, 17]. One publication demonstrated MS/MS capabilities with an ion trap prior to IM-TOF [18], but the entire instrument was not under computer control. Therefore, only relatively simple experiments were possible.

www.manaraa.com

IM has been used to analyze the products of ion-molecule reactions [19] including proton transfer [20, 21], H/D exchange [22], and solvation [23-26]. In these studies the desired reactions take place either in the atmospheric pressure ion source interface region or in the drift tube itself. Thus, only short reaction times and certain reagent ions can be used. In addition, performing reactions in the IM cell can make spectral interpretation difficult because the analysis and chemistry occur at the same time. In the current experiments, the ion/ion reaction is decoupled from the subsequent mobility and mass analysis. Therefore, the reaction time and chemistry of reagent ions are controlled more effectively, including a wider selection of reagent ions from independent ion sources.

Gas-phase ion/ion reactions provide another dimension for bioanalysis. Pioneering work by Smith and coworkers [27, 28] was followed by a continuing series of experiments by McLuckey's group [29]. Ion/ion reactions are rapid, versatile, and can be controlled via various ion manipulation schemes. The most common type of reaction has been proton transfer to manipulate the charge states of multiply-charged ions [30] and simplify complex MS/MS spectra [31, 32]. Use of product ions in low charge states can improve mass accuracy and resolution, especially with low resolution mass analyzers. Various instruments specifically for ion/ion reactions include two [33-37], three or four [38] independent ion sources arranged around an IT, although use of pulsed sources and a single ion extraction system is also possible [39, 40]. Electron transfer is another useful process, especially electron transfer dissociation (ETD) [33, 41, 42]. ETD is now becoming widely used in proteomics and for determination of post translational modifications. Several instruments combine an IT for ETD reactions with a high resolution mass analyzer, for example, the

www.manaraa.com

modified QSTAR/TOF MS spectrometer in McLuckey's group [43, 44] and the hybrid linear IT/orbitrap MS by Coon's group [45, 46].

Here we describe the first instrument to include capabilities for both ion/ion reactions and IM-TOF-MS measurements. Initial experiments and instrument characteristics are described, including use of a new ion trap controller and software to control the entire instrument. Ubiquitin is used as a test compound to compare the new results with the extensive previous studies of this protein [20, 47-53].

Experimental

Bovine ubiquitin (Sigma-Aldrich, St. Louis, MO) was used without further purification. Protein concentrations were 20 to 30 μM in 1% aqueous acetic acid for positive ion mode. Nano-ESI emitters were pulled from glass capillaries (1.5 mm o.d., 0.86 mm i.d.) by a micropipette puller (P-97, Sutter Instruments, Novato, CA). Nano-ESI was performed by applying +1 kV to +1.2 kV to the protein solution via a stainless steel wire through the back of the sample capillary. Negative ions from perfluoro-1,3-dimethylcyclohexane (PDCH, Sigma-Aldrich , St. Louis, MO) were used as the proton acceptor reagent.

Instrumentation

General. The instrument is shown to scale in Figure 1. It contains three independent ion sources: two for ESI and one for ASGDI [54]. Ions from these sources are stored in the 3D quadrupole IT for reaction. The products are separated by the IM drift tube, followed by a quadrupole-time-of-flight mass spectrometer (q-TOF).

www.manaraa.com

The vacuum chamber consists of an 8" Conflat cube, which houses the three ion sources, ion optics, and turning quadrupole deflector (TQ, Extrel, Pittsburgh, PA). The cube is evacuated by a turbomolecular pump (Turbo-V550 MacroTorr, 550 l/s N_2, Varian Inc., Palo Alto, CA) backed by a mechanical pump (SD-30, Varian, Palo Alto, CA) and is attached to a custom built rectangular chamber (304 stainless steel, 35.6 cm wide ×76.2 cm long × 33.0 cm high) that also houses the IT, IM drift tube, and quadrupole collision cell. The TOF is in an aluminum housing (8.90 cm × 25.4 cm × 66.7 cm) attached to the back of the chamber; the TOF tube is oriented vertically. The main vacuum chamber (i.e., the chamber that houses the drift cell and quadrupole collision cell) is evacuated by two diffusion pumps (Diffstak 250/2000M and 160/700M, BOC Edwards) backed by mechanical pumps (E2M40 and RV12, respectively, BOC Edwards, Wilmington, MA). The TOF is pumped by a turbomolecular pump (Turbovac 361, 400 l/s N_2, Leybold Inc., Woodbridge, Ont.), backed by a mechanical pump (RV12, BOC Edwards). Convectron and ion gauges (Series 375 and 358, Helix Technology Corporation, Mansfield, MA) measure the ion source and chamber pressures (all are uncorrected). The base pressures are 7.5×10^{-8} mbar in the main chamber and 3.3×10^{-7} mbar in the TOF when the sources are closed. In normal operation, one ESI source and the ASGDI source are open, and helium is added to the drift tube (~1.3 to 2.0 mbar) through a precision leak valve (Model 203, Granville Phillips, Boulder, CO). The main chamber pressure is then $\sim1\times10^{-4}$ mbar and the pressure in the TOF region is 9×10^{-7} mbar.

www.manaraa.com

Ion Sources. The basic design for a three ion source interface (Figure 1) has been described previously [38]. The three sources are arranged around three faces of the 8" Conflat cube. One source is on the ion optical axis of the IT and IM drift tube and the other two are orthogonal to it. The two ESI sources are identical. The interface region, which is 5.08 cm in diameter and 1.59 cm deep, is machined out of an 8" ConFlat flange. A 254 μm diameter aperture separates the interface region from atmosphere, and a 381 μm diameter aperture separates the interface region from the high vacuum region. Two lenses between the apertures focus ions through the interface region. Each ESI interface region operates at ~1 mbar during the experiment and is pumped by a mechanical pump (E2M40, BOC Edwards). The nano-ESI voltages are provided by 5 kV power supplies (ORTEC 659, Oak Ridge, TN).

The ASGDI source interface region has the same design and dimensions as the ESI sources but without the interface lenses. It is pumped by a mechanical pump (E2M40, BOC Edwards). PDCH headspace vapors are sampled via a 0.64 cm diameter Nylon tube connecting the sample container and the outer aperture plate. The source pressure (~0.79 mbar) is regulated by a bellows valve (SS-4BMW, Swagelok) inserted in the tubing between the compound headspace and the source region. The ASGDI source uses a 3 kV power supply (ORTEC 556, Oak Ridge, TN) and a high voltage pulser (PVX-4150, Directed Energy Corp., Fort Collins, CO) that is trigged by a TTL pulse from the Argos IT controller (Griffin Analytical Technologies, West Lafayette, IN), to apply a ~ -420 V pulse between the outer and inner (grounded) aperture plates. This ASGDI pulse lasts for the time required to add reagent anions to the IT, typically 5 to 20 ms.

www.manaraa.com

Each ion source has three cylindrical lenses attached to the vacuum side of the flange to focus the ions from the exit aperture of the source into the TQ. The second lens is split in half with distinct voltages applied to each half and serves as a deflector for direction focusing. The TQ was modified by severing the electrical connection between diagonally opposing rods and by applying four independent DC potentials to the four TQ rods. This allows ions to either be deflected 90^{o} onto the axis of the instrument or to be passed straight through.

After the TQ, three lenses focus the ions into the IT. Two home-built high-voltage switches, controlled by TTL signals from the Argos IT controller, switch the voltages applied to the TQ and three subsequent lenses to allow ions from the desired ion source into the IT. Six nine-channel DC power supplies (-500 V, TD9500, Spectrum Solutions, Russellton, PA) generate the potentials for the ion optics from the sources to the ion trap.

Ion Trap. The 3D quadrupole IT (ideal geometry, r_0 = 1.0 cm, z_0 = 0.707 cm, RM Jordan, Grass Valley, CA) is attached to the drift tube; the exit aperture is 1.3 cm from the front plate of the drift tube. During ion trapping the end caps are at ground, except during resonance excitation and mass selection, and the DC potential on the ring electrode is zero to prevent any asymmetric fields. The 665 kHz ion trapping voltage is generated by a home-built LC circuit that provides up to 5000 V_{0p}. The maximum low mass cutoff value is ~m/z 1220 (calculated assuming an ideal ion trap geometry). For the work presented here, the low mass cutoff is typically ~m/z 200 to allow for confinement of the $PDCH^-$ reagent anions from the ASGDI.

www.manaraa.com

A 0 to 10 V dc control signal from the Argos IT controller determines the rf trapping voltage. A custom control generates the initial low-level rf voltage, measures feedback to stabilize the rf voltage, and contains calibration data. The initial rf voltage is first amplified to 0 to 200 V_{0p} by a 50 W commercial amplifier (AG1020, T&C Power Conversion Inc., Rochester, NY) and finally by the custom LC circuit to the full 0 to 5000 V_{0p}. Measured stabilities of the full rf voltage are better than 1%. A TTL input allows the rf wave to be shut off in ~15 µs at any rf amplitude. The shutoff is not locked to the rf phase.

The ion trap timing and voltages are controlled by an Argos IT controller and software (Figure 2). The Argos provides the master clock for the entire instrument, as well as two independent arbitrary waveform outputs, digital TTL triggers, and analog control outputs (0 to 4 V). One arbitrary waveform output provides the 0 to 10 V dc control signal for the ion trap rf; the other is applied to the front endcap electrode (after being amplified by x17 to 85 V_{p-p}) to perform mass selection and resonance excitation. The TTL triggers are used to start the ASGDI source, control the high voltage switches for the ion sources, and start the ion injection pulse for the mobility experiment. A custom 8-channel driver is used to increase the power of the TTL signals to enable them to trigger 50 Ω loads. The ion injection TTL pulse enables the high voltage pulser (PVX-4150, Directed Energy Corp., Fort Collins, CO, applied to the exit endcap) to eject ions from the ion trap. Typically the ejection pulse for positive ions is -100 to -150 V applied for 3 to 5 µs to the trap end cap closest to the drift tube (Figure 1). Two analog signals are used to control the quadrupole collision cell, described below.

www.manaraa.com

Drift Tube. The drift tube (modified from a design provided by Valentine et al. [55, 56]) consists of alternating 12.7 cm diameter 304 stainless steel lenses (0.16 cm thick, 12.7 cm o.d. 4.40 cm i.d.) and Delrin insulating rings (1.27 cm thick, 12.7 cm o.d., 8.26 cm i.d.). The drift tube is 44.45 cm long (together with the ion funnel) with a 0.5 mm diameter entrance aperture. A chain of 2 MΩ resistors connects the lenses, creating an electric field (typically 12.4 V/cm) down the drift tube. The voltage applied to the front of the drift tube is typically -30 to -100 V, i.e., more negative than the grounded IT. A capacitance manometer (690A13TRC, MKS Instrument, Methuen, MA) measures the He pressure inside the drift tube, which is typically 1.33 to 2.00 mbar, controlled via another precision leak valve.

Ion Funnel. To improve ion transmission efficiency, an ion funnel [56, 57] is integrated into the back of the drift tube (Figure 1). The funnel is based on the device described by the Smith [57] and Jarrold groups [58]. After the last ring of the drift tube, a series of 25 stainless steel electrodes (0.079 cm thick, 12.7 cm o.d.) with circular apertures whose inner diameters decrease linearly from 4.293 to 0.483 cm is attached. The ion funnel electrodes are sealed together using 0.318 cm thick Delrin spacers and Viton o-rings giving a funnel length of 11.11 cm. Thus, the helium pressure in the drift tube and ion funnel are the same. The electrodes are connected to each other with a series of resistors (Vishay, 500 k **Ω,** 0.6 W, ±1%). One voltage is applied to the entrance of the drift tube, and a second voltage is applied to the exit of the ion funnel to set the axial electric field down the drift tube-ion funnel assembly. The electrode spacing and resistor voltages in the ion funnel are selected so that the axial electric field is the same as that in the rest of the drift tube.

www.manaraa.com

In the ion funnel, alternate lenses are capacitively coupled (Vishay, 1000 pF, 1.5 kV_{rms}, ±20%) to form two lens chains. RF voltages (Ardara RF power supply, # PSRF-100, Ardara Technologies, North Huntingdon, PA) that are 180° degrees out of phase from each other are applied to each chain with amplitudes ~90 V_{pp} at 360 kHz. A capacitor to ground decouples the RF voltage from the drift tube lenses. There is one DC only electrode after the exit of the ion funnel with a pressure-limiting aperture (1.0 mm diam).

In this instrument, the ion funnel increases the overall total ion signal by a factor of ~7. Here, the basis of comparison is the same number of electrodes at the end of the drift tube all with the same ID and no rf voltage. In this experiment, total ion signal is measured by extracting ions from the TOF source continuously into the flight tube and reflecting them to the TOF microchannel plate (MCP) detectors.

Another set of three lenses behind the drift tube-ion funnel focuses ions into the quadrupole collision cell (Figure 1). The voltages supplied to the ion funnel dc lens, the lenses before the collision cell, the entrance and exit lenses of the collision cell, and the lenses between the collision cell and the TOF are floated on the drift tube exit voltage using a nine-output floating power supply (TD9500HV, Spectrum Solutions Inc., Russellton, PA).

Quadrupole-TOF. The quadrupole collision cell (Figure 1) transmits ions from the ion funnel to the TOF. It also provides for CID of ions labeled by mobility (i.e., a pseudo MS/MS step) [14, 15], although this capability is not shown in this paper. The quadrupole (d_0 = 9.5 mm, 880 kHz, 3600 V_{0p} per pole, Extrel, Pittsburgh, PA) is followed by an orthogonal W-reflectron TOF (TOFWerk, Thun, Switzerland). The collision cell and its

www.manaraa.com

electronics are floated using an isolation transformer (SIT 30-1000, Stangenes Industries Inc., Palo Alto, CA). The collision cell is mounted on the vacuum side of an 8" Conflat flange that is attached to the back of the main vacuum chamber. A capacitance manometer (Model 690A01TRC, MKS Instrument, Methuen, MA) measures the pressure inside the collision cell, which is typically ~8×10^{-4} mbar of He from the drift tube. Additional collison gas can be added via another precision leak valve. The Argos IT controller (Figure 2) supplies two 0 to 4 V analog signals that are amplified to 0 to 10 and -200 to 200 V, respectively, and then used by the quadrupole power supply to control the rf amplitude and to supply the dc bias to the collision cell rods to set the collision energy.

After the ions exit the collision cell, they are focused into the source region of the TOF by a series of 10 lenses mounted in the hole machined out of the 8" Conflat flange between the collision cell and the TOF, which is mounted vertically on the air side of the flange. One lens is split into half-plates for vertical direction focusing. The ions are pulsed upwards into the TOF drift region by a 2 μs pulse and are then accelerated into the drift region by ~5800 V. The voltages on the TOF electrodes and detector are controlled by the TOF software, which communicates directly with the TOF power supply. The TOF has a W-reflectron and can be operated in V-mode or in W-mode. Only the V-mode is used in this paper; the effective flight path is ~1.5 m.

The ion detector is an eight-anode MCP (Ionwerks, Houston, TX) that has post acceleration voltage of ~6000 V. The signal is amplified ×100 by two four-channel preamplifiers (XCD quad amplifier/discriminator, Ionwerks, Houston, TX) and then sent to an 8 channel time-to-digital converter (TDC×8, Ionwerks, Houston, TX). The TOF software

www.manaraa.com

reads the data from the TDC to create 2D data that contain both drift time and mass spectral information.

The timing of the TOF data acquisition is similar to methods described previously [8, 16]. As shown by the bottom three traces in Figure 3, the TOF timing controller gets signals from the software and an external trigger and sends TTL triggers to the TDC×8 and to the TOF pulser. The mobility acquisition is started by the ion injection pulse (a trigger from the Argos), after which the TOF timing controller starts sending TTL triggers—at specific intervals depending on the mass range being acquired—simultaneously to the TDC×8 and the TOF extraction lenses. In a typical experiment 100 mass spectra are taken within each 10 ms mobility spectrum, up to a maximum m/z value of 2400. Mass spectra could be measured to higher m/z values, but there would be fewer such mass spectra over the duration of the IM peaks.

Measurement of Cross Sections. Ion cross-sections can be determined from the IM drift times [59]:

$$\Omega = \frac{(18\pi)^{1/2}}{16}\frac{ze}{(k_b T)^{1/2}}\left[\frac{1}{m_i}+\frac{1}{m_b}\right]^{1/2}\frac{1}{N}\frac{t_D E}{L}\frac{760}{P}\frac{T}{273.2} \qquad (1)$$

where z is the charge state of ions, m_i is the mass of ions, m_b is the mass of the buffer gas, E is the electric field through the drift tube, L is the length of the drift tube, t_D is the flight time through the drift tube, P is the pressure of the buffer gas, N is the number density of the collision gas and T is the temperature of the buffer gas.

www.manaraa.com

The instrument provides the time between the ejection pulse from the IT and the start pulse of the TOF. For Eqn. 1, the measured t_D value should be only the time spent inside the drift tube. Therefore, the ion flight times between the drift tube and TOF source region (i.e., through the quadrupole and the ion lenses just to the left of it in Figure 1) are calculated from the lens dimensions and applied voltages and subtracted from the total time between IT and TOF source. The calculated times through the lenses and quadrupole range from 127 μs for ubiquitin +8 to 360 μs for ubiquitin +1, i.e., the ions with the shortest and longest drift times. About 70% of this time is spent inside the quadrupole collision cell.

Many experimental parameters pertaining to the drift tube and ion funnel (e.g., axial electric field, injection pulser voltage, rf voltage on the ion funnel, etc.) were varied. Under the experimental conditions used in this work, none affected the numerical values of the measured cross sections, confirming that the ion mobility measurement is in the low field regime. The combination of four parameters did influence the number of mobility peaks observed and their relative abundances: the voltage on the first electrode of the drift cell, the pressure in the drift cell, and the duration and magnitude of the voltage pulse used to eject ions from the IT. These effects are described below.

Results and Discussion

IM-TOFMS after Ion/Ion Reactions. In early research on proton transfer reactions with IM, a basic neutral gas was introduced into the source region to create lower charge state ions through an in-source proton transfer reaction [20, 60]. In the present instrument, the total reaction time and reagent ion identity can be controlled. The experimental timing

www.manaraa.com

diagram (Figure 3) is similar to those previously shown for ion/ion reactions [38], except the usual IT mass analysis step is replaced by injection of product ions into the IM drift tube. The experiment scan function shown in Figure 3 includes acquisition of nested drift (flight) time mobility data.

These capabilities are illustrated using charge reduction reactions of multiply charged ubiquitin ions with PDCH anions. The reagent anions are mainly $[M\text{-}F^{\cdot}]^-$ and $[M\text{-}CF_3^{\cdot}]^-$ ions, as seen from a similar ASGDI source in McLuckey's group [61] and another paper recently published from our group [62]. The signal ratio $[M\text{-}F]^-$/ $[M\text{-}CF_3]^-$ is approximately 1.5 in the present device.

For a typical ion/ion reaction-IM experiment, ubiquitin ions are injected for 50 to 100 ms, $PDCH^-$ ions are injected for 5 to 50 ms, and both polarity ions are trapped in the IT to react for 20 to 150 ms, depending on the product ion charge states desired. An extraction pulse (-100 V for 3 to 10 µs) is then applied to the back end cap of the ion trap to inject ions into the drift tube. For the IM separation the He pressure in the drift tube is 1.4 mbar, and the electric field applied is 12.4 V/cm across the drift cell, with various injection voltages.

Figure 4a shows a 3D mobility-m/z spectrum of ubiquitin before proton transfer reactions. The main charge state observed for ubiquitin under these solution and source conditions is +7 with a small but measurable amount of +8. The mass resolution shown is $m/\Delta m = 1000$ at m/z 1224.6. Mass accuracies are within 28 ppm, using cytochrome *c* +8 and +9 ions as external calibrants.

Figure 4b, c and d show spectra after ion/ion charge reduction reaction of ubiquitin with PDCH. Ubiquitin +8 and +7 ions are converted to lower charge states than those

www.manaraa.com

produced directly by ESI, using longer fill and reaction times. The ions in lower charge states are better resolved in the IM dimension. Previous attempts at analysis of protein mixtures by CID after IM separation suffered because protein ions in high charge states were not resolved in the mobility separation [63]. Thus, mobility labeling for proteins is not as useful as for peptides. Ion/ion reaction combined with IM separations provides a new technique to make mobility labeling (for on-the-fly MS/MS) possible for top-down analysis of intact proteins. The capability to effectively fragment proteins behind the drift tube, especially at these lower charge states, is still under development.

Cross-section measurements for ubiquitin ions using three injection voltages are depicted in Figure 5. Numerical cross section values from the plots in Figure 5 are listed in Table 1, and conditions and scale values are given in Table 2. IM spectra and the resulting cross sections obtained at higher injection voltages do not differ appreciably from those measured at -50 V and are not shown.

First, consider the +8 and +7 ions, which come directly from the ESI source. The +8 ions are unfolded at all injection voltages, while the +7 ions are observed in up to three IM peaks, as noted above. The +6 to +1 ions come from proton transfer reaction, mainly with the +7 ubiquitin ions originally present. Reducing the charge state converts the ubiquitin ions to more compact conformers. For ions in the lower charge states, the single IM peak gets narrower as charge state is reduced. For ubiquitin +1, the FWHM of the ion mobility peak (~500 μs) is still wider than the FWHM of the diffusion limited peak (~175 μs) by a factor of about three. Thus, we suggest that the single IM peak is comprised of contributions

www.manaraa.com

from several unresolved conformers [64], and fewer such conformers are present at lower charge states.

Numerical data for cross sections are given in Table 1. Multiple entries indicate values from several discernable peaks in the IM spectra (Figure 5). The ions in low charge states have essentially a single value of cross section corresponding to folded conformer(s) of ubiquitin, even though the original ubiquitin +7 ions have a variety of conformations before the ion/ion reaction. In general, the measured cross-sections of +8 to +4 ubiquitin ions are in the range of the literature values [20]. This is the first report of cross-sections for ubiquitin +3, +2 and +1 ions.

Effects of Injection Conditions on Folding of Ubiquitin Ions. Clemmer's group [20] studied how injection energy influences mobility spectra of ubiquitin ions and the apparent number and relative abundance of protein conformers. At lower injection energy (385 eV), different conformers were observed and the distributions were expected to reflect the distribution of conformers from the ion source [20].

Similar effects were seen in the present work for ubiquitin ions in certain charge states, as shown in Figure 5, which includes results at lower injection voltages than those reported by Clemmer. The relative abundances of various peaks in the IM spectra do not change further as injection voltage is raised above 50 V (data from -60 V to -150 V are not shown). Briefly, Figure 5 shows that +8 ions remain unfolded, and +5 to +1 ions remain folded, regardless of injection voltage. For the intermediate charge states +6 and +7, lower

www.manaraa.com

injection voltage generally favors formation of more folded conformers. More open conformers are also less abundant at lower pressure inside the drift tube (data not shown).

Similar effects are seen for cytochrome c +8 ions. In general, these observations are consistent with ions being heated and unfolded initially by collisions in the short space (1.3 cm) between the trap exit and drift tube. Ions in intermediate charge states have various folded states accessible and may refold when further collisions cool the ions, either during extraction or inside the drift tube. Differential scattering of larger ions outside the acceptance of the small entrance aperture (0.5 mm diam.) of the drift tube may also contribute to these observations.

The duration and magnitude of the negative voltage pulse applied to eject ions from the IT can also affect the number of peaks in the IM spectra for the +7 ions, i.e., those ions that are prone to folding changes. Such effects are most pronounced if the ejection pulse is more negative than the voltage on the entrance to the drift tube. Figure 6 depicts an extreme example; the ejection pulse amplitude is -100 V, and the drift tube entrance is at -30 V. Ubiquitin +7 ions are mostly folded using the shortest ejction pulse (1 μs). A variety of conformers are seen at 3 μs, while the ions are unfolded when the ejection pulse lasts for 5 and 7 μs. Curiously, the ions fold if the ejection pulse is extended further to 9 and 10 μs.

We have not found descriptions of effects quite like those shown in Figure 6 in previous literature involving injection of ions into IM drift tubes. The fundamental reasons why the apparent number of IM peaks should be so sensitive to the duration of the ion ejection pulse are not clear. A long ion ejection pulse is of use mainly because it improves signals for ions in low charge states, as if ~ 10 μs are required to draw the less highly charged

www.manaraa.com

ions out of the trap. Fortunately, the ions in low charge states remain folded anyway, and a long extraction pulse is generally not needed for the ions in the intermediate charge states that are more susceptible to folding changes. Use of an extraction pulse that is less negative than the entrance to the drift tube also reduces the magnitude of these folding changes.

Badman [65] and Myung et al. [50] observed that the folding and unfolding of cytochrome c and ubiquitin ions in intermediate charge states occurred in hundreds of milliseconds in a 3-D ion trap. In the present work, changing the duration of the extraction pulse from 1 μs to 10 μs can affect the observed conformations, so folding and unfolding events apparently can occur on the microsecond time scale [52].

The charge states where folding changes are expected probably vary between proteins, so these effects should be evaluated on a case-by case basis. So far, ions in the higher and lower charge states are less prone to these folding changes. Even for these charge states, there may still be subtle changes in the distributions of closely-related conformers hidden by the relatively low IM resolution in our experiments, compared to the much narrower peaks seen in Clemmer's tandem IM work [66, 67].

CID on Intact Proteins followed by Charge Reduction. This instrument also has potential value for top-down proteomics measurements, as indicated by the following example. Figure 7a shows a spectrum obtained after isolating only the +7 charge state of ubiquitin in the ion trap. Mass selection was performed by applying a 30 kHz 12 V_{p-p} AC waveform to the front endcap of the ion trap to resonantly eject lower mass ions during an RF ramp and then a 20 kHz 10 V_{p-p} AC waveform to eject higher mass ions during another

www.manaraa.com

RF ramp [38]. These ions were stored in the ion trap for 20 ms and activated for 100 ms at 50 kHz, 23 Vp-p. The fragment spectrum (Figure 7b) shows CID product ions in a variety of relatively high charge states that are only moderately resolved in the IM dimension. Thus, it is not easy to assign them at first.

Figure 7c shows the spectrum resulting from charge reduction of the fragment ions in the ion trap with PDCH anions (injection for 20 ms, reaction for 100 ms). The spectrum shifts to higher m/z, and the dispersion in the IM dimension is greatly improved. Many of the charge-reduced CID fragments can now be assigned by comparing the observed m/z values with that of fragments generated from the known sequence of ubiquitin. The mass tolerance for these assignments is 0.6 Th. The assumption that the fragment ions in Figure 7c are in low charge states greatly simplifies these assignments. Most of the fragments observed here are b and y ions, and b_{18} and y_{58} are the most abundant fragments, in agreement with those found in other studies [38, 68].

The IM plot for the charge-reduced fragments (Figure 7c) shows distinct groups that fall along slanted lines of different slopes for peptide fragment ions in +1, +2 and +3 charge states, as noted by Clemmer and co-workers. This phenomenon provides additional evidence to help assign charge states. These groups merge closer together at higher charge states [17], which is one reason they are poorly resolved in Figure 7b.

Armed with the identities of the charge-reduced fragments (Figure 7c), many of the original, more highly charged fragments in Figure 7b can now be assigned. For example, y_{58}^{2+} is in the charge-reduced spectrum. Thus, a more highly charged version (y_{58}^{5+} in this case) should appear in the original CID spectrum (Figure 7b), along with complementary b_{18}

www.manaraa.com

ions. Here we assume that the peptide fragment ions do not dissociate further during the charge reduction reactions, as shown by McLuckey [31] . A number of other, similar cases are identified in Figure 7b.

Conclusion

This is the first instrument that combines ion/ion reactions and IM separations with full computer control of all functions. It should prove useful for study of the effects of protein charge state on conformation, which is key to the general question of the relation between gas-phase conformation and that in solution [69, 70] . Other types of ion/ion reactions, such as ETD, formation of protein-metal, protein-ligand and protein-protein complexes, should also be possible, with the added benefit of the ability to also manipulate charge state. Finally, manipulation of charge state of CID products facilitates high throughput top-down protein analysis. A number of improvements in the instrumentation, such as use of a linear ion trap instead of the 3D ion trap, CID at higher energy, CID of mobility-selected ions using the quadrupole collision cell, and multiple reflections in the TOF-MS for higher resolution, are under investigation in our laboratory. Also, a more detailed study of conformation changes in the μs time scale between the ion trap and the drift tube may prove interesting in its own right.

Acknowledgements

The authors acknowledge helpful discussions with Steve Valentine (Indiana Univ.); Scott McLuckey for the design of high-voltage switches; Brent Knecht, Garth Patterson,

www.manaraa.com

Brent Rardin, and Mitch Wells (Griffin Analytical) for assistance with the Argos and software; David Prior (Pacific Northwest National Lab) for design of the IT rf amplifier; and Randy Pedder (Ardara Technologies, North Huntingdon, PA) for advice on use of the rf supply for the ion funnel. Other custom electronics were designed and constructed by Lee Harker (Ames Lab Engineering Services Group); vacuum welding by Charlie Burg (Ames Lab); precision machining by Richard Egger, the late Steve Lee, and Terry Soseman (ISU Chemistry Machine Shop). Derrick Morast analyzed the ubiquitin sample with another ESI instrument to evaluate its purity. ERB acknowledges funding from Waters Corp. via an ASMS Research Award. Funding from Iowa State University: College of Liberal Arts and Sciences, Office of Biotechnology, Plant Sciences Institute, and the Carver Trust are gratefully acknowledged.

www.manaraa.com

References

1. Pandey, A.; Mann, M. Proteomics to Study Genes and Genomes *Nature* **2000**, *405*, 837-846
2. Loo, J. A.; Berhane, B.; Kaddis, C. S.; Wooding, K. M.; Xie, Y. M.; Kaufman, S. L.; Chernushevich, I. V. Electrospray Ionization Mass Spectrometry and Ion Mobility Analysis of the 20s Proteasome Complex *Journal of the American Society for Mass Spectrometry* **2005**, *16*, 998-1008
3. Sobott, F.; McCammon, M. G.; Hernandez, H.; Robinson, C. V. The Flight of Macromolecular Complexes in a Mass Spectrometer *Philosophical Transactions of the Royal Society of London Series a-Mathematical Physical and Engineering Sciences* **2005**, *363*, 379-389
4. St. Louis, R. H.; Hill, H. H. Ion Mobility Spectrometry in Analytical Chemistry *Critical Reviews in Analytical Chemistry* **1990**, *21*, 321-355
5. Collins, D. C.; Lee, M. L. Developments in Ion Mobility Spectrometry-Mass Spectrometry *Analytical and Bioanalytical Chemistry* **2002**, *372*, 66-73
6. Brian C. B.; Merenbloom, S. I.; Koeniger S. L.; Hilderbrand A. E.; Clemmer, D. E. Biomolecule Analysis by Ion Mobility Spectrometry *Annual Review of Analytical Chemistry* **2008**, *Vol. 1*, 293-327
7. Jarrold, M. F. Peptides and Proteins in the Vapor Phase *Annual Review of Physical Chemistry* **2000**, *51*, 179-207
8. Hoaglund, C. S.; Valentine, S. J.; Sporleder, C. R.; Reilly, J. P.; Clemmer, D. E. Three-Dimensional Ion Mobility Tofms Analysis of Electrosprayed Biomolecules *Analytical Chemistry* **1998**, *70*, 2236-2242
9. Stone, E.; Gillig, K. J.; Ruotolo, B.; Fuhrer, K.; Gonin, M.; Schultz, A.; Russell, D. H. Surface-Induced Dissociation on a MALDI -Ion Mobility-Orthogonal Time-of-Flight Mass Spectrometer: Sequencing Peptides from an "in-Solution" Protein Digest *Analytical Chemistry* **2001**, *73*, 2233-2238
10. Stone, E. G.; Gillig, K. J.; Ruotolo, B. T.; Russell, D. H. Optimization of a Matrix-Assisted Laser Desorption Ionization-Ion Mobility-Surface-Induced Dissociation-Orthogonal-Time-of-Flight Mass Spectrometer: Simultaneous Acquisition of Multiple Correlated Ms1 and Ms2 Spectra *International Journal of Mass Spectrometry* **2001**, *212*, 519-533
11. Steiner, W. E.; Clowers, B. H.; Fuhrer, K.; Gonin, M.; Matz, L. M.; Siems, W. F.; Schultz, A. J.; Hill, H. H. Electrospray Ionization with Ambient Pressure Ion Mobility Separation and Mass Analysis by Orthogonal Time-of-Flight Mass Spectrometry *Rapid Communications in Mass Spectrometry* **2001**, *15*, 2221-2226
12. Steiner, W. E.; Clowers, B. H.; English, W. A.; Hill, H. H. Atmospheric Pressure Matrix-Assisted Laser Desorption/Ionization with Analysis by Ion Mobility Time-of-Flight Mass Spectrometry *Rapid Communications in Mass Spectrometry* **2004**, *18*, 882-888
13. Smith, D. P.; Giles, K.; Bateman, R. H.; Radford, S. E.; Ashcroft, A. E. Monitoring Copopulated Conformational States During Protein Folding Events Using

www.manaraa.com

Electrospray Ionization-Ion Mobility Spectrometry-Mass Spectrometry *Journal of the American Society for Mass Spectrometry* **2007**, *18*, 2180-2190
14. Hoaglund-Hyzer, C. S.; Li, J. W.; Clemmer, D. E. Mobility Labeling for Parallel CID of Ion Mixtures *Analytical Chemistry* **2000**, *72*, 2737-2740
15. Hoaglund-Hyzer, C. S.; Clemmer, D. E. Ion Trap/Ion Mobility/Quadrupole/Time of Flight Mass Spectrometry for Peptide Mixture Analysis *Analytical Chemistry* **2001**, *73*, 177-184
16. Henderson, S. C., Valentine, S. J., Counterman, A. E., and Clemmer, D. E. ESI/Ion Trap/Ion Mobility/Time-of-Flight Mass Spectrometry for Rapid and Sensitive Analysis of Biomolecular Mixtures *Analytical Chemistry* **1999**, *71*, 291-301
17. Myung, S.; Lee, Y. J.; Moon, M. H.; Taraszka, J.; Sowell, R.; Koeniger, S.; Hilderbrand, A. E.; Valentine, S. J.; Cherbas, L.; Cherbas, P.; Kaufmann, T. C.; Miller, D. F.; Mechref, Y.; Novotny, M. V.; Ewing, M. A.; Sporleder, C. R.; Clemmer, D. E. Development of High-Sensitivity Ion Trap Ion Mobility Spectrometry Time-of-Flight Techniques: A High-Throughput Nano-LC-IMS-TOF Separation of Peptides Arising from a Drosophila Protein Extract *Analytical Chemistry* **2003**, *75*, 5137-5145
18. Badman, E. R.; Myung, S.; Clemmer, D. E. Gas-Phase Separations of Protein and Peptide Ion Fragments Generated by Collision-Induced Dissociation in an Ion Trap *Analytical Chemistry* **2002**, *74*, 4889-4894
19. Green, M. K.; Lebrilla, C. B. Ion-Molecule Reactions as Probes of Gas-Phase Structures of Peptides and Proteins *Mass Spectrometry Reviews* **1997**, *16*, 53-71
20. Valentine, S. J., Counterman, A. E., Clemmer, D. E. Conformer-Dependent Proton-Transfer Reactions of Ubiquitin Ions *Journal of the American Society for Mass Spectrometry* **1997**, *8*, 954-961
21. Valentine, S. J.; Anderson, J. G.; Ellington, A. D.; Clemmer, D. E. Disulfide-Intact and -Reduced Lysozyme in the Gas Phase: Conformations and Pathways of Folding and Unfolding *Journal of Physical Chemistry B* **1997**, *101*, 3891-3900
22. Valentine, S. J.; Clemmer, D. E. H/D Exchange Levels of Shape-Resolved Cytochrome c Conformers in the Gas Phase *Journal of the American Chemical Society* **1997**, *119*, 3558-3566
23. Woenckhaus, J.; Mao, Y.; Jarrold, M. F. Hydration of Gas Phase Proteins: Folded +5 and Unfolded +7 Charge States of Cytochrome c *Journal of Physical Chemistry B* **1997**, *101*, 847-851
24. Fye, J. L.; Woenckhaus, J.; Jarrold, M. F. Hydration of Folded and Unfolded Gas-Phase Proteins: Saturation of Cytochrome c and Apomyoglobin *Journal of the American Chemical Society* **1998**, *120*, 1327-1328
25. Woenckhaus, J. Drift Time Mass Spectrometric Protein Hydration Experiments *International Journal of Mass Spectrometry* **2002**, *213*, 9-24
26. Wyttenbach, T.; Liu, D. F.; Bowers, M. T. Hydration of Small Peptides *International Journal of Mass Spectrometry* **2005**, *240*, 221-232
27. Loo, R. R. O.; Udseth, H. R.; Smith, R. D. Evidence of Charge Inversion in the Reaction of Singly Charged Anions with Multiply Charged Macroions *Journal of Physical Chemistry* **1991**, *95*, 6412-6415

www.manaraa.com

28. Loo, R. R. O.; Udseth, H. R.; Smith, R. D. A New Approach for the Study of Gas-Phase Ion-Ion Reactions Using Electrospray Ionization *Journal of the American Society for Mass Spectrometry* **1992**, *3*, 695-705
29. Pitteri, S. J.; McLuckey, S. A. Recent Developments in the Ion/Ion Chemistry of High-Mass Multiply Charged Ions *Mass Spectrometry Reviews* **2005**, *24*, 931-958
30. Stephenson, J. L.; McLuckey, S. A. Ion/Ion Proton Transfer Reactions for Protein Mixture Analysis *Analytical Chemistry* **1996**, *68*, 4026-4032
31. Stephenson, J. L., McLuckey, S. A. Simplification of Product Ion Spectra Derived from Multiply Charged Parent Ions Via Ion/Ion Chemistry *Analytical Chemistry* **1998**, *70*, 3533-3544
32. McLuckey, S. A.; Reid, G. E.; Wells, J. M. Ion Parking During Ion/Ion Reactions in Electrodynamic Ion Traps *Analytical Chemistry* **2002**, *74*, 336-346
33. Syka, J. E. P., Coon, J. J., Schroeder, M. J., Shabanowitz, J., and Hunt, D. F. Peptide and Protein Sequence Analysis by Electron Transfer Dissociation Mass Spectrometry *Proceedings of the National Academy of Sciences of the United States of America* **2004**, *101*, 9528-9533
34. Stephenson, J. L.; McLuckey, S. A. Adaptation of the Paul Trap for Study of the Reaction of Multiply Charged Cations with Singly Charged Anions *International Journal of Mass Spectrometry and Ion Processes* **1997**, *162*, 89-106
35. Reid, G. E.; Wells, J. M.; Badman, E. R.; McLuckey, S. A. Performance of a Quadrupole Ion Trap Mass Spectrometer Adapted for Ion/Ion Reaction Studies *International Journal of Mass Spectrometry* **2003**, *222*, 243-258
36. Wu, J.; Hager, J. W.; Xia, Y.; Londry, F. A.; McLuckey, S. A. Positive Ion Transmission Mode Ion/Ion Reactions in a Hybrid Linear Ion Trap *Analytical Chemistry* **2004**, *76*, 5006-5015
37. Xia, Y.; Liang, X. R.; McLuckey, S. A. Pulsed Dual Electrospray Ionization for Ion/Ion Reactions *Journal of the American Society for Mass Spectrometry* **2005**, *16*, 1750-1756
38. Badman, E. R., Chrisman, P. A., and McLuckey, S. A. A Quadrupole Ion Trap Mass Spectrometer with Three Independent Ion Sources for the Study of Gas-Phase Ion/Ion Reactions *Analytical Chemistry* **2002**, *74*, 6237-6243
39. Liang, X. R.; Xia, Y.; McLuckey, S. A. Alternately Pulsed Nanoelectrospray Ionization/Atmospheric Pressure Chemical Ionization for Ion/Ion Reactions in an Electrodynamic Ion Trap *Analytical Chemistry* **2006**, *78*, 3208-3212
40. Liang, X. R.; Han, H. L.; Xia, Y.; McLuckey, S. A. A Pulsed Triple Ionization Source for Sequential Ion/Ion Reactions in an Electrodynamic Ion Trap *Journal of the American Society for Mass Spectrometry* **2007**, *18*, 369-376
41. Pitteri, S. J., Chrisman, P. A., Hogan, J. M., McLuckey, S. A. Electron Transfer Ion/Ion Reactions in a Three-Dimensional Quadrupole Ion Trap: Reactions of Doubly and Triply Protonated Peptides with SO_2 Center Dot *Analytical Chemistry* **2005**, *77*, 1831-1839
42. Chrisman, P. A., Pitteri, S. J., Hogan, J. M., McLuckey, S. A. SO_2^- Electron Transfer Ion/Ion Reactions with Disulfide Linked Polypeptide Ions *Journal of the American Society for Mass Spectrometry* **2005**, *16*, 1020-1030

www.manaraa.com

43. Han, H., Xia, Y., Yang, M., and McLuckey, S. A. Rapidly Alternating Transmission Mode Electron-Transfer Dissociation and Collisional Activation for the Characterization of Polypeptide Ions *Analytical Chemistry* **2008**, *80*, 3492-3497
44. Xia, Y.; Han, H.; McLuckey, S. A. Activation of Intact Electron-Transfer Products of Polypeptides and Proteins in Cation Transmission Mode Ion/Ion Reactions *Analytical Chemistry* **2008**, *80*, 1111-1117
45. McAlister, G. C., Berggren, W. T., Griep-Raming, J., Horning, S., Makarov, A., Phanstiel, D., Stafford, G., Swaney, D. L., Syka, J. E. P., Zabrouskov, V., and Coon, J. J. A Proteomics Grade Electron Transfer Dissociation-Enabled Hybrid Linear Ion Trap-Orbitrap Mass Spectrometer *Journal of Proteome Research* **2008**, *7*, 3127-3136
46. Phanstiel, D.; Zhang, Y.; Marto, J. A.; Coon, J. J. Peptide and Protein Quantification Using iTRAQ with Electron Transfer Dissociation *Journal of the American Society for Mass Spectrometry* **2008**, *19*, 1255-1262
47. Li, J. W.; Taraszka, J. A.; Counterman, A. E.; Clemmer, D. E. Influence of Solvent Composition and Capillary Temperature on the Conformations of Electrosprayed Ions: Unfolding of Compact Ubiquitin Conformers from Pseudonative and Denatured Solutions *International Journal of Mass Spectrometry* **1999**, *187*, 37-47
48. Koeniger, S. L.; Clemmer, D. E. Resolution and Structural Transitions of Elongated States of Ubiquitin *Journal of the American Society for Mass Spectrometry* **2007**, *18*, 322-331
49. Koeniger, S. L.; Merenbloom, S. I.; Sevugarajan, S.; Clemmer, D. E. Transfer of Structural Elements from Compact to Extended States in Unsolvated Ubiquitin *Journal of the American Chemical Society* **2006**, *128*, 11713-11719
50. Myung, S., Badman, E. R., Lee, Y. J., Clemmer, D. E. Structural Transitions of Electrosprayed Ubiquitin Ions Stored in an Ion Trap over Similar to 10 Ms to 30 S *Journal of Physical Chemistry A* **2002**, *106*, 9976-9982
51. Segev, E., Wyttenbach, T., Bowers, M. T., and Gerber, R. B. Conformational Evolution of Ubiquitin Ions in Electrospray Mass Spectrometry: Molecular Dynamics Simulations at Gradually Increasing Temperatures *Physical Chemistry Chemical Physics* **2008**, *10*, 3077-3082
52. Shvartsburg, A. A.; Li, F. M.; Tang, K. Q.; Smith, R. D. Distortion of Ion Structures by Field Asymmetric Waveform Ion Mobility Spectrometry *Analytical Chemistry* **2007**, *79*, 1523-1528
53. Shvartsburg, A. A.; Li, F. M.; Tang, K. Q.; Smith, R. D. Characterizing the Structures and Folding of Free Proteins Using 2-D Gas-Phase Separations: Observation of Multiple Unfolded Conformers *Analytical Chemistry* **2006**, *78*, 3304-3315
54. McLuckey, S. A.; Glish, G. L.; Asano, K. G.; Grant, B. C. Atmospheric Sampling Glow-Discharge Ionization Source for the Determination of Trace Organic-Compounds in Ambient Air *Analytical Chemistry* **1988**, *60*, 2220-2227
55. Valentine, S. J.; Koeniger, S. L.; Clemmer, D. E. A Split-Field Drift Tube for Separation and Efficient Fragmentation of Biomolecular Ions *Analytical Chemistry* **2003**, *75*, 6202-6208

www.manaraa.com

56. Him, T.; Tolmachev, A. V.; Harkewicz, R.; Prior, D. C.; Anderson, G.; Udseth, H. R.; Smith, R. D.; Bailey, T. H.; Rakov, S.; Futrell, J. H. Design and Implementation of a New Electrodynamic Ion Funnel *Analytical Chemistry* **2000**, *72*, 2247-2255
57. Tang, K.; Shvartsburg, A. A.; Lee, H. N.; Prior, D. C.; Buschbach, M. A.; Li, F. M.; Tolmachev, A. V.; Anderson, G. A.; Smith, R. D. High-Sensitivity Ion Mobility Spectrometry/Mass Spectrometry Using Electrodynamic Ion Funnel Interfaces *Analytical Chemistry* **2005**, *77*, 3330-3339
58. Julian, R. R.; Mabbett, S. R.; Jarrold, M. F. Ion Funnels for the Masses: Experiments and Simulations with a Simplified Ion Funnel *Journal of the American Society for Mass Spectrometry* **2005**, *16*, 1708-1712
59. Clemmer, D. E., Jarrold, M. F. Ion Mobility Measurements and Their Applications to Clusters and Biomolecules *Journal of Mass Spectrometry* **1997**, *32*, 577-592
60. Loo, R. R. O.; Winger, B. E.; Smith, R. D. Proton Transfer Reaction Studies of Multiply Charged Proteins in a High Mass-to-Charge Ratio Quadrupole Mass Spectrometer *Journal of the American Society for Mass Spectrometry* **1994**, *5*, 1064-1071
61. Stephenson, J. L., McLuckey, S. A. Ion/Ion Reactions in the Gas Phase: Proton Transfer Reactions Involving Multiply-Charged Proteins *Journal of the American Chemical Society* **1996**, *118*, 7390-7397
62. Soyk, M. W.; Zhao, Q.; Houk R.S. ; Badman, E. R. A Linear Ion Trap Mass Spectrometer with Versatile Control and Data Acquisition for Ion/Ion Reactions *Journal of American Society for Mass Spectrometry* **2008**, *in press*
63. Badman, E. R., Hoaglund-Hyzer, C. S., Clemmer, D. E. Dissociation of Different Conformations of Ubiquitin Ions *Journal of the American Society for Mass Spectrometry* **2002**, *13*, 719-723
64. Koeniger, S. L., Merenbloom, S. I., Sevugarajan, S., Clemmer D. E., Hudgins, R. R., Jamold, M. F. Transfer of Structural Elements from Compact to Extended States in Unsolvated Ubiquitin *Journal of American Chemical Society* **2006**, *128*, 11713-11719
65. Badman, E. R., Hoaglund-Hyzer, C. S., Clemmer, D. E. Monitoring Structural Changes of Proteins in an Ion Trap over ~10 to 200 Ms: Unfolding Transitions in Cytochrome c Ions *Analytical Chemistry* **2001**, *73*, 6000-6007
66. Koeniger, S. L., Merenbloom, S. I., Valentine, S. J., Jarrold, M. F., Udseth, H. R., Smith, R. D., and Clemmer, D. E. An IMS-IMS Analogue of MS-MS *Analytical Chemistry* **2006**, *78*, 4161-4174
67. Merenbloom, S. I., Koeniger, S. L., Valentine, S. J., Plasencia, M. D., and Clemmer, D. E. IMS-IMS and IMS-IMS-IMS/MS for Separating Peptide and Protein Fragment Ions *Analytical Chemistry* **2006**, *78*, 2802-2809
68. Xia, Y.; Liang, X. R.; McLuckey, S. A. Ion Trap versus Low-Energy Beam-Type Collision-Induced Dissociation of Protonated Ubiquitin Ions *Analytical Chemistry* **2006**, *78*, 1218-1227
69. Breuker, K., McLafferty, F. W. The Thermal Unfolding of Native Cytochrome c in the Transition from Sollution to Gas Phase Probed by Native Electron Capture Dissociation *Angrew Chem. Int. Ed.* **2005**, *44*, 4911-4914

www.manaraa.com

70. Breuker, K., and McLafferty, F. W. Native Electron Capture Dissociation for the Structural Characterization of Noncovalent Interactions in Native Cytochrome c *Angewandte Chemie-International Edition* **2003**, *42*, 4900-4904

www.manaraa.com

Table 1. Measured cross-sections for ubiquitin ions in different charge states. +7 and +8 ions are from the ESI source, ions with charge states +6 to +1 are made from mostly +7 ions by ion/ion reaction. See text for conditions. The cross-sections are determined from the apex of the various mobility peaks (Figure 5) according to Equation 1.

Charge	Cross-Section ($Å^2$) at Indicated Injection Voltage			
state	0 V	-30 V	-50 V	-100 V
+8	1428	1430	1430	428
+7	1393	1394	1394	1393
+6	863,1056,1314	863,1056, 1314	1314	1312
+5	872, 979	979	1033	1031
+4	904	861	904	902
+3	855	813	814	814
+2	854	856	857	857
+1	882	861	882	861

www.manaraa.com

Table 2. Reaction conditions and vertical scale values for cross-section plots in Figure 5. Other conditions: ubiquitin fill time 50 ms, extraction pulse from ion trap -100 V for 5 μs except for +1 ions, which were pulsed out for 10 μs at -150 V.

	Time Values (ms)		Full-Scale Signal (counts/s)		
Charge	PDCH		At Indicated Injection Voltage		
State	Fill	Reaction	0 V	-30 V	-50 V
+8*		60*	38	137	83
+7*		60*	189	546	380
+6	20	60	33	154	116
+5	20	60	136	522	373
+4	20	60	26	191	81
+3	45	150	258	642	873
+2	45	150	350	182	114
+1	50	180	18	320	159

*These ions were observed directly from the ESI source without ion/ion reaction. To keep the total trapping time constant without inducing ion/ion reactions, the ASGDI source was turned off while these ions were measured.

www.manaraa.com

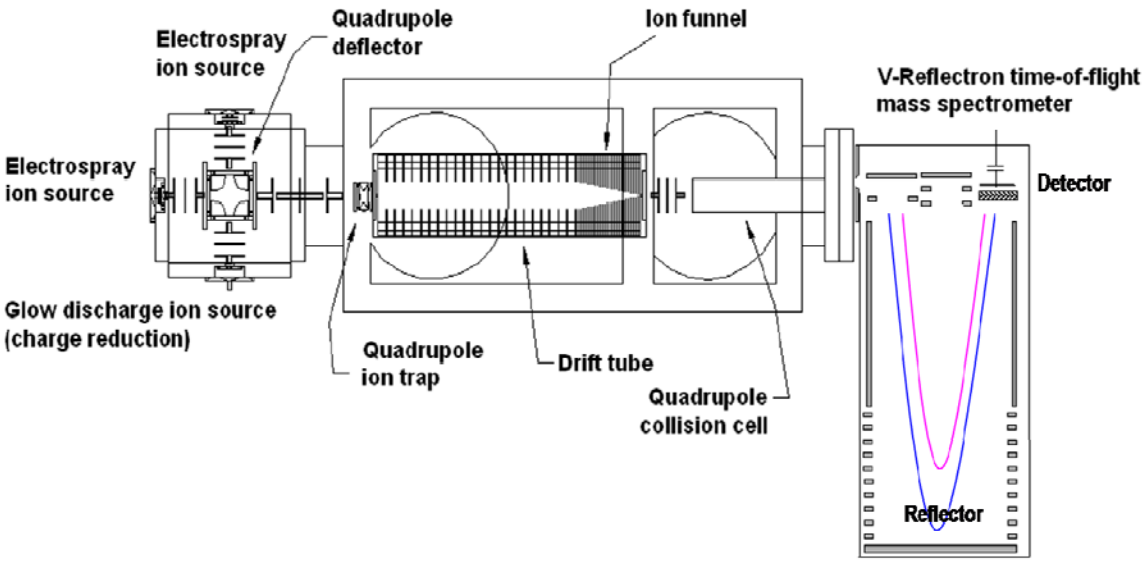

Figure 1. Scale diagram showing overall instrument, including two ESI and one ASGDI sources, ion optics, quadrupole deflector, IT, IM drift tube with ion funnel and q-TOF.

www.manaraa.com

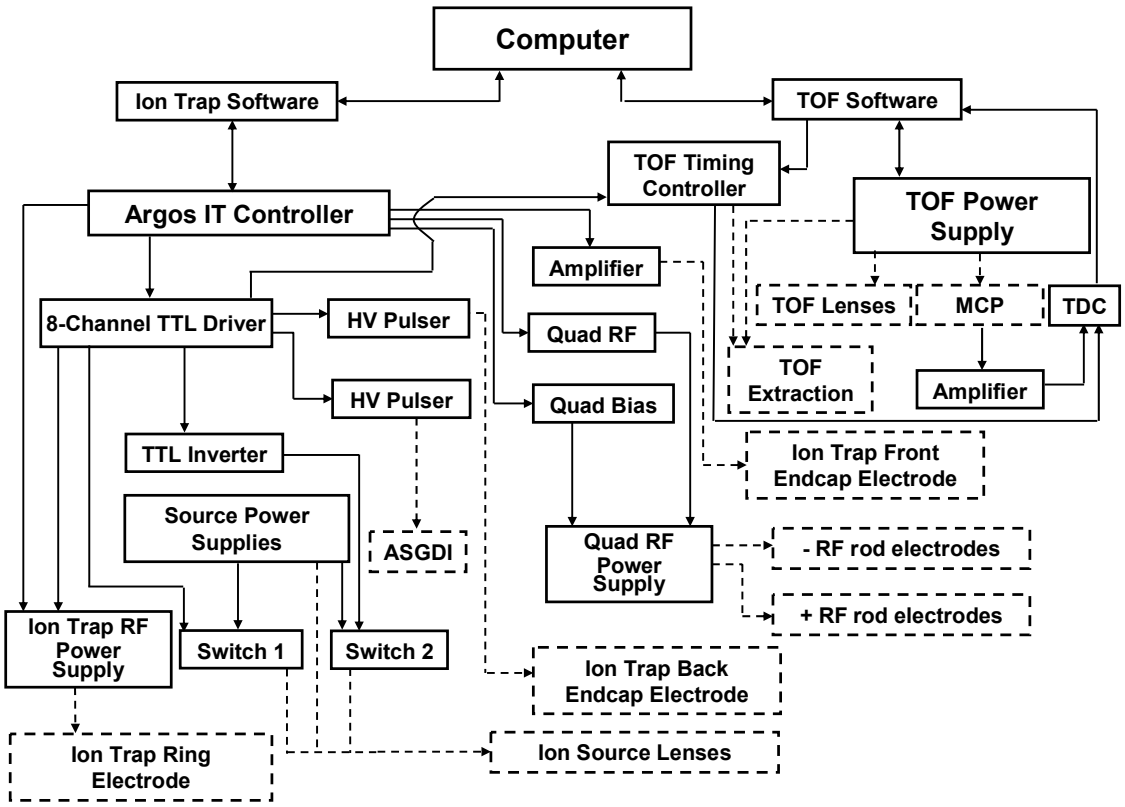

Figure 2. Electronics block diagram (see text for details). The solid lines indicate instrument control electronics, and the dashed lines indicate hardware in the vacuum chamber.

www.manaraa.com

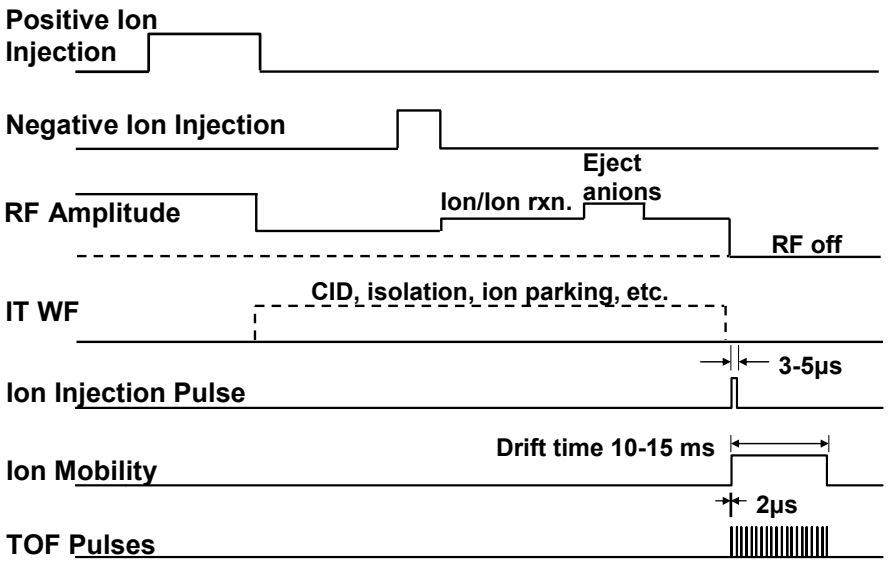

Figure 3: A generic scan function for an ion/ion reaction followed by nested flight time/ion mobility experiment. The top and second plots show the time during which positive and negative ions are injected. The third plot shows the amplitude of the rf trapping voltage applied to the ring electrode of the ion trap. The lower three plots show the times when ions after ion/ion reaction are injected into the drift tube, ion mobility data acquisition and TOF extraction pulses.

www.manaraa.com

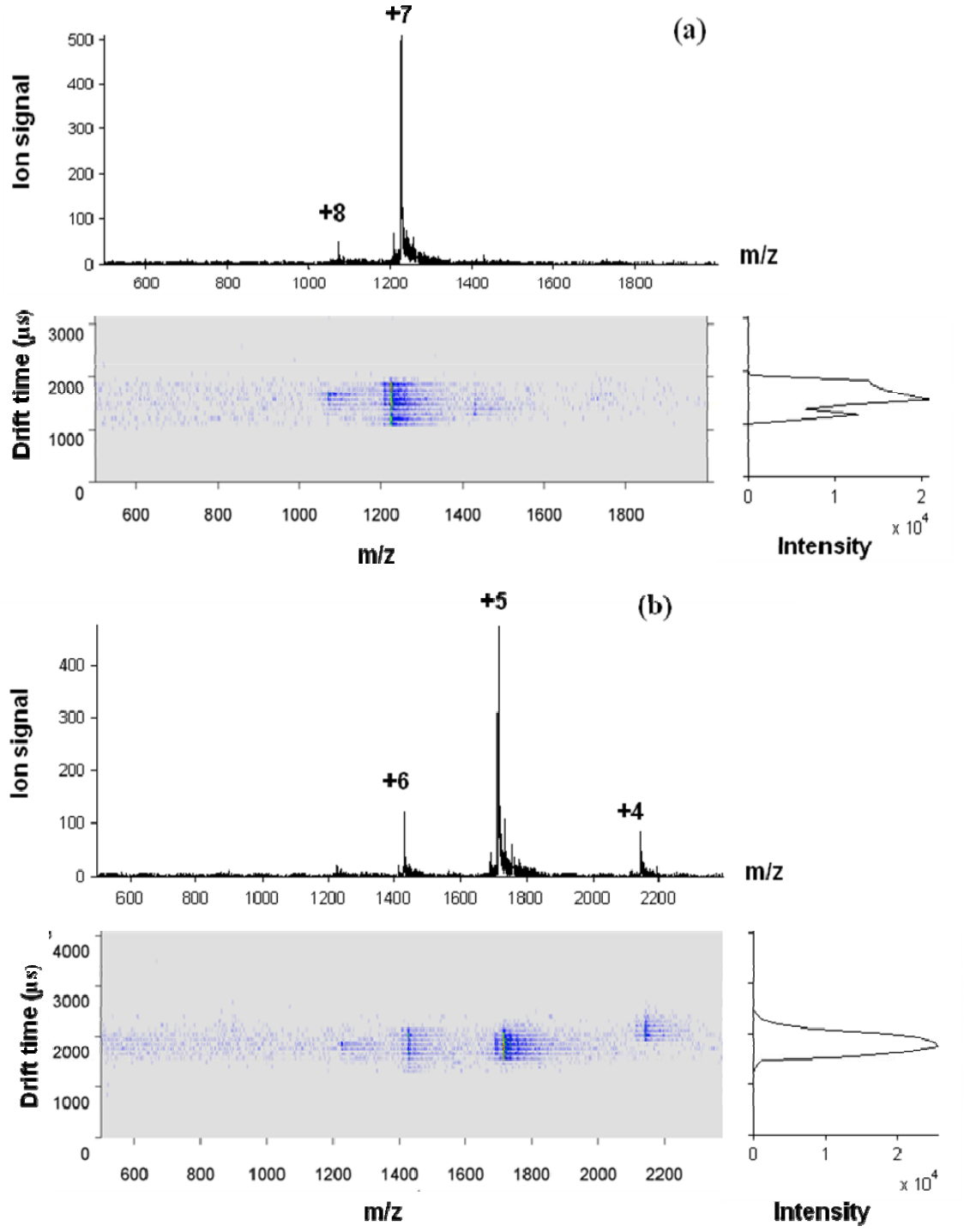

www.manaraa.com

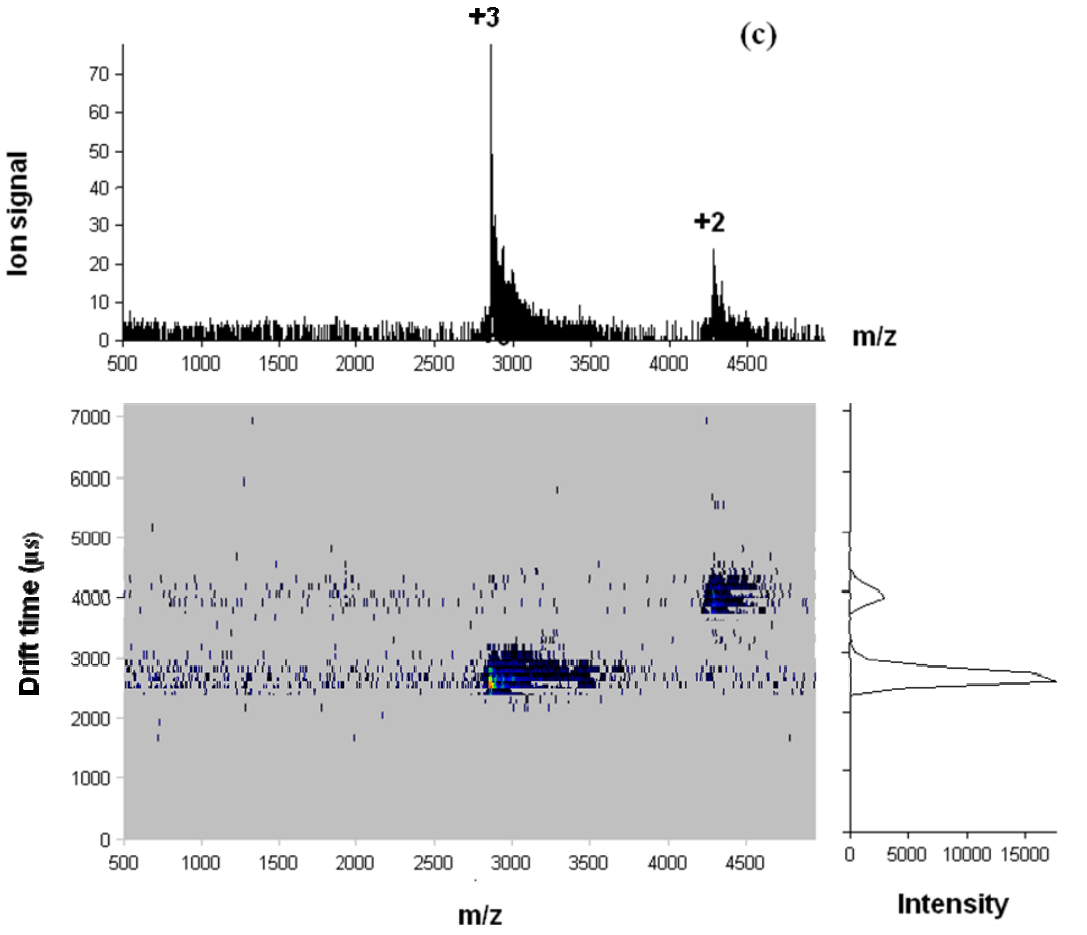

www.manaraa.com

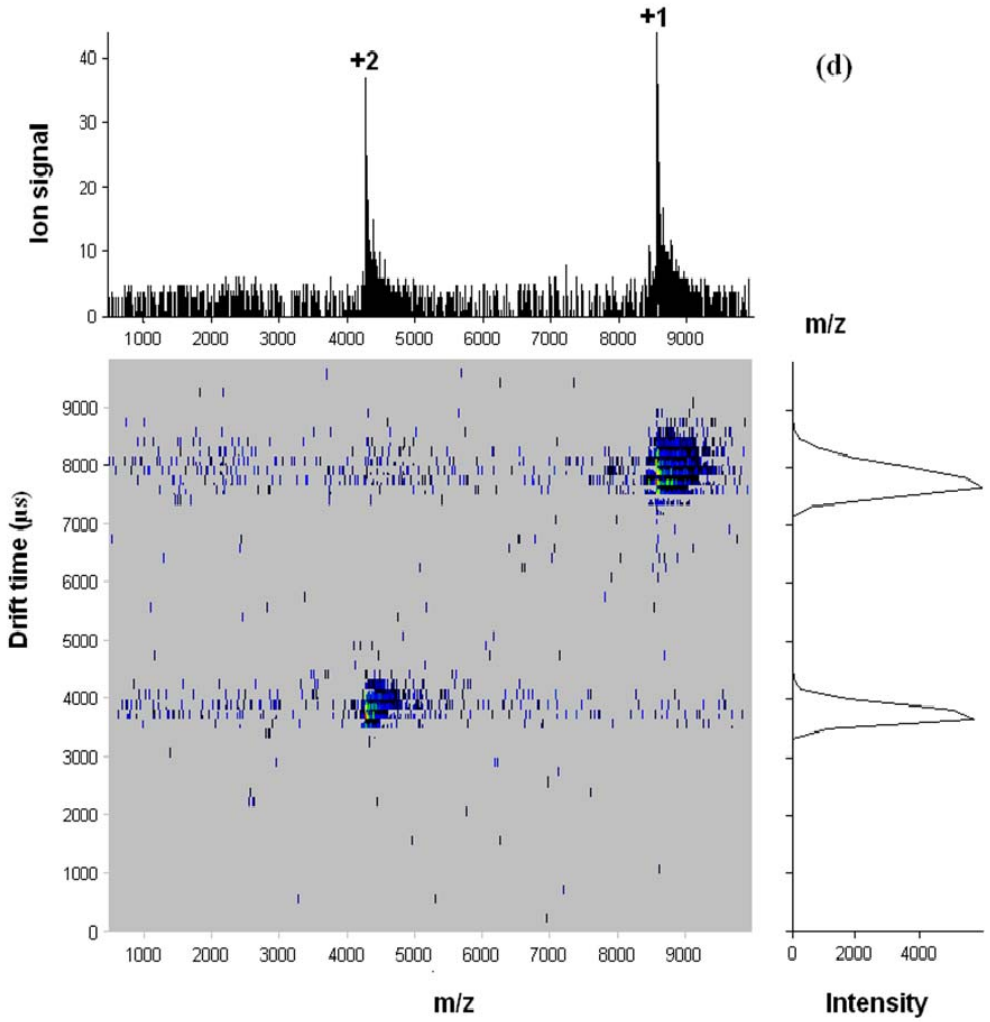

Figure 4a) 3D mobility mass spectrum of ubiquitin; 3D mobility mass spectrum of ubiquitin after reaction with PDCH negative ions: b) PDCH fill time 20 ms, ion/ion reaction time 60 ms; c) PDCH fill time 45 ms, ion/ion reaction time 150 ms; d) PDCH fill time 50 ms, reaction time 180 ms. The ions in lower charge states are more readily resolved by IM. Conditions: 0.30 mg/ml ubiquitin aqueous solution with 1% acetic acid, drift voltage -30 V to -580 V, drift pressure 1.39 mbar, IT fill time for ubiquitin 50 ms, data acquisition time: 10 s for (a), (b), (c), and 20 s for (d).

www.manaraa.com

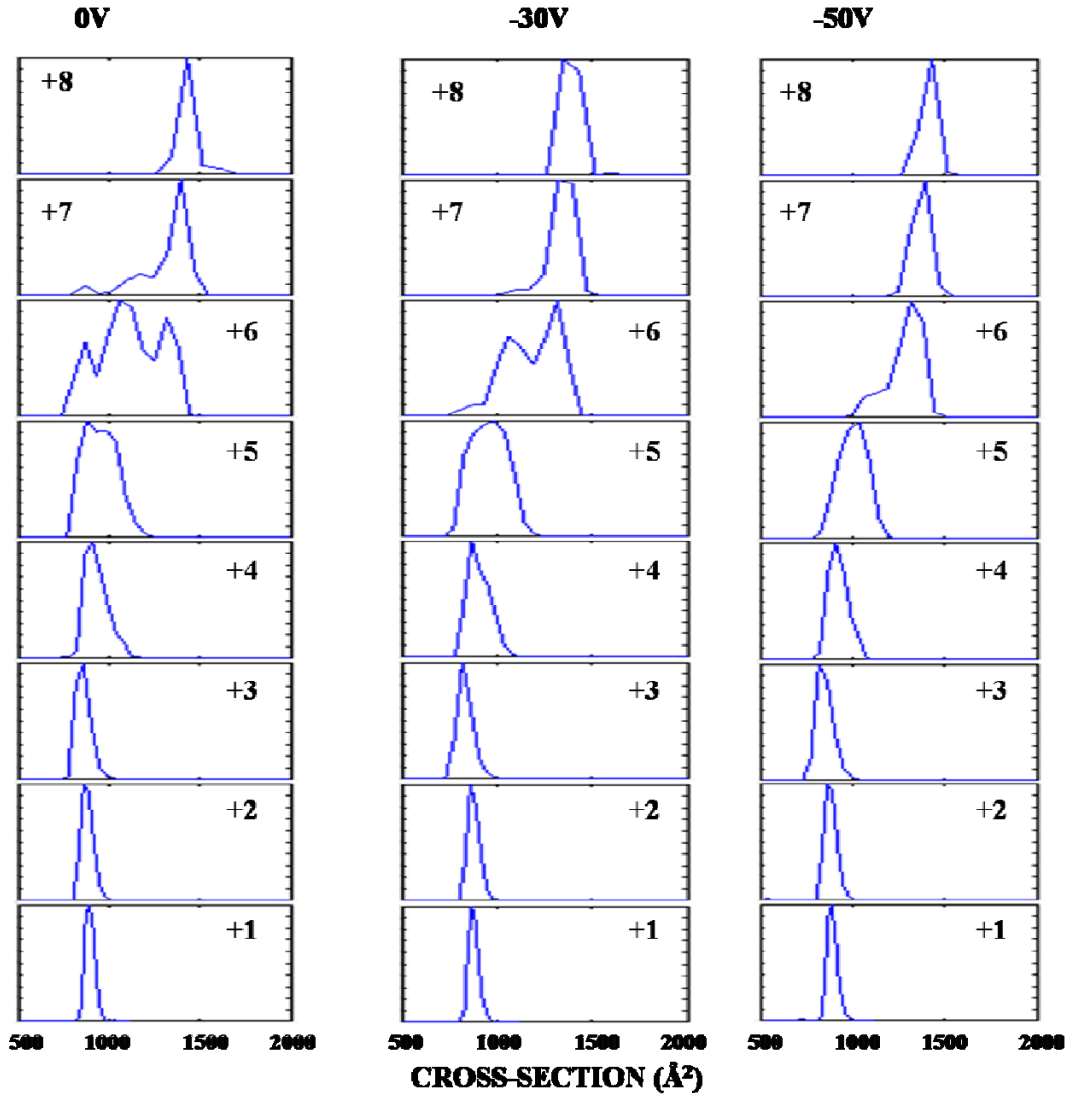

Figure 5: Cross section distributions for ubiquitin ions in various charge states. +8 and +7 ions are made from nano-ESI of 0.30 mg/ml ubiquitin aqueous solution with 1% acetic acid. The other ions are made by ion/ion reaction with PDCH anions under the conditions described in Table 2. Vertical scale values are also given in Table 2. Numerical values for cross section are listed in Table 1. The injection voltages are 0, -30 V, or -50 V, as indicated. The extraction pulse is –100V for 5 μs, and the axial electric field through the drift tube is 12.4 V/cm.

www.manaraa.com

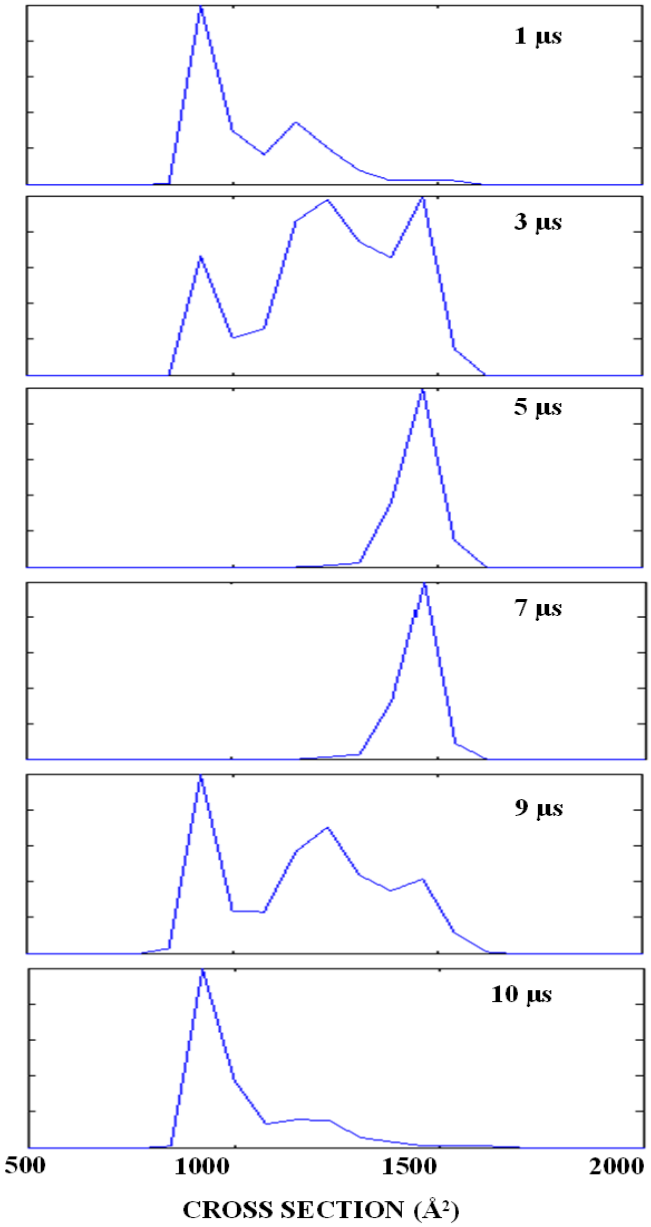

Figure 6. Effect of duration of IT ejection pulse on conformations of ubiquitin +7 ions directly from ESI source, without ion/ion reaction. IT ejection voltage = -100 V, IM injection voltage = -30 V.

www.manaraa.com

Figure 7

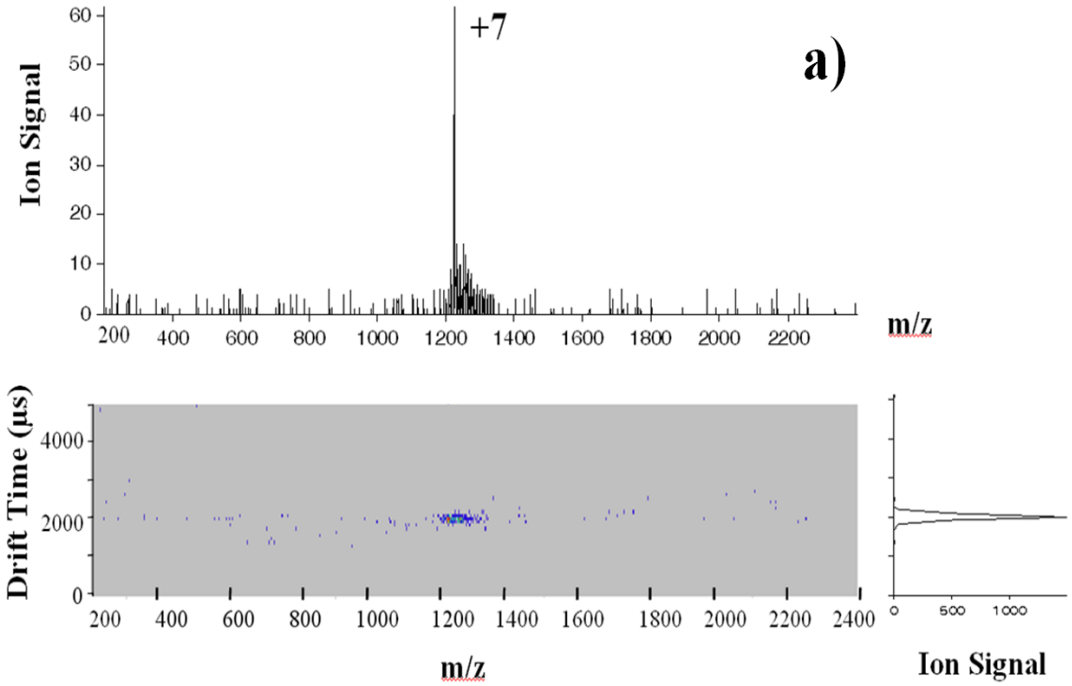

www.manaraa.com

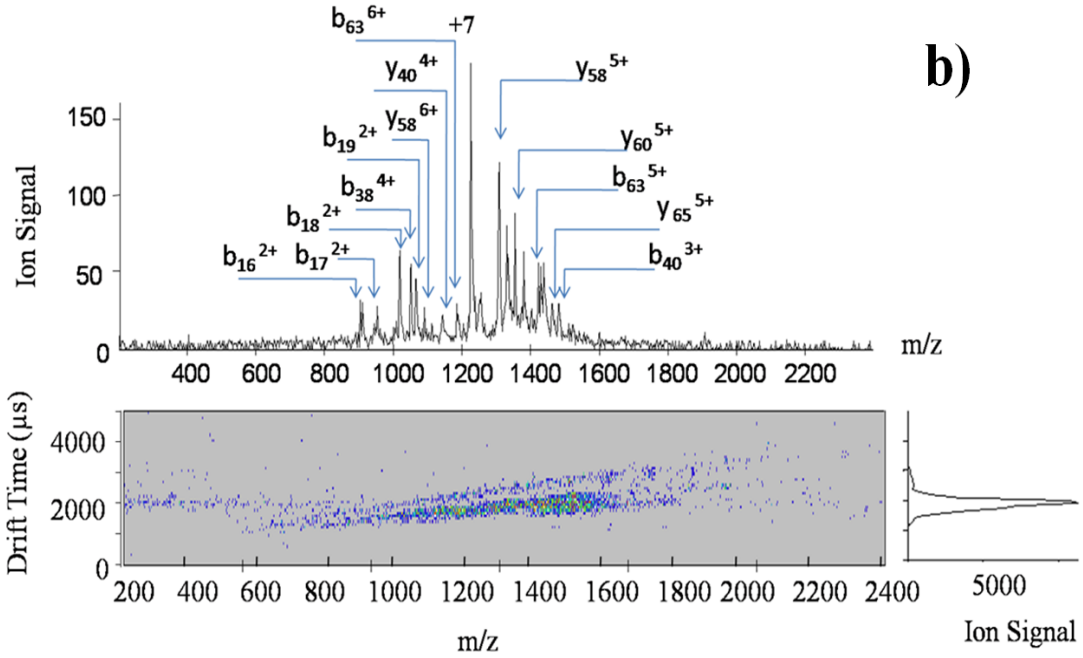

www.manaraa.com

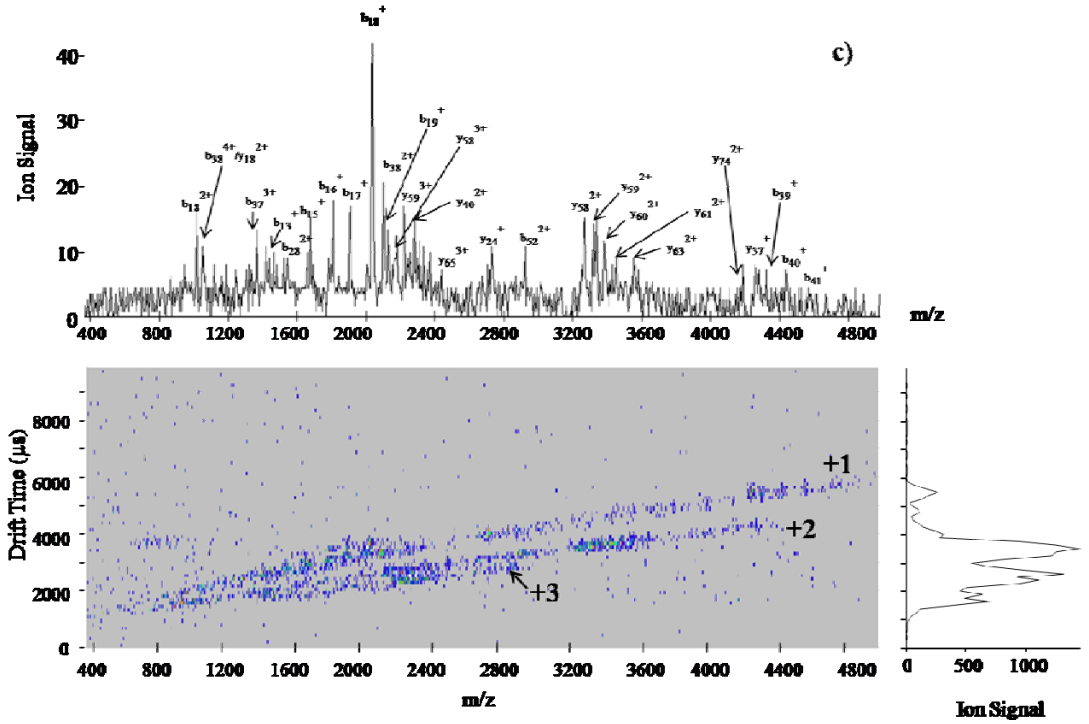

Figure 7. CID results**:** a) 3-D ion mobility spectrum of ubiquitin +7 ions isolated in 3-D IT; b) fragments directly from CID of ubiquitin +7 ions in IT; c) charge reduced CID fragments from ubiquitin +7 ions after reaction with PDCH anions for 100 ms.

www.manaraa.com

CHAPTER 3

EFFECTS OF ION/ION REACTIONS ON CONFORMATION OF GAS-PHASE CYTOCHROME *C* IONS

Qin Zhao, Mathew W. Soyk, Gregg M. Schieffer, R. S. Houk* and Ethan R. Badman‡

Department of Chemistry, Iowa State University, Ames, IA, 50011 USA

*Ames Laboratory USDOE, Iowa State University, Ames IA 50011 USA

‡ Author for correspondence

Current Address: Hoffman-La Roche Inc., Non-Clinical Safety, Nutley, NJ, 07110, USA

E-mail: ethan.badman@roche.com

Address reviews, revisions and other pre-publication matters to:

R. S. Houk

Department of Chemistry

Iowa State University

Ames IA 50011 USA

515-294-9463 fax -5233 rshouk@iastate.edu

For submission to JASMS, December 2008

www.manaraa.com

Abstract

Positive ions from cytochrome *c* are studied in a 3-D ion trap/ion mobility (IM)/quadrupole-time-of-flight (TOF) instrument with three independent ion sources. The IM separation allows measurement of the cross section of the ions. Ion/ion reactions in the 3-D ion trap that remove protons cause the cytochrome c ions to refold gently without other degradation of protein structure. The conformation(s) of the product ions generated by ion/ion reactions in a given charge state are independent of the original charge state of the cytochrome c ions. In the lower charge states (+1 to +5) cytochrome *c* ions made by the ion/ion reaction have a single conformation with cross section of ~ 1110 to 1180 $Å^2$, even if the original +8 ion started with two conformations. These cross section values are close to those of the "most folded" conformation found previously. The conformation expands slightly when the charge state is reduced from +5 to +1. In a given charge state, ions created by ion/ion reaction prefer to produce the more compact conformation in somewhat higher abundances, compared to those produced by the electrospray ionization (ESI) source alone. A variety of related studies that employ ion/ion reactions and IM to probe conformations of biomolecular ions should be possible by these methods.

www.manaraa.com

Introduction

The determination of protein conformation is important in many biological applications. Of the various methods for these measurements, mass spectrometry (MS) has certain advantages such as speed and the need for only small amounts of sample. The variations of MS for study of protein conformation include ion mobility (IM) [1-3], H/D exchange [4-8], and native electron capture dissociation (NECD)[9, 10]. Of these methods, IM provides a direct way to examine the gas-phase conformation of the ions by probing the average cross-section of the protein ions via collisions with buffer gas [3]. Early research on protein folding and unfolding was done with an IM-quadrupole instrument [1]. To study ions in lower charge states than those made directly from the electrospray ionization (ESI) source, a basic collision gas (e.g., acetophenone or 7-methyl-1, 3, 5-triazabicyclo [4,4,0] dec-5-ene(MTBD)) [11] was introduced into the source region. The collision gas extracted protons from the protein ion and created lower charge state ions through proton transfer reactions in the source. In these studies, the reactions took place only in the atmospheric pressure ion source interface region. Thus, control and variation of the reaction time and extent of reaction were difficult, and only certain reagent ions were available.

Recent instrumentation improvements have greatly extended the type of structural information and number of possible experiments available in this area. The development of a 3-D trap-IM-time of flight (TOF) instrument allows time dependent studies of gas-phase protein ions, including folding, unfolding and structural transitions [12-15]. A multi-stage IMS-MS instrument [16, 17] provides two important new functions. First, a protein ion in a specific structure can be selected by IMS, then activated and separated in the next drift

www.manaraa.com

region. Second, "state-to-state" structural transitions can be studied by structure selection-activation cycles.

Gas-phase ion/ion reactions provide another dimension for gas-phase bioanalysis by MS. To date, these reactions have been mainly used to simplify complex MS/MS spectra [18, 19] or provide fragments for structural assignment [20, 21] by methods like electron transfer dissociation (ETD) [22-24]. A three-source-ion trap-drift tube-q-TOF instrument was recently developed by our group to combine ion-ion reactions with IM-TOF measurements [25, 26]. The present paper describes how proton transfer ion/ion reactions can be used to manipulate charge state and study the effect of ion/ion reactions on the conformation change of cytochrome *c* ions. This protein is chosen because of the extensive previous studies both by experiment [10, 12, 15, 27-29] and by modeling [30-33].

Experimental

The design and general operating conditions for the home-built three source-3-D trap-IM-TOFMS are described in another paper [25]. In most experiments, Bovine heart cytochrome *c* (Sigma-Aldrich, St. Louis, MO) was dissolved without further purification at 20 to 30 μM in water with 1% aqueous acetic acid; Water alone was used as solvent for some of the results shown in the last figure. These samples were introduced through one nano-ESI source in positive mode. Perfluoro-1,3-dimethylcyclohexane (PDCH, Sigma-Aldrich, St. Louis MO) was used as the proton transfer reagent. Negative PDCH ions were created by atmospheric sampling glow discharge ionization (ASGDI) in a second source. Both positive cytochrome c ions and negative PDCH ions were trapped together in the 3-D trap and

www.manaraa.com

allowed to react for selected times between 50 ms to 200 ms. The product ions were then injected into the drift tube for IM separation, followed by m/z analysis and detection by TOF-MS. The drift tube is 44.45 cm long and contains helium gas at a pressure of 1 to 1.5 Torr. The standard operation conditions for ion mobility measurement are as follows unless stated otherwise: the injection voltage is -150 V to get the best signal, and ion trap ejection pulse is 3 μs long and -100V in magnitude. The axial electric field in the drift tube is 12 to 13 V/cm. Cross sections are calculated from the mass resolved mobility spectra in the usual fashion [3, 34].

Results and Discussion

Effect of Charge Reduction Reaction on the Conformation of Cytochrome *c* Ions. In 1% acetic acid/water solution, ESI produces cytochrome *c* ions in two main charge states (+8 and +9), as seen in the 3-D nested drift/flight [1] IM-TOF mass spectrum (Figure 1). Although their IM drift times overlap, resolved mobility peaks for the +8 and +9 ions can be extracted because these ions are m/z resolved. Note that the +8 ion has two resolvable cross sections, which are generally attributed to different gas-phase conformations.

To study how ion/ion reactions affect the conformation of protein ions, either +8 or +9 ions are isolated in the 3-D ion trap first. The mass spectra of isolated +8 and +9 ions and their cross section distributions are shown in Figure 2. The cross section plots are similar to those obtained when both +8 and +9 ions are stored and ejected into the drift tube before m/z resolution. Isolation in the 3-D trap does not heat and unfold the ions appreciably, at least at time scales up to ~ 200 ms.

www.manaraa.com

PDCH anions are then injected into the ion trap from the ASGDI source and react with cytochrome c ions to remove protons for the desired time. A typical spectrum after ion/ion reaction is shown in Figure 3. The resulting cross sections (Table 1) agree well with those reported in the literature [35]. The proton transfer reactions leave the protein ions in a range of charge states, which can be as low as +1 [25]. These reactions do not remove the covalently-bound heme group, in agreement with other reports on myoglobin, which does not lose its noncovalently-bound heme group after proton transfer reactions [36].

Cross-section values for cytochrome *c* ions in each charge state, produced by reaction of either isolated +8 or +9 ions with PDCH anions in the trap, are summarized in Table 1. The distributions of cross section observed for each charge state are indicated in Figure 4. These distribution plots indicate the relative abundances of the various folded conformations of the cytochrome c ion in a given charge state.

In general, the distributions of conformations for a given charge state are similar whether the ions started as +8 or +9. The distribution for the +7 ion made from +8 (i.e., in the left plot in Figure 4) has an additional, partly resolved peak at low cross section that is not seen in the distribution for the +7 ion made from +9. The wider peaks seen for +7 and +6 ions after ion/ion reaction suggest that there may be several additional conformations not fully resolved by ion mobility. The ions in lower charge states (+5 to +1) have only one mobility peak, even when the reactant ion was the +8 form with two mobility peaks originally.

It is tempting to assert that observation of just one mobility peak means the ions have only one conformation. The narrowest mobility peak seen for the +9 ion of cytochrome *c* has

www.manaraa.com

a full width at half maximum (fwhm) of ~180 μs (Figure 1). Calculations indicate the contribution to the fwhm of this peak from diffusion to be only ~ 16 μs. Under these experimental conditions, $Cs_7I_6^+$ ions or protonated reserpine ions (from ESI of CsI or reserpine in water) yield single mobility peaks ~80 μs fwhm, roughly half the width of the narrowest protein peaks. Thus, each of the "single" mobility peaks seen for cytochrome *c* may actually correspond to the juxtaposition of unresolved peaks from ions in several conformations of similar size. For brevity, we use phrases like "one conformation" or "a single conformation" in the discussion below, with this caveat in mind.

These results show that the protein ions can fold to one or more compact conformations during the charge reduction reaction. This observation is explained as follows. When the protein ions pass into the vacuum system, the solvent molecules evaporate, and the attraction between hydrophobic portions of the molecules diminishes. Thus, the highly charged protein ion opens rapidly to an "unfolded" conformation [11, 35]. The ion/ion reaction then removes protons, whose charges keep the protein unfolded. Intramolecular charge repulsion becomes weaker, hydrogen bonds become more important, so the protein gradually refolds as more protons are removed.

The cross-section of cytochrome *c* in the crystal structure is 1090 $Å^2$ [35, 37] . In the gas phase, ions with cross-sections from 1050 $Å^2$ to 1350 $Å^2$ are generally assigned to this "most compact" conformation [35, 37]. Thus, Figure 4 shows that the proton transfer reactions in the 3-D ion trap allow the original "unfolded" protein to pass gradually through several partially folded conformations and eventually assume the most compact conformation, with a cross section close to that of cytochrome *c* in its crystal structure.

www.manaraa.com

Close examination of the mobility plots in Figure 4 shows that the +5 ion has the smallest cross section, and cross sections for those ions in the "most compact" conformation increase slightly as charge state is reduced from +5 to +1. Apparently, as more protons are removed from the +5 ion, cytochrome c stays in one conformation, but the size of the molecule expands by a measurable amount. This effect is also observed for ubiquitin in low charge state [25], but is not as extreme as for cytochrome *c*.

Stepwise Ion/Ion Reaction. To study a "step-by-step" charge reduction, this stepwise method is demonstrated. Figure 5 shows a stepwise charge reduction of cytochrome c ions from +8 and +9. Positive ions were injected and trapped in the ion trap, and then negative ions were injected and followed by ion/ion reaction for ~60 ms. After that, the negative ions were injected again and then followed by ion/ion reaction for another~50 ms. The "negative ion injection and ion/ion reaction" were repeatedly added to the scan function. For each step of the reaction, only one charge was removed by careful control of the reaction time and reagent amount into the trap. This method is an alternative experimental way to ion parking [38] to manipulate the product ion charge state. The advantage is that it can avoid the heating of ions from ion parking, which may induce some conformation changes.

Figure 6 is the distributions of the conformation of cytochrome c ions from ion/ion reaction. The same folding pattern was observed as the charges were removed. The folding transitions from different experiment (Figure 4, 6 and 9) will be compared later.

Conformation of Ions Made by Ion/Ion Reaction Compared to Those Produced Directly by ESI. To generate ions in lower original charge states, cytochrome *c* is sprayed from water without acetic acid. These ions are then measured without ion/ion reaction, and

www.manaraa.com

the results are compared to those obtained by charge reduction reactions of more highly charged ions from water/acetic acid solutions.

Figure 7 compares cross section distributions for ions in a given charge state, prepared either by ion/ion reaction or by ESI directly. First, consider the results for the +7 and +6 charge states. Within a given charge state, either +7 or +6, the number of conformations seen and their cross sections are almost the same, but the relative abundances of the various conformations can be different. More compact conformations are more abundant for the +5, +6 and +7 ions made by ion/ion reaction than by ESI directly. For the +5 ions, the "most compact" conformation is most abundant, and at least one entirely different, more open conformation is seen only for the +5 ions made by ESI directly from water. The "closed" +5 conformer made by ion/ion reaction could not be converted to the more "open" structure by heating the +5 ions, i.e., by increasing the trapping time (as far as 4 s) or by increasing the kinetic energy used to inject ions into the drift tube. For the +4 ions in Figure 7, a "single" conformation with cross section ~ 1200 $Å^2$ predominates, although there is some of an even smaller conformation for the ions produced directly by ESI.

Effect of Solution Conditions on the Conformation of Ions Made by Ion/Ion Reaction. Even if the ions generated from electrospray or nano-ESI are solvent-free gas-phase ions, they may still have some memory of the initial solution conditions. For example, for ubiquitin water solution with 1% acetic acid, the conformations observed are less open compared with the ions formed from 50/50 water/methanol solution with 1% acetic acid [39]. As described above, protein folding was induced by removal of protons. To study the effect of initial solution conditions on the folding process induced by ion/ion reaction, cytochrome

www.manaraa.com

c in 50/50 water/methanol solution with 1% acetic acid were electrosprayed. This is done to make ions at higher charge state.

The charge states are from +16 to +9, and +12 is the most abundant charge state (Figure 8). After ion/ion reaction with PDCH negative ions from ASGDI source, +8 to +2 charge state cytochrome *c* ions were observed, and the cross-section distributions are shown in Figure 9. The same trend as in Figure 4 was found that the cytochrome *c* ions folds to the compact conformation as charges are removed. Ions tend to fold to similar conformations even when started from much high charge state. For example, +4 ions in Figure 9 have the similar conformation as +4 in Figure 6.

Folding Transitions of Cytochrome c Ions Induced by Gas-phase Ion/Ion Reaction. From all the results discussed above, the general conclusion is the ion/ion reaction between the gas-phase positive cytochrome c ions and negative PDCH ions can induce the folding of the ions, the folding of the elongated ions follows the similar pathway as that of the ions with partially folded structure, and ion/ion reaction always folds the ions to the similar conformation independent of the initial charge state. Figure 10 is a summary of all the cross-section seen for cytochrome c ions starting from different charge state, different conformations, and generated by different solutions. Even a little broad, which could result from the different solutions and experimental conditions from different day, a "belt" clearly shows the folding pathway.

Since the folding in the gas-phase follows the similar way independent of the initial conformation and charge state, there must be a folding mechanism behind these observations. Dill [40] described the gas phase folding kinetics by several possible folding funnels, and

www.manaraa.com

different conformers funnel into the native state finally. A rugged energy landscape model [40] seems to fit our observations very well, which is a bumpy bowl funnel with kinetic traps, energy barriers, and some narrow throughway paths to native state. Because the research from Houk's lab [25] and also from Clemmer's lab [11] shows that some conformations are easy to change by increasing the injection energy, but some conformations remain very stable even with heating process. The stable conformations may be at those valleys in the bumpy funnel.

Effect of Injection Conditions on Folding and Unfolding of Cytochrome c +8 Ions. Clemmer's group found that the injection energy affects the cross-section distribution of cytochrome c ions, but it is still relative high (385 eV for +6 to +10 ubiquitin ions) [41]. Lower injection energies were also studied in this work. As shown in Figure 11, at extremely low injection voltage, the cytochrome c ions were all in compact conformation. As the injection voltage increased to -30 V, some compact conformer start to unfold and some partially unfolded structure can be found in the cross-section distribution. From injection voltage of -40 V to -70 V, the compact ions gradually unfold to two structures, one is partially unfolded and the other one is elongated. The definition of compact, partially unfolded and elongated conformation is from the literature [42]. The partially unfolded structure is very stable, even at injection energy of -150 V; it still cannot completely unfold into the elongated structure.

Time Scale of Folding and Unfolding for Gas-Phase Cytochrome c +8 Ions in Gas-phase. The folding and unfolding of cytochrome c ions has been studied at different time scales by mass spectrometry. Structure transitions that occur over seconds or minutes

www.manaraa.com

can be studied by trapping in the Fourier transform-ion cyclotron resonance (FT-ICR) mass spectrometry [15, 43]. Folding and unfolding over 20 to 100 ms scale was monitored in the ion trap by Clemmer's group [12, 14]. In our previous work [25], the conformation changes were observed when the ejection pulse duration changes from 1 to 15 μs. The distributions of the ion mobility time at different ejection pulse duration (1 to 10 μs) is shown in Figure 11. For a1 μs pulse, the short drift time peak according to a compact conformation was observed. As the pulse duration increases from 3 to 7 μs, elongated structure appears. When the pulse is even longer from 7 to 10 μs, the drift time of the peak moves to short times which means smaller size conformation observed in the ion mobility spectra. So the very stable conformation in Figure 10 can refold back to partially unfolded structure if a long ejection pulse isused.

A conclusion of the observations in Figure 11 is that the changing of the structure can be observed by changing the pulse duration, and the folding and unfolding of cytochrome c +8 ions in the gas-phase could be observed in μs. Before this conclusion is safely dr4wn from the observation, the first thing needed to be confirmed is that the changing is not from the change of sampling of ions injected into the drift tube. The integration of the ion mobility peaks (Table 2) showed that the peak area for each ion mobility spectrum gradually increases as the pulse duration increasing, and in literature, the pulse durationin used by Badman and his coworker was 0.6 μs. So within the pulse duration from 3 to 10 μs, 90% of the ions should be extracted out of the trap by the pulse and ready to be sampled into the drift tube (1 and 2 μs signal was a little low compared with other duration, so maybe not all the ions were

www.manaraa.com

ejected out of the trap.), and the changing of the ion mobility spectra should come from the changing of the conformation of the ions.

The scattering effect when ions moving to the drift tube entrance (which is a 0.5 mm diameter hole) can also be ruled out as this: because the smaller ions should be scattered more than the large ions, so if the smaller conformation ions can be observed (for example at 10 μs duration), the large conformation ions if there are some could also be observed in the ion mobility spectrum. All the above changing discussed were also observed for ubiquitin +7 ions. (Figure 6 in Chapter 2 of this thesis.)

After carefully justified the possible reasons, an explanation should focus on what occurs in the small distance (1.3 cm) from the exit of the ion trap to the entrance of the drift tube. As the gas leaking from the drift tube, the pressure in this region should be in between the drift tube pressure (1 Torr) and chamber pressure (0.1 mTorr). So the collisions are a significant number (several hundred). Close analyzing the electric field changes during the injection process, as shown in Figure 12, during the pulser-on period, the electric field is opposite direction to the ion initial velocity, ions are slowed down by the electric field; during the pulser-off period, electric field is the same direction to the ion motion, ions are accelated by the electric field. The changes of the "pulser-on" time will affect the injection time or in another word, affect the time the ions in the short space from the ion trap exit to the entrance of drift tube. Different number of collisions in this space result in different ion mobility spectra for cytochrome c +8 ions.

To prove this idea, the effect of the pulse amplitude was studied. If the above proposal is reasonable, the different pulse amplitude should change the time of injection (or

www.manaraa.com

change the collision numbers ions experienced during the injection into the drift tube). The result is shown in Figure 13 at four different magnitudes: -10V (less negative than front of the drift tube),-30V (same as the front of the drift tube), -50V(slightly more negative than the front of the drift tube) and -80 V(more negative than the front of the drift tube). The changing of the electric field has been shown in Figure 12. As expected, for -10V, electric field is always the same direction as ion motion, so no change was observed in ion mobility spectra for different pulse duration; for -30V, the electric field is 0, and almost no change was observed; for -50, -80V in Figure 13 and -100 V in Figure 11, the changes were observed, but at different pulse duration time. From all the figures shown, the changes of the conformation can be observed in μs scale pulse duration, which means the folding and unfolding of gas-phase cytochrome c can be detected in micro-second.

Conclusion

Gas-phase ion-ion reactions combined with IM measurements provide a new way to study conformation changes in protein ions. Exothermic processes like these multiple proton transfer reactions might be expected to simply heat the ions and unfold them [44] . However the collisions with the bath gas in the 3-D trap cools the ions [45], the protein ions after proton transfer reaction are still in folded states . Thus, ion/ion reactions can be performed while the ions remain in, or perhaps re-fold into, biologically-interesting conformations.

In addition to the charge reduction reactions described here, this three source-ion trap-IM-TOFMS should facilitate a variety of ion/ion reaction studies pertinent to bioanalysis. The identity and amount of reagent ion and the reaction time can be controlled

www.manaraa.com

over wide ranges. Other reactions such as electron transfer dissociation [22, 23], metal addition [46] , and some sequential reactions (e.g., ETD followed by charge reduction to simplify assignment of the ETD fragments) should be possible. The time progression of kinetic processes that change either the m/z value or the conformation of the ions should be measurable, at least for processes that occur on time scales long compared to the duration of the measurement (~ 1 s). These and other studies are underway in our laboratory.

Changing of the ejection pulse duration and magnitude can cause the unfolding and folding of cytochrome c +8 ions in μs scale if the pulse is more negative than the front of the drift tube. Till now, we only observed this on cytochrome c +8, +9 and ubiquitn +7 ions from ESI of 100% water solution with 1% acetic acid and ubiquitn +7 ions from ESI of 50/50 methanol and water solution with 1% acetic acid. These ions are in the intermediate charge state and have more variable conformations [14, 42]. For lower charge state ubiqutin ions (+5 to +2), no changes were observed as changing the pulse duration. So these effects should be evaluated on a case-by case basis and study on this effect is still undergoing.

Acknowledgments

This work was funded by a grant from the Vice Provost for Research, Iowa State University. QZ and MS acknowledge the Conoco-Phillips Fellowship (Iowa State University, 2006-2007 and 2007-2008) for financial support. MS also acknowledges the GAANN Fellowship (Iowa State University, 2008) and the Velmer A. and Mary K. Fassel Fellowship (Iowa State University, 2006-2007)

www.manaraa.com

Reference

1. Hoaglund, C. S., Valentine, S. J., Sporleder, C. R., Reilly, J. P., and Clemmer, D. E. Three-Dimensional Ion Mobility TOFMS Analysis of Electrosprayed Biomolecules *Analytical Chemistry* 1998, *70*, 2236-2242
2. Clemmer, D. E., Hudgins, R. R., Jarrold, M. F. Naked Protein Conformations - Cytochrome c in the Gas-Phase *Journal of the American Chemical Society* 1995, *117*, 10141-10142
3. Clemmer, D. E., Jarrold, M. F. Ion Mobility Measurements and Their Applications to Clusters and Biomolecules *Journal of Mass Spectrometry* 1997, *32*, 577-592
4. Wood, T. D., Chorush, R. A., Wampler, F. M., Little, D. P., Oconnor, P. B., McLafferty, F. W. Gas-Phase Folding and Unfolding of Cytochrome-c Cations *Proceedings of the National Academy of Sciences of the United States of America* 1995, *92*, 2451-2454
5. Cassady, C. J., and Carr, S. R. Elucidation of Isomeric Structures for Ubiquitin $[M+12H]^{(12+)}$ Ions Produced by Electrospray Ionization Mass Spectrometry *Journal of Mass Spectrometry* 1996, *31*, 247-254
6. Freitas, M. A., Hendrickson, C. L., Emmett, M. R., Marshall, A. G. Gas-Phase Bovine Ubiquitin Cation Conformations Resolved by Gas-Phase Hydrogen/Deuterium Exchange Rate and Extent *International Journal of Mass Spectrometry* 1999, *187*, 565-575
7. Freitas, M. A., Hendrickson, C. L., Marshall, A. G. Correlation between Solution and Gas-Phase Protein Conformation: H/D Exchange, IRMPD, and ESI FT-ICR MS *Proc. SPIE-Int. Soc. Opt. Eng.* 2000, *3926*, 61-68
8. Robinson, E. W.; Williams, E. R. Multidimensional Separations of Ubiquitin Conformers in the Gas Phase: Relating Ion Cross Sections to H/D Exchange Measurements *Journal of the American Society for Mass Spectrometry* 2005, *16*, 1427-1437
9. Breuker, K., and McLafferty, F. W. Native Electron Capture Dissociation for the Structural Characterization of Noncovalent Interactions in Native Cytochrome c *Angewandte Chemie-International Edition* 2003, *42*, 4900-4904
10. Breuker, K., and McLafferty, F. W. The Thermal Unfolding of Native Cytochrome c in the Transition from Sollution to Gas Phase Probed by Native Electron Capture Dissociation *Angrew Chem. Int. Ed.* 2005, *44*, 4911-4914
11. Valentine, S. J., Counterman, A. E., Clemmer, D. E. Conformer-Dependent Proton-Transfer Reactions of Ubiquitin Ions *Journal of the American Society for Mass Spectrometry* 1997, *8*, 954-961
12. Badman, E. R.; Hoaglund-Hyzer, C. S.; Clemmer, D. E. Monitoring Structural Changes of Proteins in an Ion Trap over Similar to 10-200 ms: Unfolding Transitions in Cytochrome c Ions *Analytical Chemistry* 2001, *73*, 6000-6007
13. Badman, E. R., Hoaglund-Hyzer, C. S., Clemmer, D. E. Dissociation of Different Conformations of Ubiquitin Ions *Journal of the American Society for Mass Spectrometry* 2002, *13*, 719-723

www.manaraa.com

14. Myung, S., Badman, E. R., Lee, Y. J., Clemmer, D. E. Structural Transitions of Electrosprayed Ubiquitin Ions Stored in an Ion Trap over Similar to 10 ms to 30 s *Journal of Physical Chemistry A* 2002, *106*, 9976-9982
15. Badman, E. R.; Myung, S.; Clemmer, D. E. Evidence for Unfolding and Refolding of Gas-Phase Cytochrome c Ions in a Paul Trap *Journal of the American Society for Mass Spectrometry* 2005, *16*, 1493-1497
16. Koeniger S. L.; Merenbloom S. I.; Clemmer David E. Evidence for Many Resolvable Structures within Conformation Types of Electrosprayed Ubiquitin Ions *Journal of Physical Chemstry B* 2006, *110*
17. Koeniger S. L., Merenbloom S. I., Sevugarajan S., Clemmer D. E., Hudgins, Robert R., Jamold Martin F. Transfer of Structural Elements from Compact to Extended States in Unsolvated Ubiquitin *Journal of American Chemical Society* 2006, *128*, 11713-11719
18. Stephenson, J. L., McLuckey, S. A. Simplification of Product Ion Spectra Derived from Multiply Charged Parent Ions via Ion/Ion Chemistry *Analytical Chemistry* 1998, *70*, 3533-3544
19. Stephenson, J. L., McLuckey, S. A., Reid, G. E., Wells, J. M., Bundy, J. L. Ion/Ion Chemistry as a Top-Down Approach for Protein Analysis *Current Opinion in Biotechnology* 2002, *13*, 57-64
20. Breuker, K., Oh, H. B., Lin, C., Carpenter, B. K., McLafferty, F. W. Nonergodic and Conformational Control of the Electron Capture Dissociation of Protein Cations *Proceedings of the National Academy of Sciences of the United States of America* 2004, *101*, 14011-14016
21. Ge, Y., Lawhorn, B. G., Einaggar, M., Strauss, E., Park, J. H., Begley, T. P., McLafferty, F. W. Top Down Characterization of Larger Proteins (45 kDa) by Electron Capture Dissociation Mass Spectrometry *Journal of the American Chemical Society* 2002, *124*, 672-678
22. Syka, J. E. P., Coon, J. J., Schroeder, M. J., Shabanowitz, J., and Hunt, D. F. Peptide and Protein Sequence Analysis by Electron Transfer Dissociation Mass Spectrometry *Proceedings of the National Academy of Sciences of the United States of America* 2004, *101*, 9528-9533
23. Pitteri, S. J., Chrisman, P. A., Hogan, J. M., McLuckey, S. A. Electron Transfer Ion/Ion Reactions in a Three-Dimensional Quadrupole Ion Trap: Reactions of Doubly and Triply Protonated Peptides with SO_2 Center Dot *Analytical Chemistry* 2005, *77*, 1831-1839
24. Chrisman, P. A., Pitteri, S. J., Hogan, J. M., McLuckey, S. A. SO_2^- Electron Transfer Ion/Ion Reactions with Disulfide Linked Polypeptide Ions *Journal of the American Society for Mass Spectrometry* 2005, *16*, 1020-1030
25. Zhao, Q., Soyk, M., Schieffer Gregg, Badman, Ethan R. and Houk, R., S. An Ion Trap - Ion Mobility - Time of Flight Mass Spectrometer with Three Ion Sources for Ion-Ion Reactions submitted to *J. Am. Soc. Mass Spectrum*.
26. Badman, E. R., Schieffer, G.M., Soyk, M., Zhao, Q., Anderson, T.J. An ESI-Ion Trap-Ion Mobility-q-TOF to Study Ion-Ion Reactions of Intact

www.manaraa.com

Biopolymers,*Proceedings of the 53rd ASMS Conference on Mass Spectrometry and Allied Topics* San Antonio, TX, June 6-9, 2005.

27. Valentine, S. J.; Clemmer, D. E. H/D Exchange Levels of Shape-Resolved Cytochrome c Conformers in the Gas Phase *Journal of the American Chemical Society* 1997, *119*, 3558-3566
28. Englander, S. W.; Sosnick, T. R.; Mayne, L. C.; Shtilerman, M.; Qi, P. X.; Bai, Y. W. Fast and Slow Folding in Cytochrome c *Accounts of Chemical Research* 1998, *31*, 737-744
29. McLafferty, F. W., Guan, Z. Q., Haupts, U., Wood, T. D., Kelleher, N. L. Gaseous Conformational Structures of Cytochrome c *Journal of the American Chemical Society* 1998, *120*, 4732-4740
30. Hoang, L.; Maity, H.; Krishna, M. M. G.; Lin, Y.; Englander, S. W. Folding Units Govern the Cytochrome c Alkaline Transition *Journal of Molecular Biology* 2003, *331*, 37-43
31. Krishna, M. M. G.; Lin, Y.; Rumbley, J. N.; Englander, S. W. Cooperative Omega Loops in Cytochrome c: Role in Folding and Function *Journal of Molecular Biology* 2003, *331*, 29-36
32. Krishna, M. M. G.; Englander, S. W. A Unified Mechanism for Protein Folding: Predetermined Pathways with Optional Errors *Protein Science* 2007, *16*, 449-464
33. Maity, H., Rumbley, J. N., and Englander, S. W. Functional Role of a Protein Foldon - an Omega-Loop Foldon Controls the Alkaline Transition in Ferricytochrome c *Proteins-Structure Function and Bioinformatics* 2006, *63*, 349-355
34. Chrisman, P. A., Newton, K. A., Reid, G. E., Wells, J. M., McLuckey, S. A. Loss of Charged Versus Neutral Heme from Gaseous Holomyoglobin Ions *Rapid Communications in Mass Spectrometry* 2001, *15*, 2334-2340
35. Badman, E. R., Hoaglund-Hyzer, C. S., Clemmer, D. E. Monitoring Structural Changes of Proteins in an Ion Trap over ~10 to 200 ms: Unfolding Transitions in Cytochrome C Ions *Analytical Chemistry* 2001, *73*, 6000-6007
36. Stephenson, J. L., VanBerkel, G. J., McLuckey, S. A. Ion-Ion Proton Transfer Reactions of Bio-Ions Involving Noncovalent Interactions: Holomyoglobin *Journal of the American Society for Mass Spectrometry* 1997, *8*, 637-644
37. David E. Clemmer, R. R. H., and Martin F. Jamold Naked Protein Conformations: Cytochrome c in the Gas Phase *Journal of American Chemical Society* 1995, *117*, 10141-10142
38. McLuckey, S. A.; Reid, G. E.; Wells, J. M. Ion Parking During Ion/Ion Reactions in Electrodynamic Ion Traps *Analytical Chemistry* 2002, *74*, 336-346
39. Li, J. W.; Taraszka, J. A.; Counterman, A. E.; Clemmer, D. E. Influence of Solvent Composition and Capillary Temperature on the Conformations of Electrosprayed Ions: Unfolding of Compact Ubiquitin Conformers from Pseudonative and Denatured Solutions *International Journal of Mass Spectrometry* 1999, *187*, 37-47
40. Dill, K. A.; Chan, H. S. From Levinthal to Pathways to Funnels *Nature Structural Biology* 1997, *4*, 10-19

www.manaraa.com

41. Valentine, S. J., Counterman, A. E., and Clemmer, D. E. Conformer-Dependent Proton Transfer Reactions of Ubiquitin Ions *Journal of American Society for Mass Spectrometry* 1997, *8*, 954-961
42. Badman, E. R., Myung, S., Clemmer, D. E. Evidence for Unfolding and Refolding of Gas-Phase Cytochrome c Ions in a Paul Trap *Journal of the American Society for Mass Spectrometry* 2005, *16*, 1493-1497
43. Horn, D. M.; Breuker, K.; Frank, A. J.; McLafferty, F. W. Kinetic Intermediates in the Folding of Gaseous Protein Ions Characterized by Electron Capture Dissociation Mass Spectrometry *Journal of the American Chemical Society* 2001, *123*, 9792-9799
44. Stephenson, J. L., McLuckey, S. A. Ion/Ion Reactions in the Gas Phase: Proton Transfer Reactions Involving Multiply-Charged Proteins *Journal of the American Chemical Society* 1996, *118*, 7390-7397
45. Wells, J. M., Chrisman, P. A., McLuckey, S. A. Formation and Characterization of Protein-Protein Complexes in Vacuo *Journal of the American Chemical Society* 2003, *125*, 7238-7249
46. Badman, E. R., Chrisman, P. A., and McLuckey, S. A. A Quadrupole Ion Trap Mass Spectrometer with Three Independent Ion Sources for the Study of Gas-Phase Ion/Ion Reactions *Analytical Chemistry* 2002, *74*, 6237-6243

www.manaraa.com

Table 1. Average cross-sections of cytochrome c in different charge states

*Cross-section of ions from charge reduction of isolated +9 cytochrome c ions

#Cross-section of ions from charge reduction of isolated +8 cytochrome c ions

Charge State	m/z	*Cross-section ($Å^2$)	#Cross-section ($Å^2$)
+9	1359.6	2116.3	
+8	1529.6	1601.0, 1847.6	1798.0, 2032.8
+7	1748.0	1616.6, 1832.4	1612.4,1827.6
+6	2039.2	1293.2, 1478.1	1197.6, 1474.3
+5	2446.8	1077.7	1074.9
+4	3058.3	1108.3	1162.4
+3	4077.3	1154.5	1151.5
+2	6115.5	1120.8	1179.2
+1	12230	1185.4	1182.3

The standard deviation for the cross-section of cytochrome c +8 ions is ± 56$Å^2$ for measurement of the same solution at different days.

www.manaraa.com

Table 2 Integration of the area of the ion mobility spectra of cytochrome c +8 at different ejection pulse duration, injection voltage:-30V, pulse -100V

Pulse duration (µs)	Integrated Area
1	1.71×10^{5}
2	6.65×10^{5}
3	8.15×10^{5}
4	1.04×10^{6}
5	1.05×10^{6}
6	1.25×10^{6}
7	1.15×10^{6}
8	1.41×10^{6}
9	1.16×10^{6}
10	1.13×10^{6}

www.manaraa.com

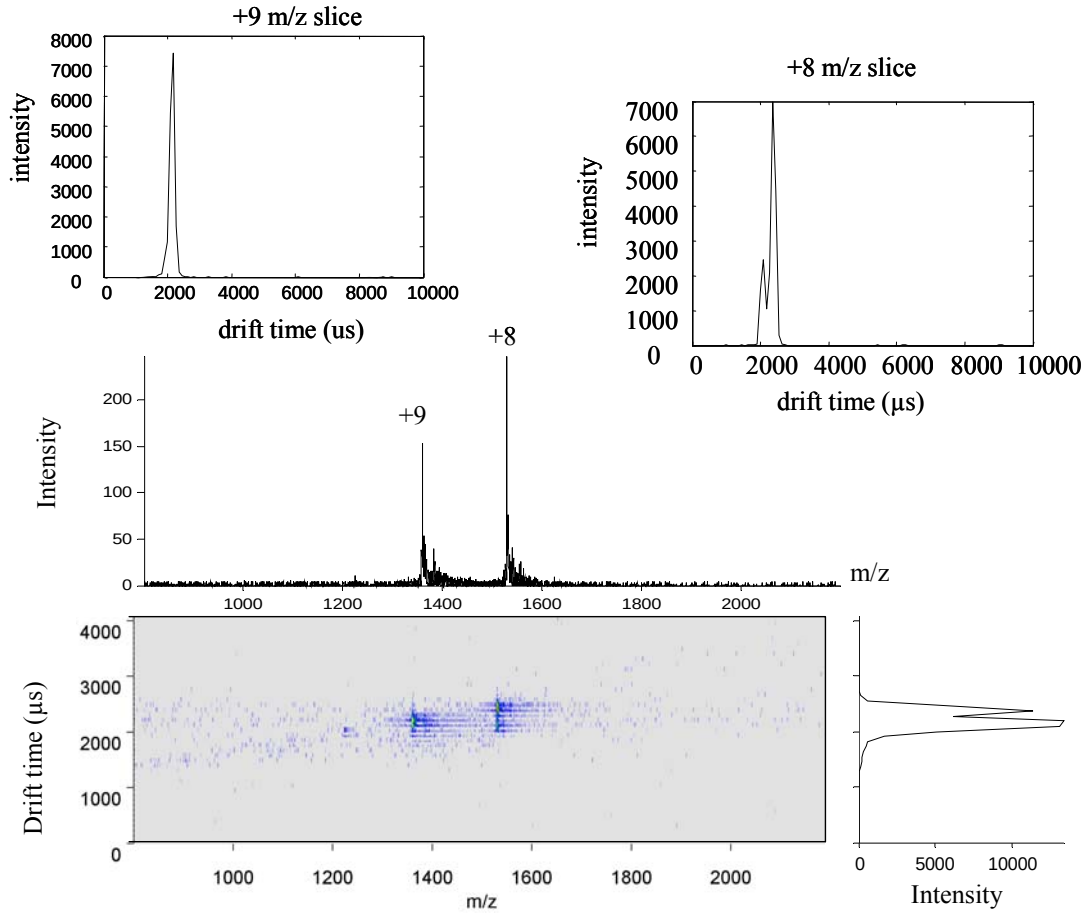

Figure 1. Nested 3-D IM-TOF mass spectrum of 30 µM cytochrome c in water with 1% acetic acid. The summed mass and ion mobility spectra are in the middle and at the lower right, respectively. The extracted IM spectra for cytochrome c +8 and +9 ions are displayed at the top.

www.manaraa.com

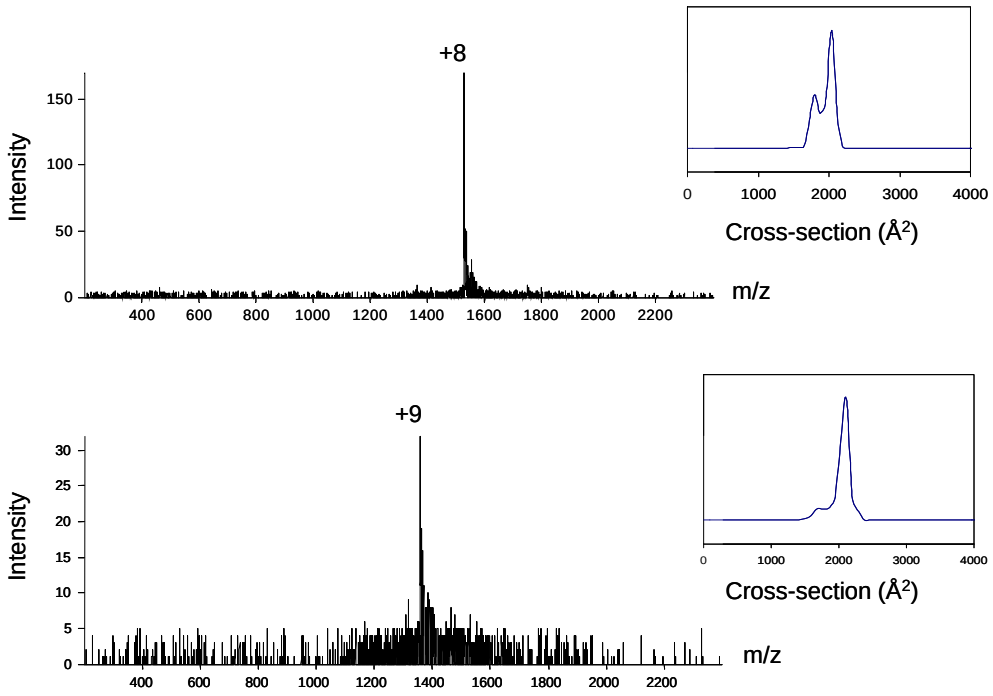

Figure 2. Mass spectra and cross-section distributions of +8 and +9 cytochrome c ions after isolation in the ion trap.

www.manaraa.com

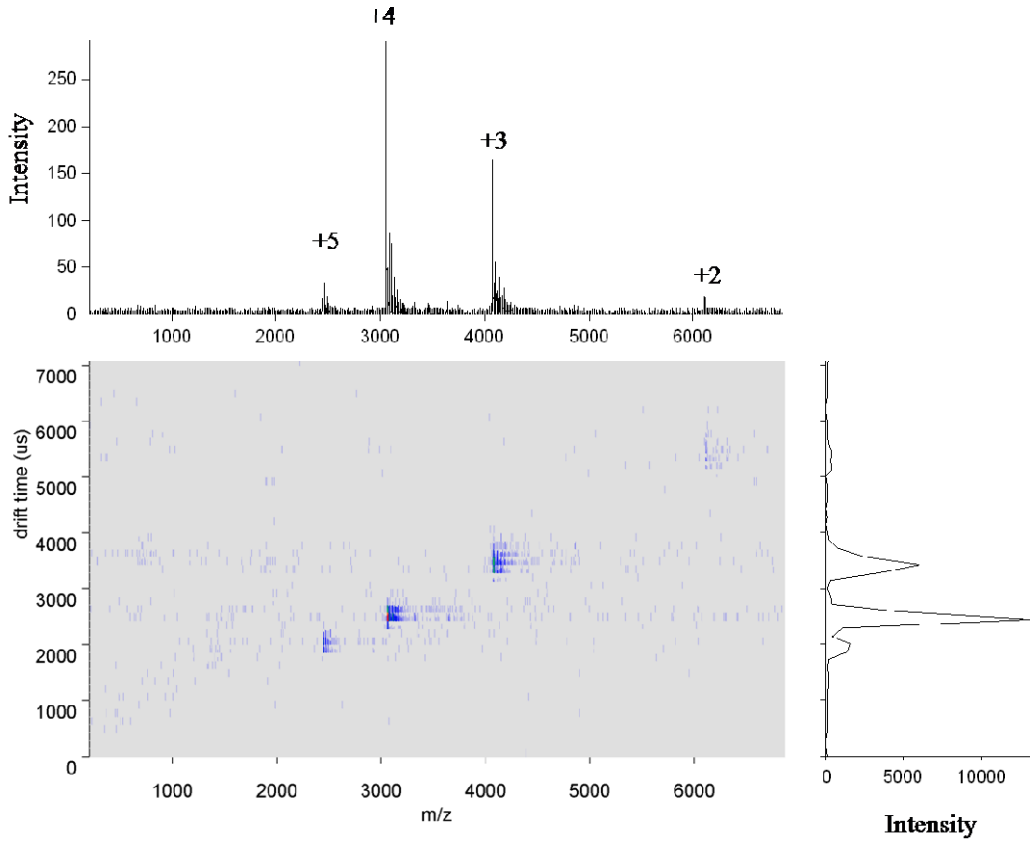

Figure 3. 3-D spectrum after isolated +8 cytochrome c ions react with PDCH anions in the ion trap for 100 ms.

www.manaraa.com

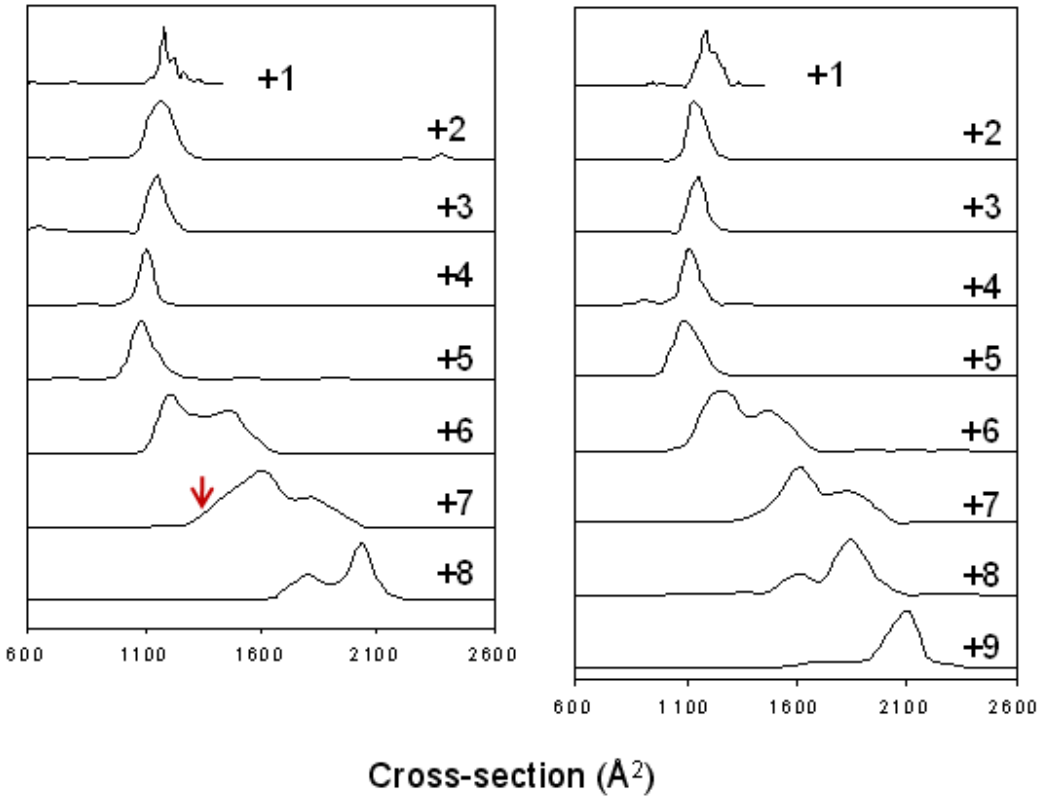

Figure 4. Distribution of cross sections for cytochrome *c* ions in each charge state. For the plots at the left, the cytochrome c ions were initially in the +8 state; ion/ion reaction time was 50 ms to go to +4 and 110 ms to go to +1. The right plots are for charge reduction of +9 cytochrome c ions for 40 ms to go to +4 and 80 ms to go to +1.

www.manaraa.com

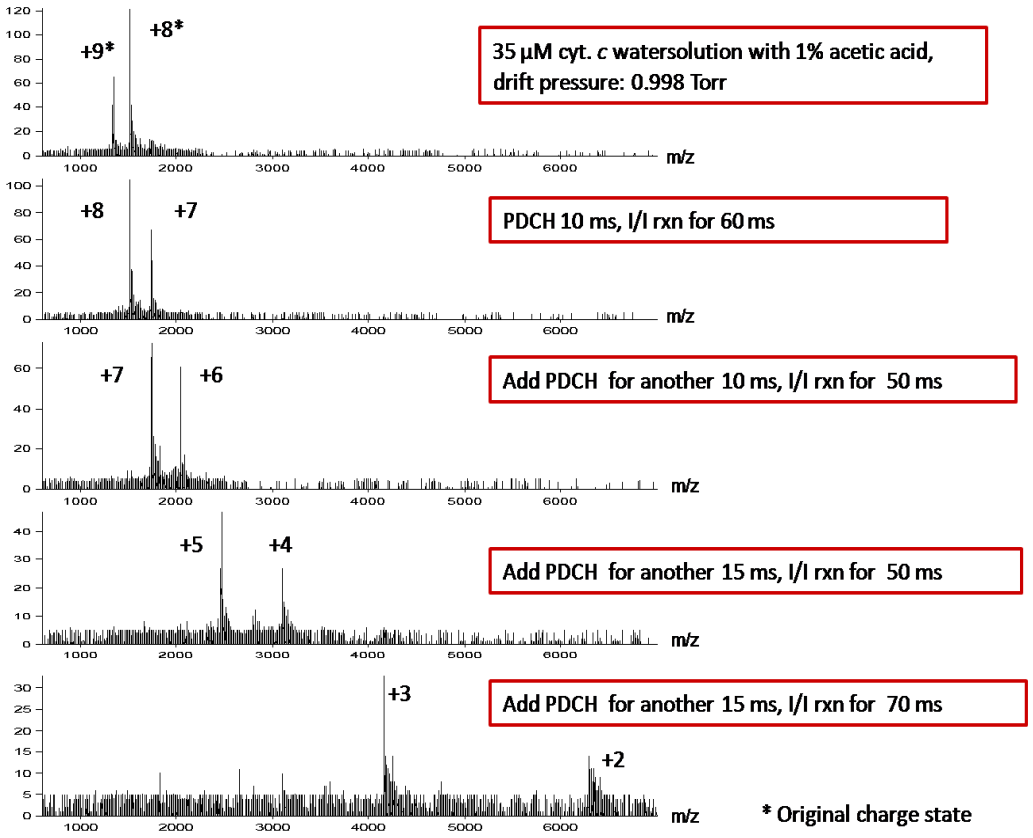

Figure 5 Mass spectra of cytochrome c ions from charge state +9 to +2 in four steps by stepwise charge reduction reaction with PDCH negative ions.

www.manaraa.com

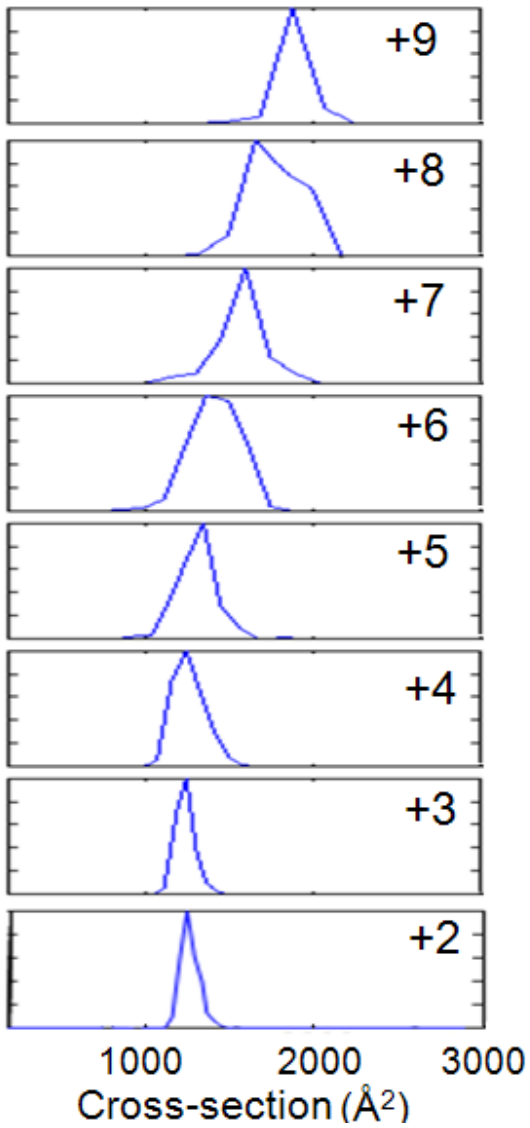

Figure 6. Distribution of cross sections for cytochrome *c* ions in each charge state. For the plots at the left, the initial charge state of cytochrome c ions were +8 and +9, +7 to +2 are made from stepwise ion/ion reaction described in Figure 5.

www.manaraa.com

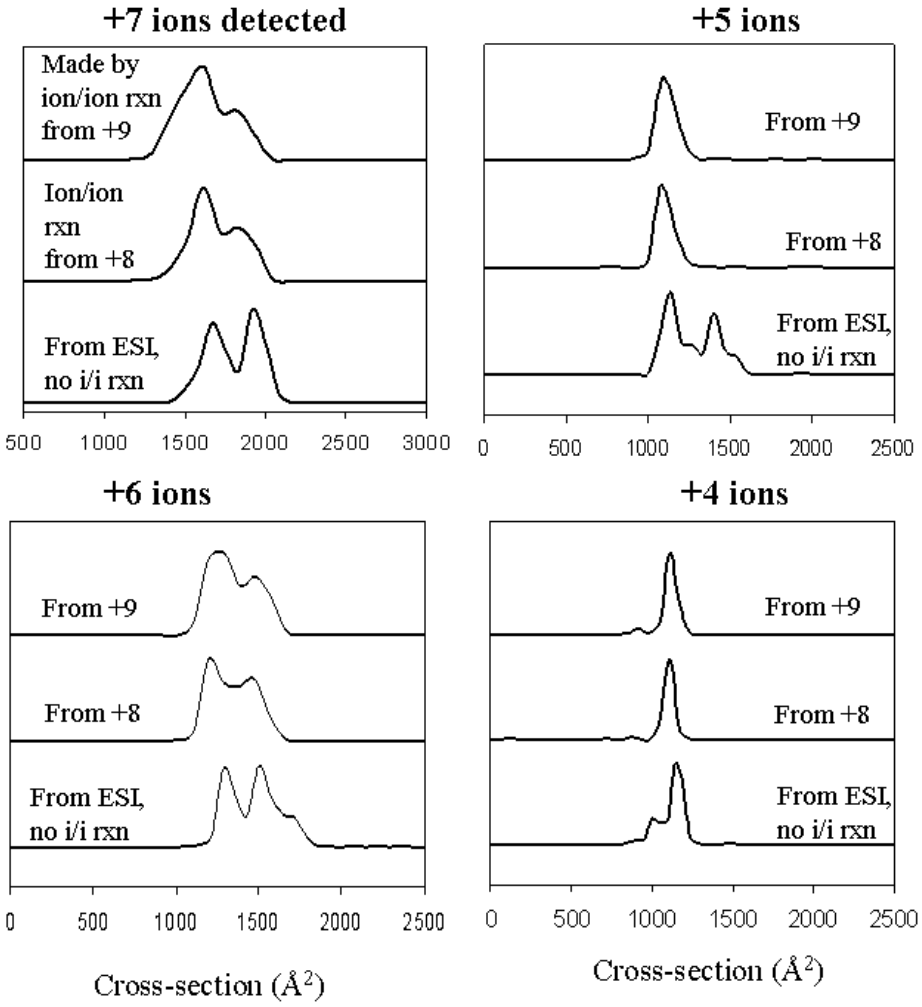

Figure 7. Distribution of cross sections for cytochrome *c* ions in each charge state. The charge state of the ions observed is noted outside each box. The top curve in each box is for ions made from +9 by ion/ion reaction (40 ms). The middle curves are for ions made from +8 (50 ms). The bottom curves are for the ions in the indicated charge state observed directly from ESI from water, without acetic acid.

www.manaraa.com

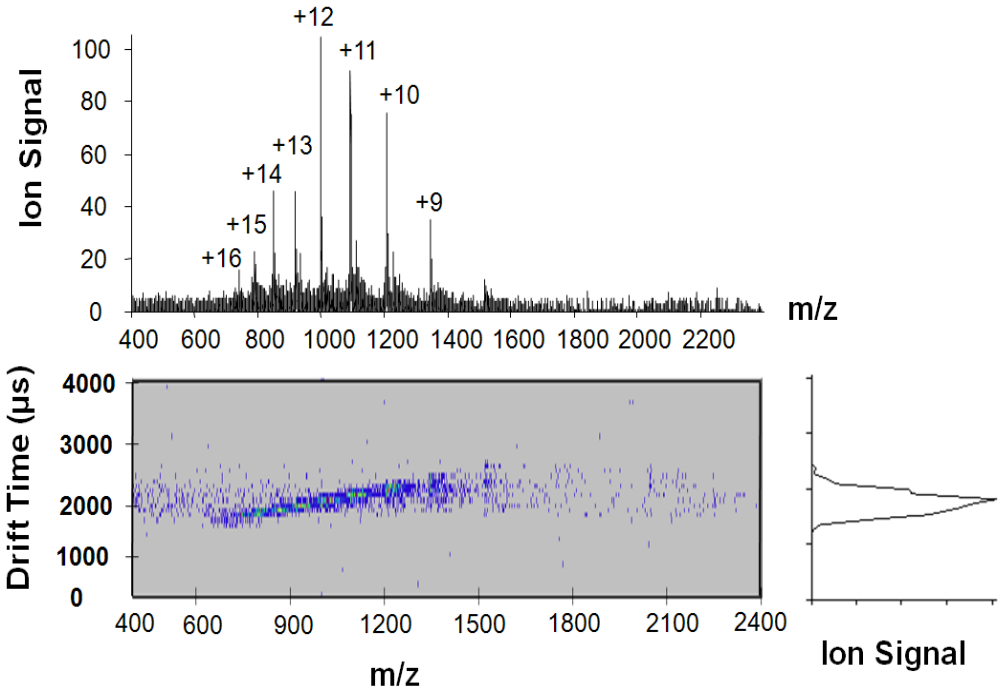

Figure 8. 3D mass spectra of cytochrome *c* (25 µM) 50/50 water/methanol solution with 1% acetic acid, the charge states are from +16 to +9.

www.manaraa.com

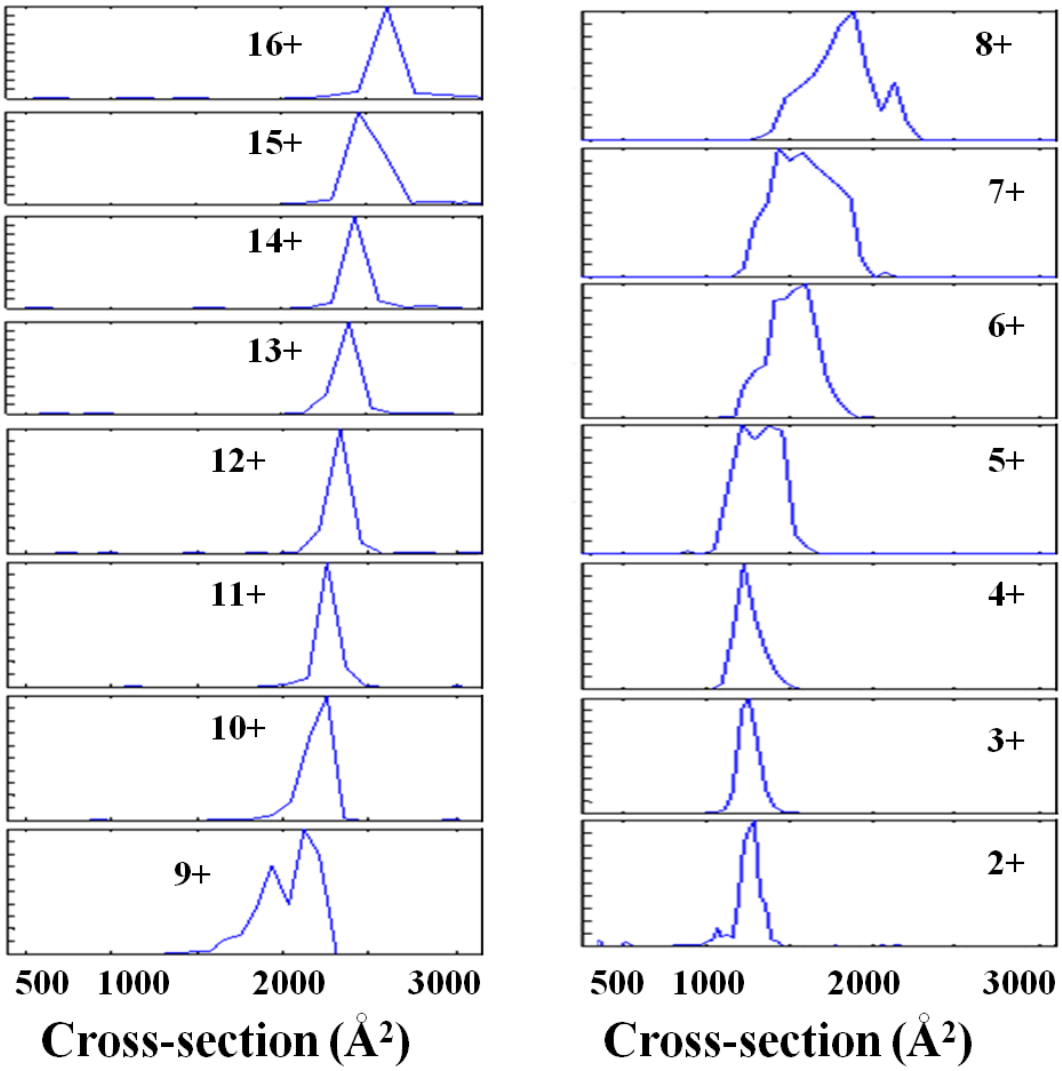

Figure 9. Distribution of cross sections for cytochrome *c* ions in each charge state. For the plots at the left, the initial charge state of cytochrome c ions were +16 to +9 and +8 to +2 are from ion/ion reaction.

www.manaraa.com

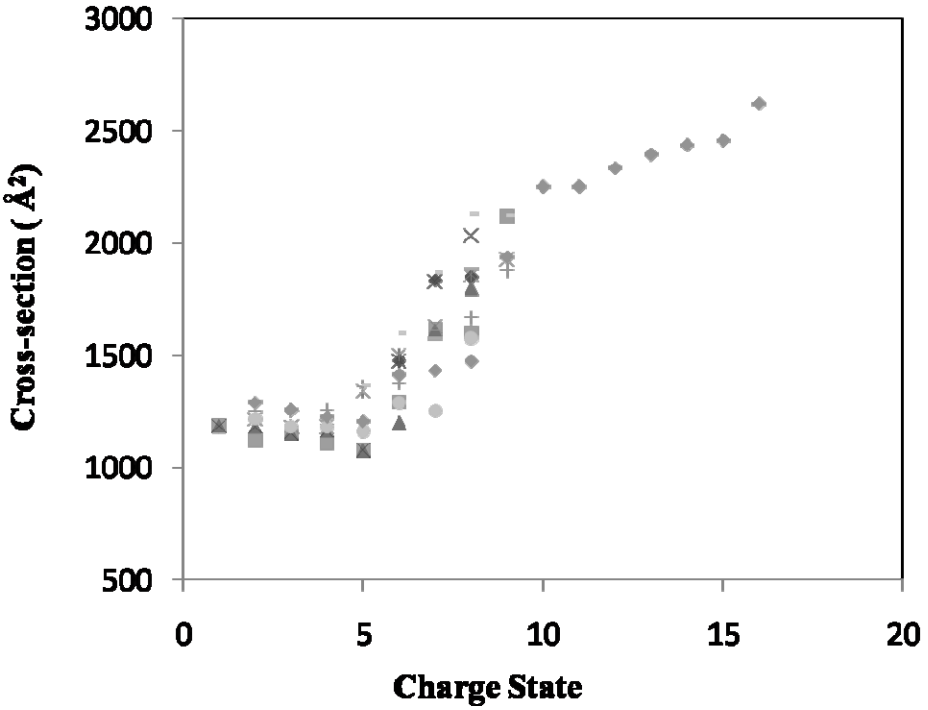

Figure 9. Summary of all cross-sections of cytochrome c ions at different charge states determined by several ion mobility measurements of ions directly formed from electrospray source or from ion/ion reactions.

www.manaraa.com

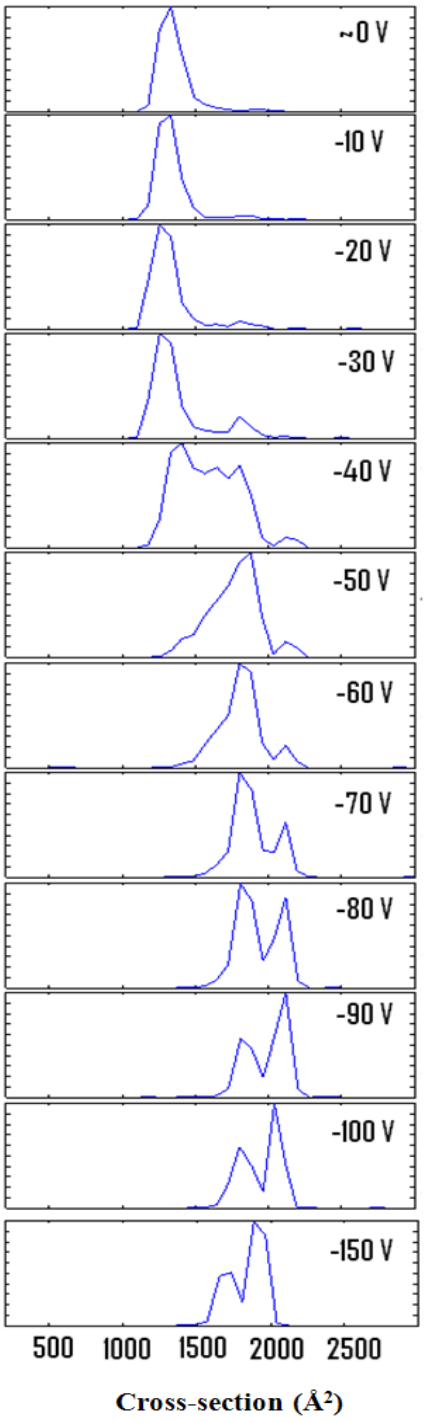

Figure 10. Cross-section distributions for cytochrome *c* +8 ions at different injection voltage into the drift tube.

www.manaraa.com

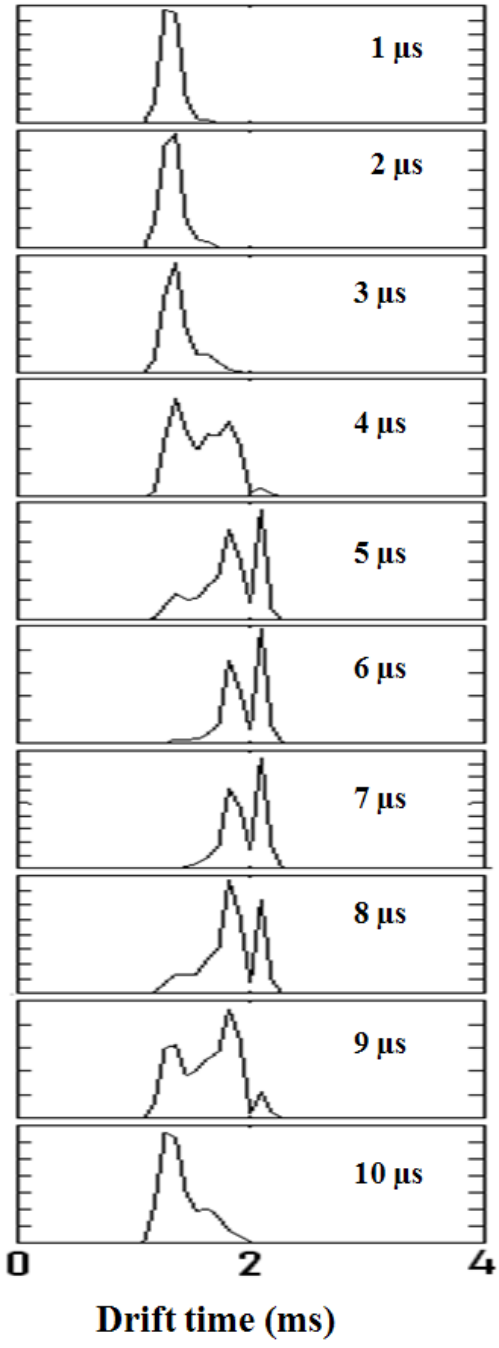

Figure 11. Ion mobility distributions for cytochrome c +8 ions. Injection voltage: -30 V, the ejection pulse: -100 V, ejection duration: from 1 to 10 µs.

www.manaraa.com

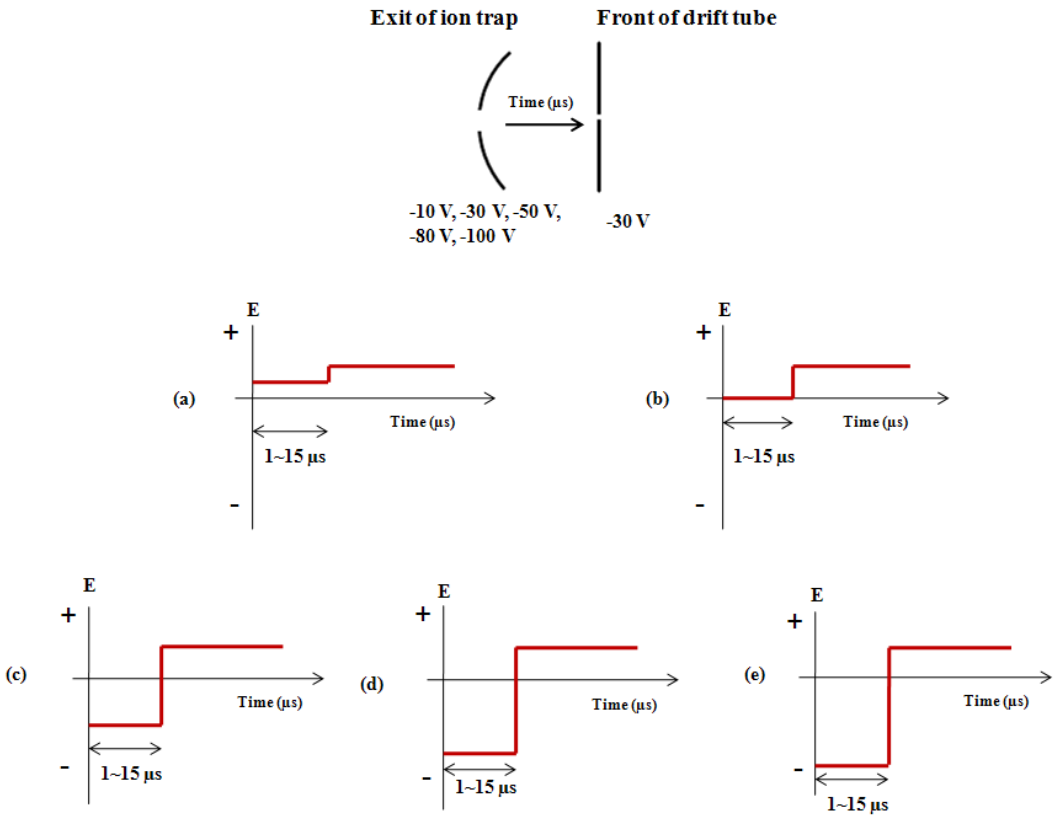

Figure 12. The change of electric field in the short space between the exit of the ion trap and entrance of the drift tube during the μs scale ion injection time period. Font of the drift tube is at -30 V, the pulse duration changes from 1 to 15 μs, pulse magnitude for (a): -10 V, (b): -30 V, (c): -50 V, (d): -80 V, and (e): -100 V. + E means the electric field accelates the ion motion and – E means the electric field slows down the ion motion.

www.manaraa.com

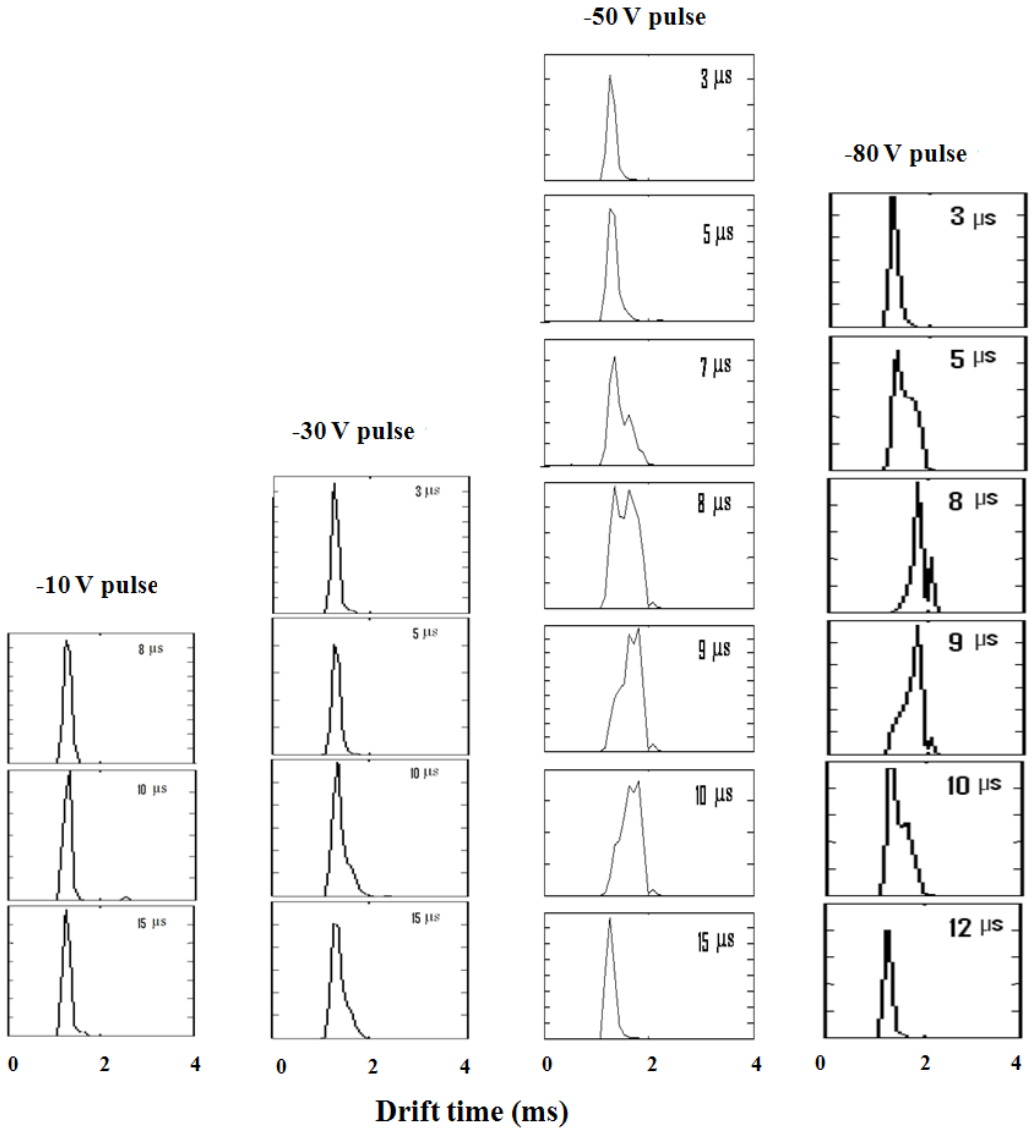

Figure 13. Ion mobility distributions for cytochrome c +8 ions. Injection voltage: -30 V, the ejection pulse: -10 V,-30 V, -50 V, and – 80 V. Pulse duration: from 1 to 15 µs.

www.manaraa.com

CHAPTER 4

A METHOD TO SEPARATE PROTEIN IONS WITH SIMILAR ION MOBILITIES VIA MASS-SELECTIVE EJECTION FROM AN ION TRAP

Qin Zhao, Ethan R. Badman, R.S. Houk

Chemistry Department, Iowa State University, Ames, IA, 50011,USA

Introduction:

Ion mobility spectrometry (IMS) provides a rapid way for the gas-phase separation of protein mixtures based on conformation [1]. The combination of IMS and mass spectrometry (IMS/MS) is currently receiving a lot of attention in peptide/protein mixture analysis [2, 3]. An ion trap /ion mobility/ q-TOF instrument has been developed around 2000 by Clemmer's group [4-7]. Ions of similar m/z ratio but different ion mobilities can be separated in the drift tube first and then injected into collision cell to generate fragments by CID. Because the parent ion has the same mobility time as its fragments, the sequence information of the parent ion can be obtained from the CID fragments.

IMS-CID-TOF analysis offers the possibility of performing parallel MS/MS of many species. Unfortunately, for complex mixtures or ESI-generated proteins with wide distributions of charge-state, many ions do not have unique mobilities. Therefore, parallel MS/MS [4] results in spectra that are the sum of many fragment ions from several parent ions. It is hard to relate the fragments to just one parent ion solely by drift time and difficult to interpret the spectra and get sequence information. This paper demonstrates one possible

www.manaraa.com

remedy for this problem: to sacrifice some of the parallel ability by selecting parent ions in specific m/z ions followed by fragmentation and mass analysis.

In this work, the mass-selective scanning ability of the ion trap was used to eject the ions out of the trap followed by injection into the drift tube. This configuration still retains the high duty cycle of ion trap-TOF experiment.

Experimental:

A home-built nano-ESI-quadrupole/ ion trap/ion mobility/TOF instrument was used in this work (Figure 1) [8]. This device has complete control over the RF amplitude, waveform, and timing of the ion trap, via an Argos ion trap controller (Griffin Analytical Technologies). Bovine cytochrome *c* (Sigma-Aldrich, St. Louis, MO, MW=12228), porcine trypsin (Sigma-Aldrich, St. Louis, MO, MW= 23463), and porcine albumin (Sigma-Aldrich, St. Louis, MO, MW= 69,950) of 20-30 μM solutions aqueous 1% acetic acid solutions were used for nano-ESI. For some initial experiments, only ion mobility spectra were obtained and the quadrupole collision cell was operated in RF only mode to transmit ions through to a detector instead of TOF.

For previous work with the conventional ion trap ejection method, a high voltage (50 to 200 V) was applied to the exit end cap of the ion trap. In this mode, all ions are rapidly and simultaneously ejected from the ion trap and injected into the ion mobility drift cell [7]. In the present work, the ion trap mass-selective instability scan [9, 10] was used. Figure 2 shows the scan function of each individual run. Proteins ions from nano-ESI were injected, cooled and stored in the ion trap. The RF voltage on the ring electrode was then ramped

www.manaraa.com

while a fixed frequency, ramped voltage sine wave was applied to the front cap of the ion trap to extend the mass range.

Results and Discussions:

Figure 3 shows the 3-D mass spectra for the two ion trap ejection method, pulsed ejection (PE) and mass-selective ejection (MSE). For ion trap pulsed ejection method (Figure 3 a), the ion mobility peaks for trypsin +11, +10, and +9 ions overlap, the drift tube cannot separate three charge states just by ion mobility. This will often be the problem for protein ions at high charge state. Instead of this typical ejection method, the ions are ejected from the ion trap in a time dependent manner (sequentially): scanning the RF from 1 to 5 kV while a fixed frequency (47 kHz) sine wave was applied to the front cap of the ion trap with ramping amplitude from 4 V to 41 V. The three charge states are well separated in the ion mobility cell (Figure 3 bottom spectrum).

The typical scan rate (50 V/ms) in the ion trap scan generates mobility peaks in a range from 20 to 40 ms. This result is compared to standard pulsed mobility spectra with unresolved peaks all within 2 to 3 ms. Note that high resolution in the mass ejection is not necessary; therefore, scan rates and duty cycles can remain relatively high.

Reverse ramping RF amplitude (ramping the RF from high to low) was used to optimize the performance for albumin. In Figure 4, the ion mobility spectra showed that approximately 20 different charge states are base-line separated for albumin ions, whereas spectrum contains only one unresolved peak.

www.manaraa.com

A mixture of cytochrome c and trypsin was also tested (Figure 5). By the traditional rapid pulsed ejection method, the various ion mixtures have similar mobilities, all peaks are condensed between 2 and 3 ms (not shown in this paper), and cannot be distinguished by the drift time from this ~0.45 m long drift tube. With the mass-selective scan ejection, cytochrome c ions and trypsin ions fall into two groups, each of which has the similar ion mobility spectra as those from the pure samples (Figure 5 top and middle). In each group, the ions at different charge states were also separated well in the ion mobility spectra (Figure 5 bottom). This ion trap ejection method provides another option for the separation of protein mixture ions, which have similar mobility but different mass to charge ratio. This capability could expand the ability of the ion mobility labeling parallel experiement to handle complex mixtures.

www.manaraa.com

Reference

1. Clemmer, D.E., Jarrold, M. F., Ion Mobility Measurements and their Applications to Clusters and Biomolecules. *Journal of Mass Spectrometry*, 1997. **32**(6): p. 577-592.
2. Kanu, A.B., Dwivedi, P., Tam, M., Matz, L., and Hill, H. H., Ion Mobility-Mass Spectrometry. *Journal of Mass Spectrometry*, 2008. **43**(1): p. 1-22.
3. Bohrer, B.C., Merenbloom, S. I. , Koeniger,S. L. , Hilderbrand, A. E., and Clemmer, D. E., Biomolecule Analysis by Ion Mobility Spectrometry. *Annual Review of Analytical Chemistry,* 2008. **1**: 293-327.
4. Hoaglund-Hyzer, C.S. and Clemmer, D.E. Ion Trap/Ion Mobility/Quadrupole/Time of Flight Mass Spectrometry for Peptide Mixture Analysis. *Analytical Chemistry,* 2001. **73**(2): p. 177-184.
5. Hoaglund, C.S., Valentine, S. J., and Clemmer, D. E., An Ion Trap Interface for ESI-Ion Mobility Experiments. *Analytical Chemistry*, 1997. **69**(20): p. 4156-4161.
6. Hoaglund-Hyzer, C.S., Lee, Y. J., Counterman, A. E., and Clemmer, D. E., Coupling Ion Mobility Separations, Collisional Activation Techniques, and Multiple Stages of MS for Analysis of Complex Peptide Mixtures. *Analytical Chemistry*, 2002. **74**(5): p. 992-1006.
7. Henderson, S.C., Valentine, S. J., Counterman, A. E., and Clemmer, D. E., ESI/Ion Trap/Ion Mobility/Time-of-Flight Mass Spectrometry for Rapid and Sensitive Analysis of Biomolecular Mixtures. *Analytical Chemistry*, 1999. **71**(2): p. 291-301.
8. Zhao, Q., Soyk, M., Schieffer G., Badman, E. R. and Houk, R., S., An Ion Trap - Ion Mobility - Time of Flight Mass Spectrometer with Three Ion Sources for Ion-Ion Reactions. submitted to *J. Am. Soc. Mass Spectrum*.
9. March, R.E., An Introduction to Quadrupole Ion Trap Mass Spectrometry. *Journal of Mass Spectrometry*, 1997. **32**(4): p. 351-369.
10. Jonscher, K.R., and Yates, J. R., The Quadrupole Ion Trap Mass Spectrometer - A Small Solution to a Big Challenge. *Analytical Biochemistry*, 1997. **244**(1): p. 1-15.

www.manaraa.com

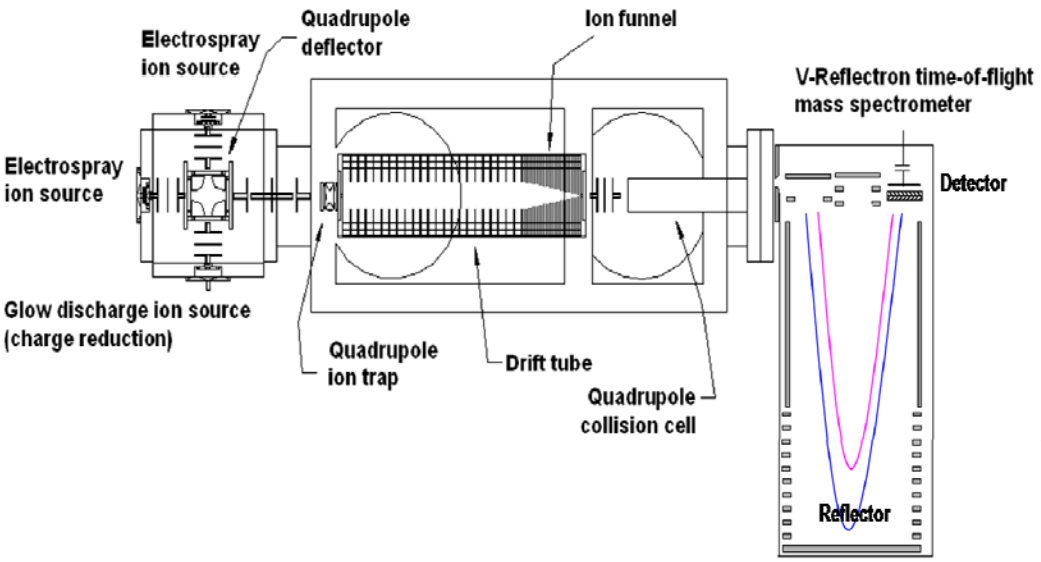

Figure 1. Scale diagram showing overall instrument, including two ESI and one ASGDI sources, ion optics, quadrupole deflector, IT, IM drift tube with ion funnel and q-TOF.

www.manaraa.com

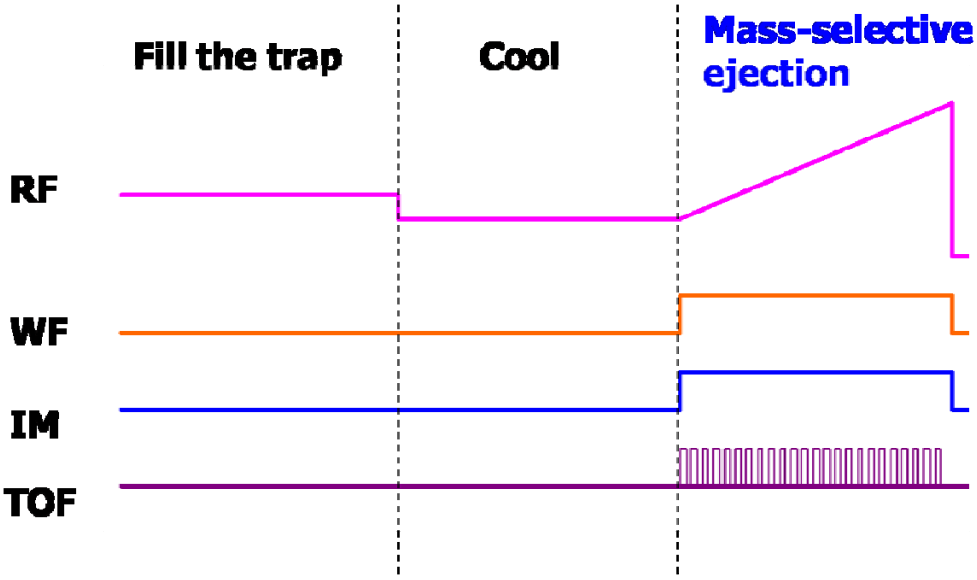

Figure 2. A generic scan function for mass selective ejection from the ion trap. The top plot shows the amplitude of the RF trapping voltage applied to the ring electrode of the ion trap. The second plot shows the time function when the waveform is applied. The lower two plots show the times when ions are injected into the drift tube, ion mobility data acquisition and TOF extraction pulses.

www.manaraa.com

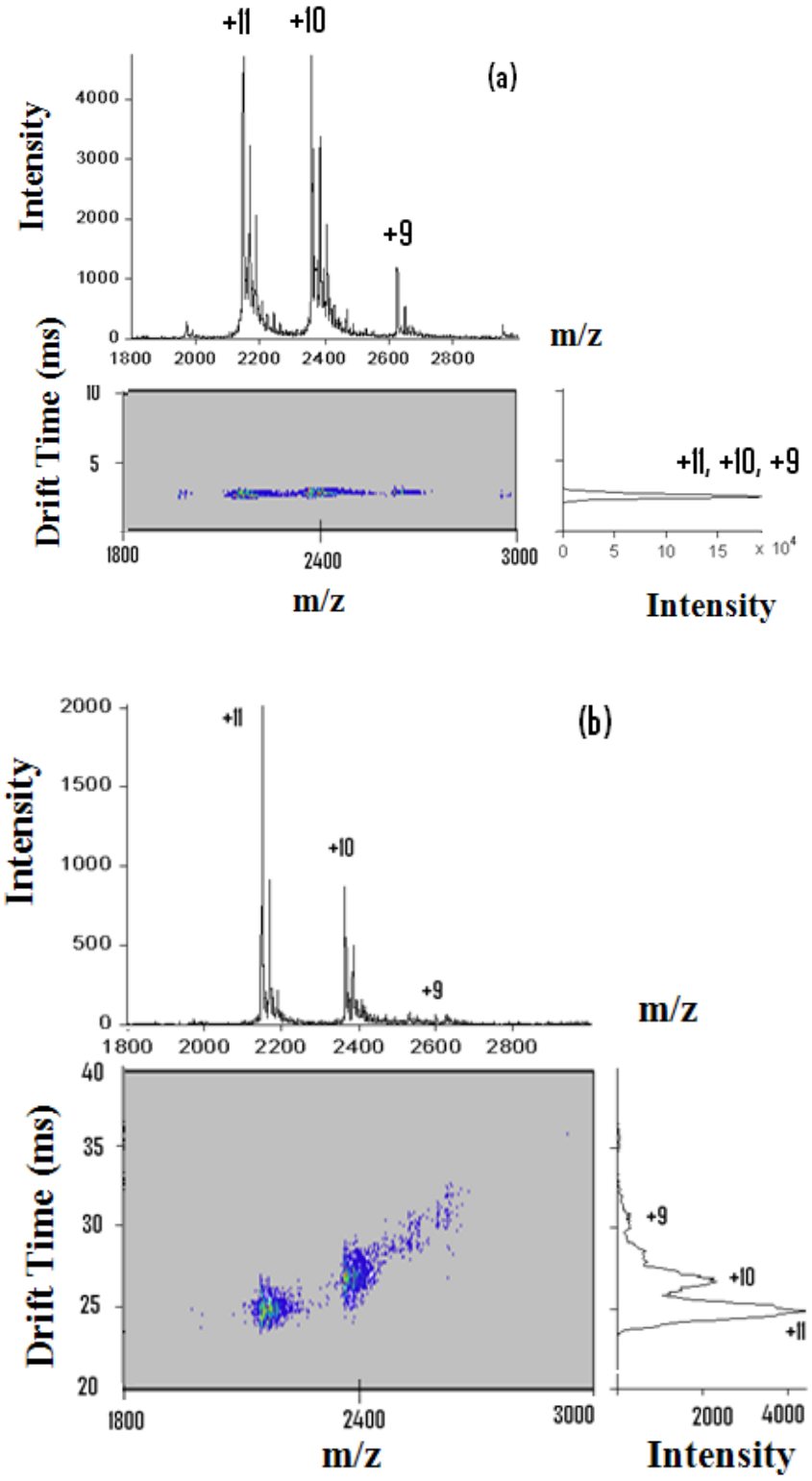

www.manaraa.com

Figure 3. Comparison of the ion mobility spectra of trypsin from the two ejection method. ~25 μM trypsin in water with 1% acetic acid. Drift pressure: 1.59 Torr, electric field: ~13 V/cm. For the pulsed ejection (PE) (a): 3 μs, -100V DC pulser was applied to the end cap of the ion trap. For the mass selective ejection (MSE) (b): RF was ramped from 1 kV to 5 kV in 80ms while a 47 kHz waveform was applied to the front cap of the ion trap with amplitude rampping up from 4 V to 41V in 80 ms.

www.manaraa.com

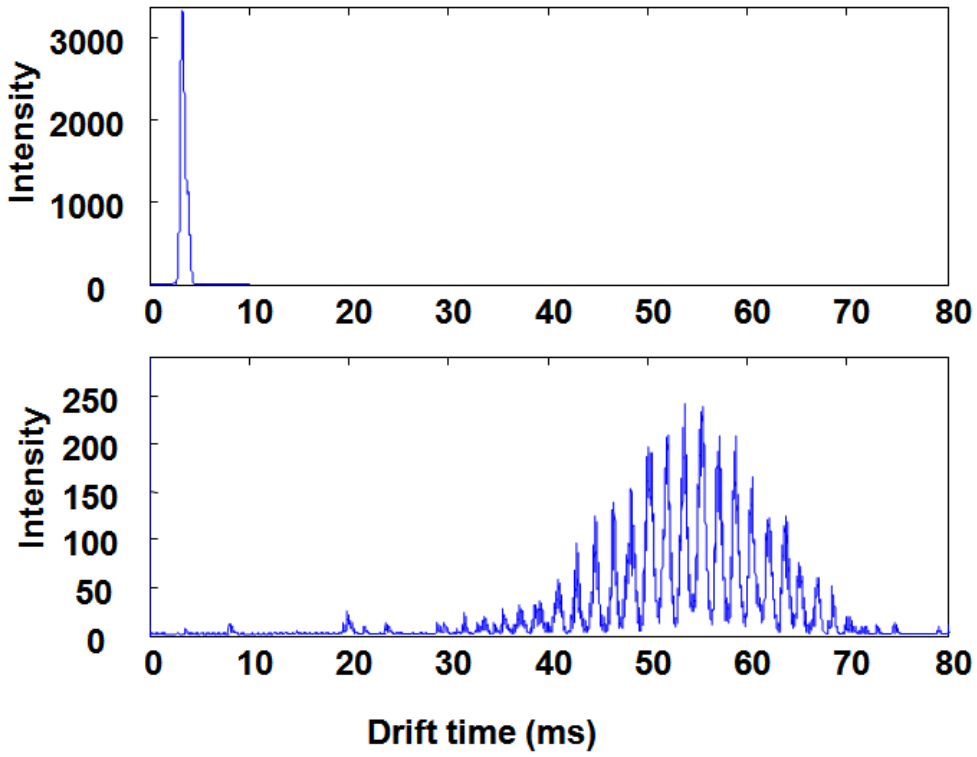

Figure 4. Comparison of the ion mobility spectra of albumin from the two ejection methods. ~20 µM Albumin in 100% water solution with 1% acetic acid. Drift pressure: 1.59 Torr, electric field: ~13 V/cm. For the pulsed ejection (PE) (top): 3 µs, -100V DC pulser was applied to the end cap of the ion trap. For the mass selective ejection (MSE) (bottom): RF was reverse- ramped from 5 kV to 1kV in 80ms while a 35 kHz waveform was applied to the front cap of the ion trap with an amplitude of 10 V.

www.manaraa.com

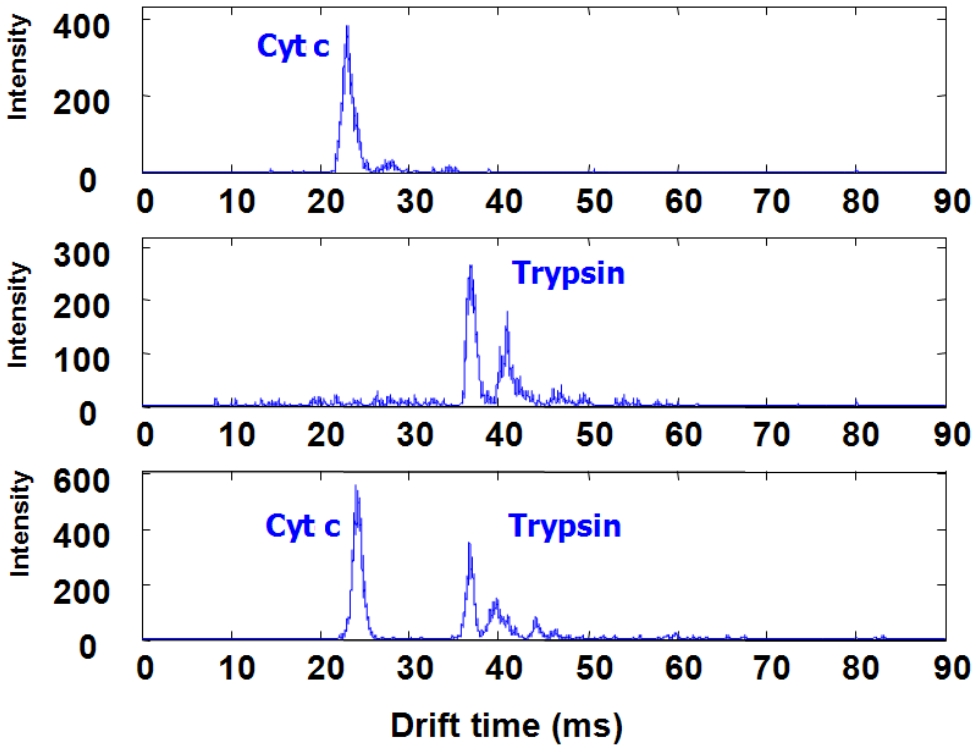

Figure 5. Comparison of the ion mobility spectra of a mixture of cytochrome c and trypsin obtained by mass selective ejection (MSE). Top: ~25 µM cytochrome c in water with 1% acetic acid. Middle: ~25 µM trypsin in water with 1% acetic acid. Bottom: mixture of ~13 µM cytochrome c and ~ 13 µM trypsin in water with 1% acetic acid. For the mass selective ejection (MSE) : RF was ramped from 1 kV to 5kV in 80 ms while a 47 kHz waveform was applied to the front cap of the ion trap with amplitude ramping from 4 V to 41 V.

www.manaraa.com

CHAPTER 5

CONCLUSION AND OVERVIEW OF FUTURE DIRECTIONS

The main work of this thesis is to combine ion mobility spectrometry with ion/ion reaction technique for mass spectrometry analysis of biological mixture. The first generation of the instrument on this purpose is a 3-D ion trap - ion mobility – time of flight mass spectrometer with three ion sources. Two sources are designed for positive and negative electrospray (ESI), and the third source is designed for atmospheric sampling glow discharge ionization (ASGDI). The amount of reagent and reaction time can be accurately controlled by software. The proton transfer reaction has been successfully performed on ubiquitin ions, reducing the charge state down to +1. Top-down protein analysis is also demonstrated on this instrument with ubiquitin ions. The intact uniquitin +7 ions can be fragmented by collision-induced dissociation (CID) in the IT and then charge reduced by ion/ion reactions also in the ion trap. The following ion mobility separation spreads the same charge state product ions in lines with the same slope and helps to identify the charge state and assignment of the fragments.

Although a lot of progress has been made to this instrument, a major factor preventing us from doing further experiments we have in mind is the sensitivity of the instrument. Since this instrument was designed and started from 2003, at a time that linear ion trap was not known, a 3-D ion trap was used to do ion/ion reactions. Based on the signal observed on the time –of –flight detector and the percentage of the ions transferring between the elements of the instrument, the number of ions trapped in the 3-D trap for each scan is

www.manaraa.com

close to the capacity of the 3-D ion trap. So, to improve the sensitivity of the instrument by a significant factor, the only way is to replace the 3-D ion trap with a linear ion trap.

A research-grade linear ion trap was built from all commercial available tri-filter quadrupole, controller and power supplies. The dual polarity trapping mode ion/ion reaction, transmission mode ion/ion reaction, and ion parking mode ion/ion reaction were also demonstrated with protein ions.

An important advantage of the linear ion trap is the dramatic increase in the trapping capacity and the varieties of ion/ion reaction capabilities. A future direction for the instrumentation area is to replace the 3-D ion trap in the instrument described in chapter 2 with a linear ion trap. The linear ion trap is very promising to improve the sensitivity and help the alignment with the drift tube so that signal won't be an issue bothering us all the time. The possible problem we have in mind now for replacing with a linear ion trap may be that the ejection of the ions from the linear ion trap won't be as fast as 3-D trap and this may affect the next ion mobility measurement. The way to solve this is to work with a smaller size linear ion trap (for example the same size as what has been used by Lee and his coworkers.)

The effect of charge reduction reaction on the conformation change of protein ions were studied in chapter 2 and chapter 3. The charge reduction reaction always forms the similar compact conformation for lower charge state ions, independent of the initial charge states, conformation, and solution conditions. And the lower charge state gas-phase ions have the cross-section close to that from the crystal structure. So the gas-phase ion/ion reaction provides a way to restore the folded structure of protein ions even they are unfolded during the transferring into gas-phase and vacuum system. Changing of the ejection pulse duration

www.manaraa.com

and magnitude can cause the unfolding and folding of cytochrome c +8 ions in μs scale if the pulse is more negative than the front of the drift tube. More studies on this should be carried on in the future.

Further studies on the conformation change from other type of other ion/ion reactions can also be studies on the new instrument, such as the effect from these reactions: electron transfer dissociation, protein-protein complex formation, and protein-metal or protein-ligand complex from ion exchange reaction.

A stepwise charge reduction method can be performed with the instrument control in this work, which is alternative experimental way to manipulate the product ion charge state to ion parking. A mass-selective ion trap ejection method was also developed, which improve the separation of ion mixtures with similar ion mobility but different m/z and maintain the ion mobility labeling ability for high throughput top-down parallel protein analysis.

The development of the instrumentation and methodology provides new analytical capabilities and enables the new biological studies to be envisioned. Although future development on the instrumentation is still needed and new technical problems may appear, this complicated instrument has included almost all the possible capabilities in the following areas:

1. Ionization: both positive and negative electrospray sources which are easy to couple with chromatographic method, and ASGDI source
2. Fragmentation: traditional CID in ion trap and transmission CID in quadrupole, and new complementary fragmentation ETD

www.manaraa.com

3. Separation: Ion mobility separation by size from the pulsed ejection, and by both size and mass from the mass-selective ejection.
4. Ion/ion reaction: charge reduction, complex formation and ETD
5. Identification: high resolution time-of-flight mass spectrometer
6. Computer control: precise power and timing control for each element.

We believe the application of this powerful instrument on top-down analysis of biological mixtures will be a lot of room to explore in the future.

www.manaraa.com

ACKNOWLEDGEMENTS

Funding for this work from Iowa State University: College of Liberal Arts and Sciences, Office of Biotechnology, Plant Sciences Institute, the Carver Trust and the Iowa State University Vice Provost for research are gratefully acknowledged. I would also like to thank the Dow Chemical for the Awards in Analytical Chemistry (ISU 2005-2006), Proctor & Gamble for the Awards in Analytical Chemistry (ISU 2007-2008) and Conoco-Phillips for the Fellowship (ISU 2007-2008).

There are a lot of acknowledgements I would like to address here in this last chapter. First of all, I would give my greatest appreciations to two professors, Dr. R.S. Houk and Dr. Ethan R. Badman, who lead me to walk through the research life for my Ph.D degree. I joined Dr. Badman's group in 2003, and he trained me from a mass spectrometry freshman to a Ph.D candidate. His mentoring in research, experimental expertise, smart mind and strict work rules benefit my work a lot. After Dr. Badman left ISU, Dr. Houk decided to accept me, and other my two members Matt and Gregg and help out to keep the whole lab from breaking apart. Without his effort in this event, I won't continue to work on the instrument we spent two years to built, and won't be able to finish my Ph.D now. Thanks a lot for Dr. Houk's guidance on my research and tremendous support.

I would like to thank my graduate committee members, Professor R.S. Houk, Professor Mei Hong, Professor Victor Shang-yi Lin, Professor Emily Smith, Professor Hans Stauffer, for spending so much time and help on my research work.

I would like to thank my great coworkers, Matt and Gregg, for their help with construction and maintenance of the instrument and the scientific discussion between us. I

www.manaraa.com

would also give my gratitude to all the brothers and sisters in Dr. Houk's group. Although I am not good at words to express myself, all of you provided a friendly home that always makes me feel not alone.

There are a lot of people in my life I would like to say more than thank you to them: my late mother - I know she is somewhere smiling and watching me and waiting for this moment in the other world, and she would be the most happy one to see this moment; my father, for his support on my studies and his understanding of me being away from home; my younger brother for his love and friendship; my major professors in Dalian University of Technology, professor Tianxi Cai and Professor Xinping Wang, for their encouragement and motivation to pursue my education in chemistry in the United States.

I would like to leave my last acknowledgement for my big families in Ames. I would like to thank Haitao, my husband, for his deep love, for teaching me of hope about life and positive attitude on things, and for his encouragement throughout some stressful times. I would like to thank Annie, my lovely daughter, for her eating and sleeping on time and making me smile all the time. And I also like to thank my parents-in-law for their taking care of Annie and their help on my life in Ames to finish this degree.

Qin Zhao

December 2008, Ames

www.manaraa.com

Appendix

A Linear Ion Trap Mass Spectrometer with Versatile Control and Data Acquisition for Ion/Ion Reactions

Matthew W. Soyk*†, Qin Zhao*, R.S. Houk*†, and Ethan R. Badman‡

*Iowa State University, Department of Chemistry, Ames, IA 50011 USA

†Ames Laboratory, U. S. Department of Energy, Ames, IA 50011 USA

‡Hoffman-La Roche Inc., Non-Clinical Safety, 340 Kingsland St., Nutley, NJ, 07100 USA

A manuscript accepted with revisions by the *Journal of the American Society for Mass Spectrometry*, 2008.

Abstract

A linear ion trap (LIT) with electrospray ionization (ESI) for top-down protein analysis has been constructed. An independent atmospheric sampling glow discharge ionization (ASGDI) source produces reagent ions for ion/ion reactions. The device is also meant to enable a wide variety of ion/ion reaction studies. To reduce the instrument's complexity and make it available for wide dissemination, only a few simple electronics components were custom built. The instrument functions as both a reaction vessel for gas-phase ion/ion reactions, and a mass spectrometer using mass-selective axial ejection. Initial results demonstrate trapping efficiency of 70 to 90% and the ability to perform proton

www.manaraa.com

transfer reactions on intact protein ions, including dual polarity storage reactions, transmission mode reactions, and ion parking.

Introduction

Linear quadrupole ion traps (LITs)[1] have been a subject of recent interest, primarily because of their higher performance compared to 3d ion traps. Until recently, LITs were mainly used as ion storage devices or as collision cells for tandem mass spectrometry (MS/MS) preceding another type of mass analyzer (e.g. TOF[2, 3] or FT-ICR[4, 5]). Compared to 3d traps, LITs offer higher injection efficiency (<10% vs. almost 100%, respectively) and, because of their larger volume, higher ion storage capacity, while still maintaining the ability to perform MS^N in a single device. More recently, two major innovations have led to widespread use of LITs as mass analyzers: radial[6] or axial[7] ejection methods. These LIT's still have high trapping efficiency and storage capacity, with the added benefits of mass analysis in a single device [8].

For top-down protein analysis, linear and 3d ion traps cannot achieve the ultrahigh mass resolution and accuracy of FT-ICR[9] or orbitrap instruments[10] necessary to resolve and unambiguously identify the isotopic distributions of highly multiply-charged ions. However, traps are well-suited to ion/ion reactions [11-13] like proton transfer to simplify the resulting complex, overlapping product ion spectra. Electron transfer dissociation (ETD)[11] ion/ion reactions also provide an alternative tool for protein ion dissociation. Ion/ion reaction experiments have been carried out in both types of LITs, and although ETD capabilities are

www.manaraa.com

becoming more readily available on commercial ion traps, proton transfer reaction capabilities are not yet commercially available.

In addition, many researchers would like greater control and flexibility over instrumental parameters than is typically available in commercial devices, especially for fundamental experiments and development of new methods. Here we discuss the development of an electrospray ionization (ESI)-linear ion trap mass spectrometer that has been constructed to enable complete control over all functions of the device. Mass scanning by radial ejection requires machining an exit slit and channel in least one of the quadrupole rods. To simplify measurment of mass spectra and allow the future addition of subsequent components, e.g., ion mobility and time of flight analysis, this device is operated using mass-selective axial ejection (MSAE) [14]. Commercially available components were used primarily to reduce the complexity of the development and allow wide dissemination of this device to other researchers. Initial performance characteristics for MS and gas phase ion/ion reactions are described, as well as future uses for this device in bioanalytical MS and as a source for ion mobility-TOF instruments.

McLuckey and co-workers have demonstrated the great value of commercial LITs with multiple pulsed ion sources, e.g. positive ESI for analyte ion formation plus negative ESI,[15-18] negative atmospheric pressure chemical ionization,[16, 18-21] or negative atmospheric sampling glow discharge ionization (ASGDI)[12, 22] for reagent ion formation. The present paper demonstrates the first work using an LIT with multiple continuous ion sources interfaced through a turning quadrupole that has proven valuable with 3d ion traps [23, 24].

www.manaraa.com

Experimental

Cytochrome *c*, ubiquitin and trypsin were purchased from Sigma-Aldrich (St. Louis, MO) and were used without further purification. Solutions of proteins were prepared at 20 to 30 μM in 1% aqueous acetic acid solutions for positive nano-ESI. Nano-ESI ionization emitters were pulled from glass capillaries (1.5 mm o.d., 0.86 mm i.d.) with a micropipette puller (Model P-97, Sutter Instruments, Novato, CA). The nano-ESI voltage was +1 kV to +1.2 kV applied to a stainless steel wire through the back of the capillary. Perfluoro-1, 3-dimethylcyclohexane (PDCH) was purchased from Sigma-Aldrich (St. Louis, MO) and was used as the reagent ion for proton transfer ion/ion reactions. The PDCH was ionized using an ASGDI source identical to that described by Zhao and co-workers [25].

Instrumentation

Figure 1 shows a schematic diagram of the LIT with two ion sources: one ESI and one pulsed ASGDI source that are interfaced to the LIT through a quadrupole deflector. It should be noted that a third ion source could be added to the blank flange of the ion source cube shown in Figure 1. The LIT is a standard quadrupole mass filter modified to enable LIT functionality. Ions are detected with a conversion dynode/electron multiplier. Instrument control is via a commercially available ion trap controller and software. Figure 2 shows a schematic diagram of how the ion trap controller and software communicate with and control all components of the LIT. Details about each part of the instrument are given below.

www.manaraa.com

Vacuum System. The two ion sources and ion optics are housed in an 8" conflat cube, and the LIT is housed in an 8" conflat 5-way cross. One turbo pump (Turbo-V550 MacroTorr, 550 l/s N_2, Varian Inc., Palo Alto, CA) is attached to the top of the cube that houses the ion sources, and a second, identical turbo pump is attached to the 5-way cross that houses the LIT. The turbo pump on the source cube is backed by a SD-301 mechanical pump (Varian Inc., Palo Alto, CA), and the turbo pump on the LIT 5-way cross is backed by an E2M40 mechanical pump (BOC Edwards, Wilmington, MA). The chamber pressure is measured by a Micro-Ion Gauge (Helix Technology, Longmont, CO). The baseline pressure of the system is ~5 x 10^{-7} mbar.

Ion Sources and Ion Optics. Both ion sources have been described [24, 25]. Typical pressures in the ion source interface regions (i.e. behind the first 254 μm aperture to atmosphere and before the second 381 μm aperture to the high vacuum region) are 0.90 mbar and 0.80 mbar for the nano-ESI and ASGDI source, respectively. Each is pumped by a separate E2M40 mechanical pump. The pulsed ASGDI was initiated via a -400 V high voltage pulse supplied via a power supply (Model 556, Ortec, Oak Ridge, TN) through a fast pulser (Model PVX4150, Directed Energy Inc., Fort Collins, CO). Voltages for the interfaces and the first three lenses are supplied via 9 output power supplies (Model TD9500, Spectrum Solutions, Russelton, PA). The voltages on the quadrupole deflector (Model 81989, Extrel CMS, Pittsburgh, PA) and on the three lenses between the quadrupole deflector and the LIT are supplied via additional 9 output power supplies, but are switched using a computer-controlled fast relay switch to enable ions from each source to be focused separately to the

www.manaraa.com

LIT as required. The ASGDI source is the default ion source. A single TTL trigger is used to switch the optics to allow ESI ions to enter the trap, and a second TTL trigger is used to pulse on the ASGDI discharge.

Linear Ion Trap. The LIT is a commercially available tri-filter quadrupole in a collision cell housing (r_0 = 9.5 mm, Extrel CMS, Pittsburgh, PA). The rf trapping voltage is supplied by a standard Extrel 300 W rf only power supply providing 3600 $V_{0\text{-}p}$ (pole to ground) at 880 kHz. In order to operate the quadrupole as an LIT, and perform MSAE [14] and MS/MS experiments, modifications were made to the quadrupole and rf electronics.

As described by Paul,[26] additional waveforms can be added to quadrupole rods to resonantly excite ions. Douglas and coworkers [2, 3] add dipolar excitation across a pair of opposite quadrupole rods to excite trapped ions for collision-induced dissociation and MS/MS. We implemented dipolar excitation by cutting the connections between one set of rods and add an extra rf post and hole through the collision cell housing. To add the dipolar excitation voltage to the rf trapping voltage on one set of rods, a toroidal transformer was used. The toroid (Model 5977003801, Fair-Rite, Wallkill, NY) was housed in a metal casing outside the vacuum chamber. The turn ratio between the primary and secondary was 1:1 using 16 turns of 22 gauge magnet wire (Belden Corporation, Chicago, IL). One of the outputs of the rf power supply was connected to the center tap of the secondary. The outputs of the secondary are then fed to the quadrupole rods through rf feedthroughs (Model 810998, Extrel CMS, Pittsburgh, PA). One side of the primary was grounded, and the other was connected to the waveform generator.

www.manaraa.com

The MSAE and MS/MS waveforms were generated from the ion trap controller. The original 5 $V_{0\text{-}p}$ was amplified to 35.5 $V_{0\text{-}p}$ using a custom amplifier (PA09 op-amp, Apex Microtechnology, Tucson, AZ) and applied to the primary of the transformer through a 50 Ω, 51 W resistor.

Two additional modifications to the quadrupole were required for effective trapping and m/z analysis. The post-filter was removed, and the pre-filter was shorted to the center quad section. The center rod section is the only section that is aligned with high precision. Therefore, removing the post-filter ensures that the fringe fields necessary for MSAE occur between the optimally-aligned center rod section and the exit aperture IQ2. Shorting the front and center sections together applies the full rf voltage to the entire trapping length and minimizes ion loss (from unequal potential well depths) as ions are trapped. This modification is especially important during charge reduction ion/ion reactions. As ions with a lower z –and correspondingly higher m/z—are formed, they will reside in increasingly shallower potential wells. Without the full rf voltage on both the center and the pre-filter section, ions at high m/z are no longer trapped and are lost.

DC voltages (0-4 V) from an Argos ion trap controller (described in detail below) are amplified to ± 200 V (PA97 op-amp, Apex Microtechnology, Tucson, AZ), and controlled in the scan function with the ion trap controller. These dc voltages are applied to the entrance and exit lenses (IQ1, IQ2) and LIT rods (Q). The IQ1 and IQ2 lenses are 8 mm diameter and both are covered with nickel mesh (90% transparency, 70 lines per inch, InterNet Inc., Anoka, MN) on the interior side of the lenses. The distance from the IQ1 lens to the end of

www.manaraa.com

the quadrupole rods is ~5 mm. The IQ2 lens was modified to make the distance from the lens to the end of the quadrupole rods ~2 mm.

In order to fully resonate the rf power supply after adding the toroidal transformer and changing the arrangement of the quad sections, the overall capacitance of the load was reduced by the following measures. 1) The original rf cable between the power supply and the transformer was shortened by 53 cm, from 166.3 cm to 113.3 cm. 2) the magnet wire used in the toroidal transformer was covered with Teflon tubing (1.7 mm O.D., 1.1 mm I.D.). 3) A 3 pF capacitor in the rf power supply near the output on both the toroid and non-toroid sides was removed. 4) The tap of the rf coil was moved to remove 2.25 turns on the toroid side and 1 turn on the non-toroid side. By performing these steps, the power supply could generate nearly the maximum original rf voltage, as read by the internal feedback circuit.

To make sure similar rf voltages were applied to each of the quadrupole rods, two duplicate rf detector circuits identical to those used by the Extrel power supply were built. These devices convert the rf voltage to a current that can be read with a digital multimeter. Using this method, the two sides of the rf output could be tuned to be within 1.99 ± 0.25% of each other, limited by the accuracy of the digital multimeter.

The nitrogen buffer gas pressure in the LIT is adjusted using a variable leak valve (Model 203, Helix Technology, Longmont, CO) and measured by the pressure in the main chamber using the Micro-Ion Gauge. During a typical experiment, the chamber pressure is maintained at ~1.3×10^{-4} mbar with both sources open and nitrogen gas added to the LIT. Of course, the pressure inside the LIT is higher than that measured by the ion gauge. From the sizes of the IQ1 and IQ2 lenses (8 mm diameter), the 90% mesh covering the lenses, the

www.manaraa.com

measured pressure in the vacuum chamber ($1.3x10^{-4}$ mbar), and the pumping speed (550 l/s), the pressure inside the LIT is estimated to be $5x10^{-3}$ mbar, assuming effusive flow out of IQ1 and IQ2.

Mass spectra are acquired using MSAE by ramping the rf voltage while applying a dipolar resonance excitation frequency and a small, constant, repulsive voltage to IQ2 (typically +1 to +3 V for positive ions), while the dc voltage on the LIT rods is kept at ground. Ejected ions are detected with an electron multiplier with conversion dynode (402A-H, Detector Technology Inc., Palmer, MA). Scans were measured only in the forward direction, from low m/z to high m/z.

Modifications for Ion/Ion Reactions with Dual Polarity Trapping. In order to perform dual polarity storage mode ion/ion reactions, and store both positive and negative ions simultaneously, AC voltages are applied to IQ1 and IQ2 during PDCH injection and subsequent reaction time [11]. This axial trapping voltage is generated via a multifunction PC card (Model 6251, National Instruments, Austin TX) with custom software written in Labview 8.0. The frequency and amplitude are set in the software—and are, therefore, fixed during an experiment—and the waveform is switched on and off via a TTL trigger (1 μs delay). The initial 0-5 $V_{0\text{-}p}$ sine wave is amplified via a custom amplifier (PA90, Apex Microtechnology, Tucson, AZ) up to 175 $V_{0\text{-}p}$ and split into two 180° out-of-phase signals. The ac voltages are added to the dc voltage for IQ1 and IQ2 using a simple mixer circuit. Typically, the waveform is applied at 100 kHz, with an amplitude of ~50 $V_{0\text{-}p}$, empirically

www.manaraa.com

determined to minimize ion loss during the reaction period. The amplitude and frequency of this waveform are lower than those used by McLuckey and coworkers [17].

In the first scan function segment of a dual polarity trapping ion/ion reaction, three processes are done simultaneously—the dc potentials on the IQ1 and IQ2 lenses are set to 0V (the same potential as the quadrupole rods), the axial trapping waveform is turned on, and the ASGDI source is pulsed on. In the second segment, the ASGDI source is turned off, and the analyte and reagent ions are allowed to react. To end the reaction, the axial trapping waveform is turned off and the dc potentials on the IQ1 and IQ2 lenses are, simultaneously, set to repel (i.e., trap) the positive analyte ions, while excess negative reagent ions are ejected out both ends of the LIT.

Ion/Ion Reactions in Transmission Mode and Ion Parking. Another method for enabling ion/ion reactions, transmission mode reactions, has been described previously [15, 19]. Transmission mode reactions are enabled by trapping the analyte ions using small repulsive dc voltages (typically 2 to 5 V) on the IQ1 and IQ2 lenses and passing the reagent ions, continuously generated by the ASGDI source during the reaction time, through the population of trapped analyte ions. Any unreacted reagent ions pass completely through the LIT and are lost. Ending the transmission mode reactions simply requires turning off the ASGDI source, thus turning off the reagent ion beam. The reaction product ions remain trapped in the LIT because they are the same polarity as the unreacted analyte ions.

Ion/ion reactions carried out using this method do not require the use of the axial trapping waveform, and there is only one scan segment for the reaction period. Therefore, the

www.manaraa.com

scan function for transmission mode ion-ion reactions is simpler than that for dual polarity trapping ion-ion reactions. Additionally, the electronics required to add the dual polarity trapping waveform to the containment lenses are not required, making the LIT hardware for transmission mode reactions much simpler than that for dual polarity storage mode reactions.

Ion parking [27] is a technique that was developed by McLuckey and co-workers in which the rate of reaction for ions at a single m/z value [27] or multiple m/z values [28, 29] are selectively reduced. Increasing the relative velocity of reactant ions, which reduces the ion/ion reaction capture cross section, during an exothermic ion/ion reaction decreases the rate of reaction between those ions [27]. To enable ion parking, a low amplitude auxiliary sine wave (~1$V_{0\text{-}p}$, ~ 40 kHz for the ions chosen here) is added to the x-rods of the LIT during the ion/ion reaction period. The auxiliary sine wave resonantly excites a particular product ion formed during the ion/ion reaction. The frequency and amplitude of the sine wave are chosen so that the ion being parked is excited enough to inhibit the reaction rate but not so much that it is ejected from the LIT. These values are fine-tuned empirically to produce the desired results. As the reaction proceeds and the ion chosen to be parked is formed, it is resonantly excited by the applied auxiliary sine wave. The velocity of the excited ion relative to the reagent anion increases, thereby reducing its ion/ion reaction rate and minimizing further reaction. For the proton transfer ion/ion reactions on intact protein ions studied here, the result of an ion parking experiment is the concentration of most of the ions into a single charge state below that of the original ions.

www.manaraa.com

Electronics. An Argos ion trap controller (Griffin Analytical Technology, West Lafayette, IN) controls the entire instrument and acquires data. The scan function is generated by the Argos software. TTL pulses ("relays") trigger the ASGDI source, switch the fast relay switch to enable injection of oppositely-charged ions, and toggle on the ion/ion trapping voltage. The two waveform outputs control the rf level (0-10 V control 0-3600 $V_{0\text{-}p}$ of rf) and generate MS/MS waveforms, respectively. Different from previous versions of the Argos software, this version provides time dependent dc voltages (0-4 V "registers") that control the voltages applied to IQ1, IQ2, and the LIT rods.

Data are acquired using the Argos data input (at a 250 kHz sampling rate), but as a result, the data acquisition time is limited to 250 ms or less. Primarily, this limits the ability to perform slow mass scans over a wide mass range.

Results and Discussion

LIT Performance. Initial characterization of the LIT includes determination of trapping efficiency, ion capacity, mass analysis efficiency, and measurement of mass accuracy. To determine the trapping efficiency, ions are gated into the trap for a specified time, cooled, and then dumped to the detector (in a non-mass selective manner) by dropping the IQ2 voltage. The response from the trapped ions is then compared to the response acquired during operation of the quadrupole as an rf-only ion guide for the same time as the trap fill time at the same rf level.

Table 2 shows trapping efficiencies at 4 different fill times for positive ions of cytochrome *c* and trypsin generated by ESI. Efficiencies average 83% with a range from 68

www.manaraa.com

to 92%. These values agree with those determined previously from other LIT instruments [6, 7].

Figure 3 shows a plot of total ion current (TIC) vs. LIT fill time for cytochrome *c* that is used to measure the ion capacity of the LIT. The response is nearly linear from 5 to 40 ms, after which the signal levels off. The ion current on IQ1 was then measured—with all LIT and ion detector voltages turned off—using a picoammeter (Model 6485, Keithley Instruments, Cleveland, OH) to determine the real number of ions delivered to the trap. It was assumed that the rate of ions that strike the wires of the Ni mesh covering IQ1, after accounting for the 90% transmission, approximates the rate at which ions are delivered to the LIT during the fill step of a trapping experiment. Using the average measured ion current from the IQ1 Ni mesh (7.97 pA), the correction for the 90% transmission, the fill time at which the response levels off (40 ms), the measured trapping efficiency (83%), and the average charge state of the cytochrome *c* ions used for the measurement (+8.5), it was determined that approximately 1.9×10^6 ions can be trapped in the LIT. The maximum total charge in the LIT is thus ~ 1.6×10^7 charges. In order to avoid space charge effects, the LIT is not filled to this capacity during normal operation.

Mass Spectra. A typical protein mass spectrum taken using MSAE is shown in Figure 4. The inset of Figure 4 shows the peak shape for the +9 charge state of cytochrome *c*. This peak has a full-width at half maximum (fwhm) of 1.11 Th, corresponding to a resolution of 1230. The measured fwhm from the LIT is about 1.4x larger than the calculated width of

www.manaraa.com

the isotopic envelope (0.77 Th, fwhm). Of course, resolving the isotopic distribution of this peak requires resolution in excess of ~18000 (50% valley).

Table 1 shows the trapping voltages and ejection conditions used to take the spectrum shown in Figure 4. These operating conditions are typical for mass spectra taken with the LIT. The spectrum in Figure 4 shows adduct or impurity peaks at 54 Da, 90 Da, and 130 Da above each protein peak. The scan function used to generate this spectrum includes a heating ramp in which a 1.9 $V_{0\text{-}p}$, 150 kHz sine wave is applied to the x-rods while the rf amplitude is ramped to bring the protein ions into resonance with the applied sine wave. Thus the ions are heated, and the adducts/impurities are dissociated. Without this heating ramp, the overall protein peak is very wide, encompassing the protein and all the adduct/impurity ions into a single wide peak. The adduct/impurity peaks could not be totally eliminated without severely reducing the intensity of the protein peak. It should also be noted that these same adduct peaks are seen from the same protein samples on another home-built MS in our lab [25].

The mass analysis efficiency is measured using a similar procedure as the trapping efficiency measurement. Protein ions are gated into the LIT for a specified time, cooled, and non-mass selectively emptied to the detector by dropping the potential on IQ2. In a second experiment, protein ions are gated into the LIT for the same specified time—ensuring that the number of ions inside the trap is approximately the same for both experiments—cooled, and mass analyzed using MSAE. The ratio of the TIC of the ions ejected under MSAE conditions to the TIC of all the ions trapped (measured by non-mass selectively ejecting ions) yields an average measured MSAE efficiency of 7.4±2.2%. Using the average measured MSAE efficiency and the overall length of the LIT (18.7 cm), it was calculated that the extraction

www.manaraa.com

region is 18.7 x 0.074 = 1.4 cm long. The measured efficiency and extraction region length are less than the results obtained by Hager [7] at similar LIT pressure. Conversely, the measured MSAE efficiency is slightly higher than recent results obtained by Douglas and co-workers [30]. Our measured efficiency may be higher due to higher pressure in the LIT and the lower spectral resolution than in the results recorded by Douglas.

Table 2 shows MSAE efficiency measurements for different fill times of cytochrome *c* and trypsin. The data shows that as fill time increases the MSAE efficiency decreases. Space charge effects may degrade the MSAE efficiency at longer fill times.

Mass accuracy was determined by spraying a 50:50 mixture of cytochrome *c* and ubiquitin. The peak maxima for $[M+9H]^{9+}$ and $[M+8H]^{8+}$ of the cytochrome *c* ions (m/z ~ 1360 and 1530) were used to calibrate the m/z axis and the m/z at the peak maxima of $[M+7H]^{7+}$ and $[M+6H]^{6+}$ ions of ubiquitin (m/z ~ 1224 and 1429) were measured. Measured mass accuracies range from 900 to 2200 ppm. The accuracy limitations are likely due to voltage stability for the rf trapping voltage, resonance excitation voltage, and/or IQ2 dc voltage. The use of calibrant ions in a m/z window that span that of the analyte may also improve mass measurement accuracy.

To illustrate the performance of the LIT as a mass analyzer at moderate m/z values, a spectrum of the PDCH reagent anions from the glow discharge source is shown in Figure 5a. These ions are a mixture of $[M-F]^-$ and $M^{\cdot-}$ [31]. The inset shows the peak shape and resolution for the $[M-F]^-$ ion. The ^{13}C isotope peak is cleanly resolved from the main peak at m/z 381. The nominal resolution value $m/\Delta m$ = ~1080 at fwhm.

www.manaraa.com

It should be noted that nonlinear resonance ejection peaks can be seen under certain conditions. These "ghost peaks" [32] occur at a q_z value of 0.64 (β=0.5 or 220 kHz in this system) consistent with octopolar field ejection [33]. Use of resonance ejection frequencies near this nonlinear resonance can produce asymmetric or split peaks. Therefore, the resonance ejection frequency is selected to avoid this nonlinear resonance value.

Dual Polarity Trapping Mode Ion/Ion Reactions. The application of the dual polarity storage mode waveform used for ion/ion reactions is similar to that described previously [11]. The dual polarity storage mode proton transfer ion/ion reaction scan function consists of the following steps: filling the trap with protein cations, a cooling segment, a heating ramp to eliminate adduct peaks from the protein, another cooling segment, a PDCH fill segment, an additional reaction segment, a final cooling segment, and mass analysis.

The results of such a dual polarity storage mode reaction between trypsin positive ions and negative PDCH ions are shown in Figure 5. The mass spectrum of the trypsin ions formed directly from ESI is shown in Figure 5b. The main ions observed under these sample and source conditions are the $[M+11H]^{11+}$ and $[M+10H]^{10+}$ charge states, with small amounts of the $[M+9H]^{9+}$ and $[M+12H]^{12+}$ charge states. In the subsequent parts of Figure 5, the LIT is also filled with negative ions from PDCH (Figure 5a) for either 15 or 20 ms. The PDCH fill step is followed by a period of dual polarity storage where the positive trypsin ions and negative PDCH ions are allowed to react further. The amplitude of the LIT rf voltage during the ion/ion reaction periods is set at 360 $V_{0\text{-}p}$, leaving the most abundant PDCH ion ($[M\text{-}F]^-$) at q=0.74. This amplitude rf was empirically chosen to maximize the amount of high mass

www.manaraa.com

product ions that are trapped while still trapping the PDCH reagent ion. The dual polarity trapping waveform added to IQ1 and IQ2 during the ion/ion reaction periods is a 100 kHz sine wave with an amplitude of 50 $V_{0\text{-}p}$.

A PDCH fill time of 15 ms and additional reaction time of 100 ms converts the trypsin ions shown in Figure 5a to the $[M+3H]^{3+}$, $[M+2H]^{2+}$, and $[M+H]^{+}$ charge states (Figure 5c). Continuing the reaction for times in excess of 100 ms does not result in further conversion of trypsin ions to lower charge states (data not shown). Thus, all the PDCH anions that were trapped in a 15 ms fill time have been reacted after a 100 ms reaction.

Figure 5d results when this dual polarity storage mode reaction experiment is repeated with a PDCH fill time of 20 ms and an additional reaction time of 100 ms. The multiply charged trypsin ions from Figure 5b are converted to primarily $[M+H]^{+}$, m/z = ~24,000. The fwhm of the peak for this ion is 673 Th, and the resolution is 34. At this time, the $[M+H]^{+}$ ion of trypsin is the highest m/z ion created and ejected from this LIT. To achieve the mass range extension required to eject the $[M+H]^{+}$ ion of trypsin, a 35 kHz sine wave was added to the LIT rods during the mass scan. The amplitude of this resonant excitation sine wave was ramped from 8.9 $V_{0\text{-}p}$ to 24.8 $V_{0\text{-}p}$. The dc voltage on the IQ2 lens was set to be 2.5 V relative to the LIT rod bias (0 V dc).

Transmission Mode Ion/Ion Reactions. Results of proton transfer ion/ion reactions of multiply charged ubiquitin cations with PDCH anions are shown in Figure 6. During the transmission mode reaction period, the amplitude of the LIT rf voltage is set at 360 $V_{0\text{-}p}$, leaving the most abundant PDCH ion ($[M-F]^{-}$) at q=0.74, an equivalent value to dual polarity

www.manaraa.com

trapping mode experiments. Also, injecting reagent anions at high q-values results in the greatest spatial overlap between the analyte and reagent ions, maximizing the ion/ion reaction rate [15, 19]. The dc voltages on IQ1 and IQ2 were set at 3 V repulsive relative to the rod dc bias (0 V).

Figure 6a shows the mass spectrum of ubiquitin obtained directly from ESI. The solution and ESI source conditions yield ubiquitin ions primarily in the $[M+6H]^{6+}$ to $[M+8H]^{8+}$ charge states. As shown in Figure 6b, transmission mode reaction with PDCH anions for 40 ms converts approximately half these ions to the $[M+3H]^{3+}$ to $[M+5H]^{5+}$ charge states, while the other half of the ions are lost. Extending the reaction period to 70 ms converts the ions to roughly equal amounts of $[M+H]^{+}$ and $[M+2H]^{2+}$ (Figure 6c). In the latter experiment, continuing the reaction long enough to reduce the ions to $[M+H]^{+}$ and $[M+2H]^{2+}$ results in peaks that are only ~10% as high as those for the original spectrum. Most of this is due to ion losses from the ion/ion reaction, but some is attributed to loss in detector response for ions with lower charge. The same effect is seen in Figure 5 for trypsin in dual polarity storage mode. Others also report ion losses of similar magnitude as a consequence of ion/ion reactions, in either 3d ion traps or LITs [15, 27].

Ion Parking. Ion parking should alleviate some of the ion losses during proton transfer reactions. Results from such an experiment involving cytochrome *c* ions are shown in Figure 7. Here the vertical scales have been kept constant so the signals can be compared more easily. The pre-ion/ion reaction spectrum of cytochrome *c* (Figure 7a) shows mostly the $[M+9H]^{9+}$ and $[M+8H]^{8+}$ charge states. A transmission mode reaction enabled by passing

www.manaraa.com

PDCH anions through the population of trapped cytochrome *c* ions for 20 ms yields a variety of peaks from $[M+7H]^{7+}$ to $[M+4H]^{4+}$, all with low abundances (Figure 7b). In Figure 7c, a waveform selected to excite the $[M+7H]^{7+}$ ion (1.8 V_{0-p} and 42 kHz) is applied to the x-rods during the transmission mode reaction period. With ion parking enabled, most of the resulting product ions remain in the $[M+7H]^{7+}$ charge state; about 20% react further to form $[M+6H]^{6+}$ and a small amount of $[M+5H]^{5+}$. The signal in the $[M+7H]^{7+}$ charge state after the reaction with ion parking (Figure 7c) is about half of the total ion signal present in the $[M+9H]^{9+}$ and $[M+8H]^{8+}$ charge states created directly from the ESI source (Figure 7a), which is a much less severe compromise of signal than that shown for ion/ion reactions without ion parking in Figures 5 and 6.

Conclusion

A research-grade LIT with multiple ion sources was designed and constructed using primarily commercially available components. Preliminary experiments show that its trapping efficiency is similar to that of commercial LITs and its performance as a mass spectrometer is good compared to the theoretical peak width of the cytochrome *c* charge states. Ion/ion reaction capabilities in both dual polarity storage mode and transmission mode were also demonstrated. The device operates under versatile computer control that should facilitate application to various schemes for ion/ion reactions and other ways to manipulate ions.

Future plans for this instrument include: enabling top-down protein analysis, including both collision induced dissociation followed by proton transfer ion/ion reactions as

www.manaraa.com

well as electron transfer dissociation (ETD) [11]. A second plan for this instrument is writing a data acquisition program in Labview 8.0 to enable data acquisition with the National Instruments multifunction PC card mentioned earlier. This modification should allow measurement times longer than the 250 ms limit of the Argos data acquisition system. Another future use for this instrument is to replace the 3d ion trap as the source for an ion mobility-time-of-flight (IMS-TOF) device that was built in our lab [25].

Acknowledgments

The authors acknowledge the following individuals: Chris Doerge and Don Douglas for helpful discussions and advice on construction of the toroidal transformer; Gregg Schieffer for help with testing of the custom electronics; Dick Egger, the late Steve Lee, and Terry Soseman (ISU Chemistry Machine Shop) for precision machining; Charlie Burg (Ames Lab ESG) for vacuum welding; Lee Harker (Ames Lab ESG) and Chuck Reese (ISU Chemistry) for custom electronics design, construction, and maintenance; Brian Regel and Brian Lippert at Extrel CMS for helpful discussion about the rf electronics; Brent Knecht, Brent Rardin and Mitch Wells (Griffin Analytical Technologies) for development and testing of the LIT software; Scott McLuckey for the plans for the computer-controlled fast relay switch; and James Hager, MDS Sciex, for discussions about improving the performance of the LIT. This work was funded by a grant from the Iowa State University Vice Provost for Research. MS acknowledges Extrel CMS for the Richard A. Schaeffer Memorial Travel Award to present this work at the 2006 ASMS Conference. MS also acknowledges the Velmer A. and Mary K. Fassel Fellowship (Iowa State University, 2006-2007), the Conoco-

www.manaraa.com

Phillips Fellowship (Iowa State University, 2006-2007), and the GAANN Fellowship (Iowa State University, 2008) for financial support.

www.manaraa.com

References

1. Douglas, D. J.; Frank, A. J.; Mao, D. M. Linear ion traps in mass spectrometry *Mass Spectrom. Rev.* **2005**, *24*, 1-29
2. Campbell, J. M.; Collings, B. A.; Douglas, D. J. A new linear ion trap time-of-flight system with tandem mass spectrometry capabilities *Rapid Commun. Mass Spectrom.* **1998**, *12*, 1463-1474
3. Collings, B. A.; Campbell, J. M.; Mao, D. M.; Douglas, D. J. A combined linear ion trap time-of-flight system with improved performance and MSn capabilities *Rapid Communications in Mass Spectrometry* **2001**, *15*, 1777-1795
4. Harkewicz, R.; Belov, M. E.; Anderson, G. A.; Pasa-Tolic, L.; Masselon, C. D.; Prior, D. C.; Udseth, H. R.; Smith, R. D. ESI-FTICR mass spectrometry employing data-dependent external ion selection and accumulation *J. Am. Soc. Mass Spectrom.* **2002**, *13*, 144-154
5. Syka, J. E. P.; Marto, J. A.; Bai, D. L.; Horning, S.; Senko, M. W.; Schwartz, J. C.; Ueberheide, B.; Garcia, B.; Busby, S.; Muratore, T.; Shabanowitz, J.; Hunt, D. F. Novel linear quadrupole ion trap/FT mass spectrometer: Performance characterization and use in the comparative analysis of histone H3 post-translational modifications *J. Proteome Res.* **2004**, *3*, 621-626
6. Schwartz, J. C.; Senko, M. W.; Syka, J. E. P. A two-dimensional quadrupole ion trap mass spectrometer *J. Am. Soc. Mass Spectrom.* **2002**, *13*, 659-669
7. Hager, J. W. A new linear ion trap mass spectrometer *Rapid Commun. Mass Spectrom.* **2002**, *16*, 512-526
8. Jonscher, K. R.; Yates, J. R. The quadrupole ion trap mass spectrometer - A small solution to a big challenge *Anal. Biochem.* **1997**, *244*, 1-15
9. Reid, G. E.; McLuckey, S. A. 'Top down' protein characterization via tandem mass spectrometry *J. Mass Spectrom.* **2002**, *37*, 663-675
10. Hu, Q. Z.; Noll, R. J.; Li, H. Y.; Makarov, A.; Hardman, M.; Cooks, R. G. The Orbitrap: a new mass spectrometer *J. Mass Spectrom.* **2005**, *40*, 430-443
11. Syka, J. E. P.; Coon, J. J.; Schroeder, M. J.; Shabanowitz, J.; Hunt, D. F. Peptide and protein sequence analysis by electron transfer dissociation mass spectrometry *Proc. Natl. Acad. Sci. U. S. A.* **2004**, *101*, 9528-9533
12. Yu, X.; Jin, W.; McLuckey, S. A.; Londry, F. A.; Hager, J. W. Mutual storage mode ion/ion reactions in a hybrid linear ion trap *J. Am. Soc. Mass Spectrom.* **2005**, *16*, 71-81
13. Stephenson, J. L.; McLuckey, S. A. Simplification of product ion spectra derived from multiply charged parent ions via ion/ion chemistry *Anal. Chem.* **1998**, *70*, 3533-3544
14. Londry, F. A.; Hager, J. W. Mass selective axial ion ejection from a linear quadrupole ion trap *J. Am. Soc. Mass Spectrom.* **2003**, *14*, 1130-1147
15. Liang, X. R.; McLuckey, S. A. Transmission mode ion/ion proton transfer reactions in a linear ion trap *J. Am. Soc. Mass Spectrom.* **2007**, *18*, 882-890

www.manaraa.com

16. Liang, X. R.; Han, H. L.; Xia, Y.; McLuckey, S. A. A pulsed triple ionization source for sequential ion/ion reactions in an electrodynamic ion trap *J. Am. Soc. Mass Spectrom.* **2007**, *18*, 369-376
17. Xia, Y.; Liang, X. R.; McLuckey, S. A. Pulsed dual electrospray ionization for ion/ion reactions *J. Am. Soc. Mass Spectrom.* **2005**, *16*, 1750-1756
18. Xia, Y.; Chrisman, P. A.; Erickson, D. E.; Liu, J.; Liang, X. R.; Londry, F. A.; Yang, M. J.; McLuckey, S. A. Implementation of ion/ion reactions in a quadrupole/time-of-flight tandem mass spectrometer *Anal. Chem.* **2006**, *78*, 4146-4154
19. Liang, X. R.; Hager, J. W.; McLuckey, S. A. Transmission mode Ion/Ion electron-transfer dissociation in a linear ion trap *Anal. Chem.* **2007**, *79*, 3363-3370
20. Liang, X. R.; Xia, Y.; McLuckey, S. A. Alternately pulsed nanoelectrospray ionization/atmospheric pressure chemical ionization for ion/ion reactions in an electrodynamic ion trap *Anal. Chem.* **2006**, *78*, 3208-3212
21. Han, H. L.; Xia, Y.; McLuckey, S. A. Ion trap collisional activation of c and z(center dot) ions formed via gas-phase ion/ion electron-transfer dissociation *J. Proteome Res.* **2007**, *6*, 3062-3069
22. Wu, J.; Hager, J. W.; Xia, Y.; Londry, F. A.; McLuckey, S. A. Positive ion transmission mode ion/ion reactions in a hybrid linear ion trap *Anal. Chem.* **2004**, *76*, 5006-5015
23. Wells, J. M.; Chrisman, P. A.; McLuckey, S. A. "Dueling" ESI: Instrumentation to study ion/ion reactions of electrospray-generated cations and anions *J. Am. Soc. Mass Spectrom.* **2002**, *13*, 614-622
24. Badman, E. R.; Chrisman, P. A.; McLuckey, S. A. A quadrupole ion trap mass spectrometer with three independent ion sources for the study of gas-phase ion/ion reactions *Anal. Chem.* **2002**, *74*, 6237-6243
25. Zhao, Q.; Soyk, M. W.; Schieffer, G. M.; Houk, R. S.; Badman, E. R.; Fuhrer, K.; Gonin, M. An Ion Trap-Ion Mobility-Time of Flight Mass Spectrometer with Three Ion Sources for Ion/Ion Reactions *J. Am. Soc. Mass Spectrom.* **2008**, *Submitted*
26. Paul, W.; Reinhard, H. P.; Vonzahn, U. The Electric Mass Filter as Mass Spectrometer and Isotope Separator. *Zeitschrift Fur Physik* **1958**, *152*, 143-182
27. McLuckey, S. A.; Reid, G. E.; Wells, J. M. Ion parking during ion/ion reactions in electrodynamic ion traps *Anal. Chem.* **2002**, *74*, 336-346
28. Chrisman, P. A.; Pitteri, S. J.; McLuckey, S. A. Parallel ion parking: Improving conversion of parents to first-generation products in electron transfer dissociation *Anal. Chem.* **2005**, *77*, 3411-3414
29. Chrisman, P. A.; Pitteri, S. J.; McLuckey, S. A. Parallel ion parking of protein mixtures *Anal. Chem.* **2006**, *78*, 310-316
30. Moradian, A.; Douglas, D. J. Mass selective axial ion ejection from linear quadrupoles with added octopole fields *J. Am. Soc. Mass Spectrom.* **2008**, *19*, 270-280
31. Stephenson, J. L.; McLuckey, S. A. Adaptation of the Paul Trap for study of the reaction of multiply charged cations with singly charged anions *Int. J. Mass Spectrom. Ion Process.* **1997**, *162*, 89-106

www.manaraa.com

32. Mo, W.; Langford, M. L.; Todd, J. F. J. Investigation of 'Ghost' Peaks Caused by Non-Linear Fields in the Ion Trap Mass Spectrometer *Rapid Commun. Mass Spectrom.* **1995**, *9*, 107-113
33. Franzen, J.; Gabling, R. H.; Schubert, M.; Wang, Y. In *Practical Aspects of Ion Trap Mass Spectrometry*; March, R. E.;Todd, J. F. J., Eds.; CRC Press: Boca Raton, FL, 1995; Vol. 1, pp 49-167.

www.manaraa.com

Table 1. Typical LIT conditions used to trap and eject ions over 1100-1800 m/z range.

Scan Step	IQ1 (V)	IQ2 (V)	RF Amplitude (V_{0-p})	Resonance Amplitude (V_{0-p})	Resonance Frequency (kHz)	Scan Rate (Da/s)
Fill (10-20 ms)	-10	10	360	--	--	--
Cool (30 ms)	10	10	360	--	--	--
Heating Ramp (100 ms)	10	10	540 to 1260	1.9	150 (q=0.46)	12,300
Cool (30 ms)	10	10	1080	--	--	--
Mass Scan (250 ms)	10	2	1080 to 1800	2.8 to 3.7	275 (q=0.75)	3000

Table 2. Trapping efficiency and MSAE efficiency at various ion fill times for cytochrome *c* and trypsin ions. Uncertainties represent the standard deviations of four to six such measurements.

Fill Time (ms)	Trapping Efficiency (%)	MSAE Efficiency (%)
5	68.9 ± 11.1	9.6 ± 1.8
10	85.3 ± 4.6	7.7 ± 1.6
15	84.9 ± 8.2	6.4 ± 1.7
20	92.0 ± 4.8	5.1 ± 0.86

www.manaraa.com

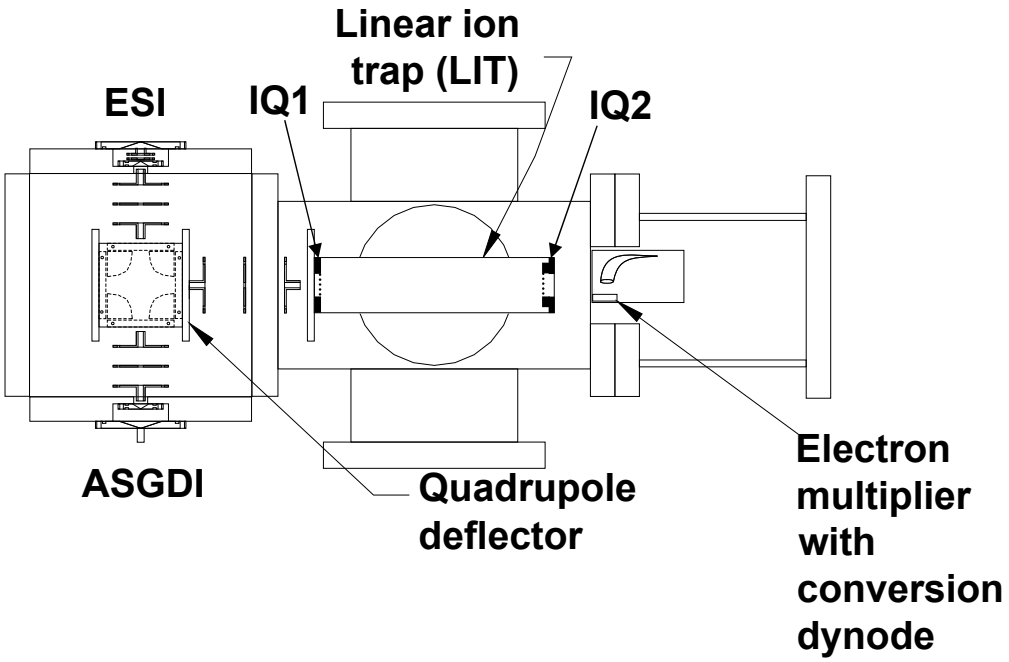

Figure 1. Instrument hardware schematic drawn to scale.

www.manaraa.com

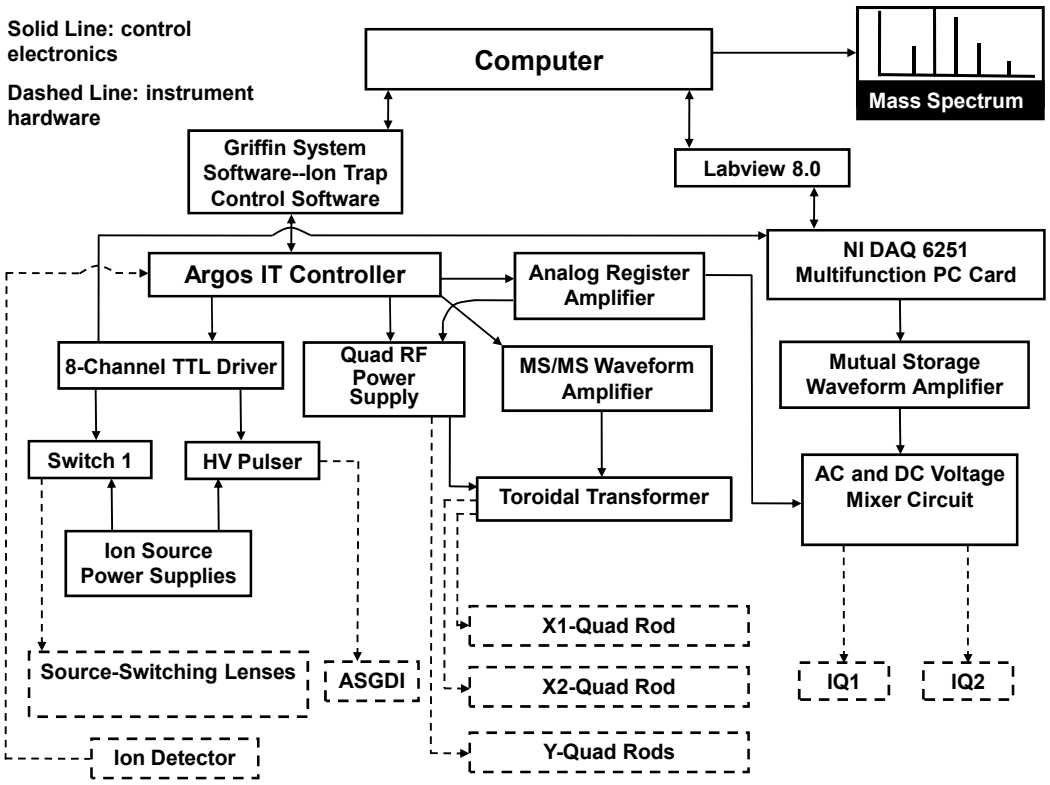

Figure 2. Instrument communication and control diagram.

www.manaraa.com

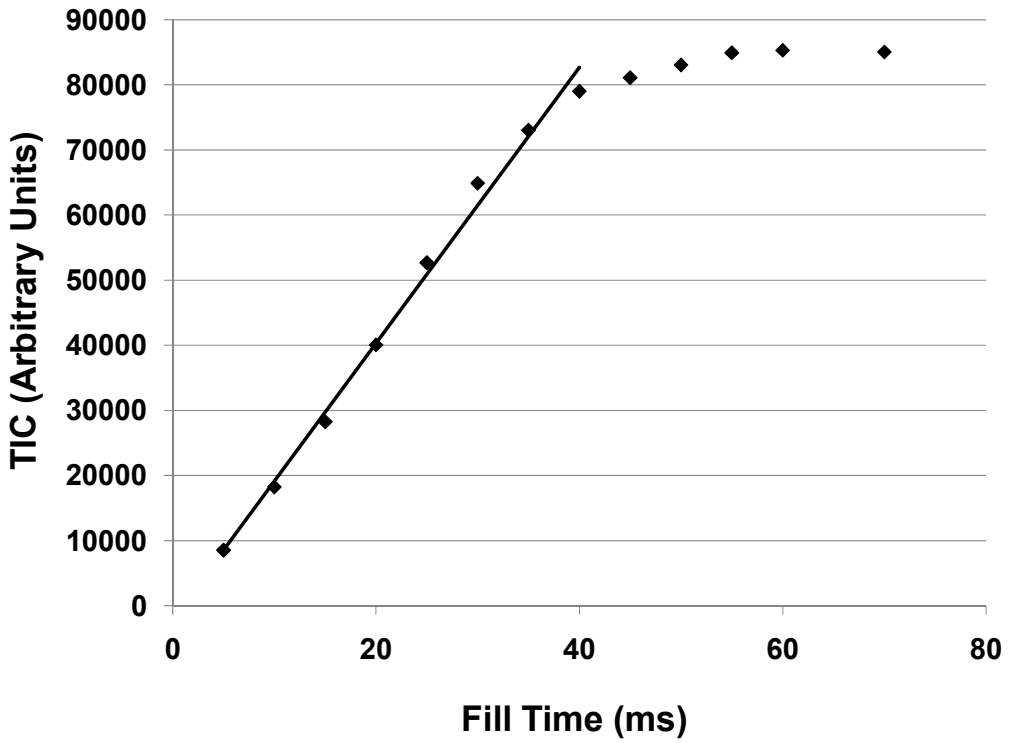

Figure 3. Plot of total ion current vs fill time used to measure the ion capacity of the LIT.

www.manaraa.com

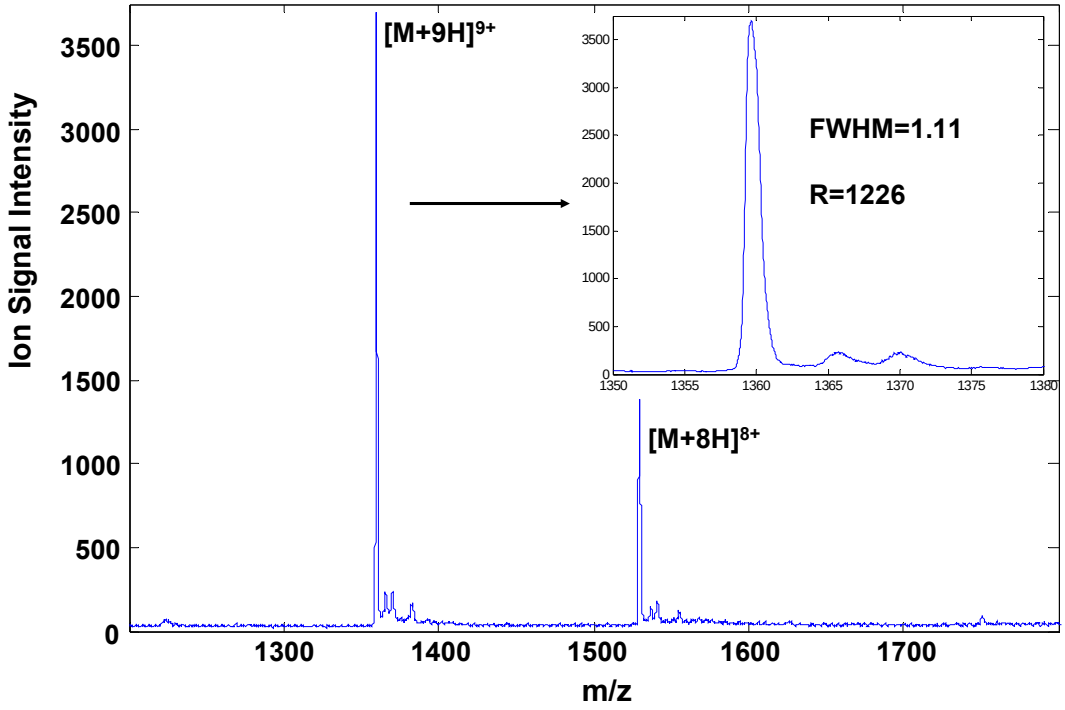

Figure 4. Cytochrome *c* mass spectrum. A heating ramp (100 ms, 540 to 1260 $V_{0\text{-}p}$ rf, 1.9 $V_{0\text{-}p}$, 150 kHz sine wave) reduced the intensity of the adduct peaks that are visible at 54 Da, 90 Da, and 130 Da above each protein peak.

www.manaraa.com

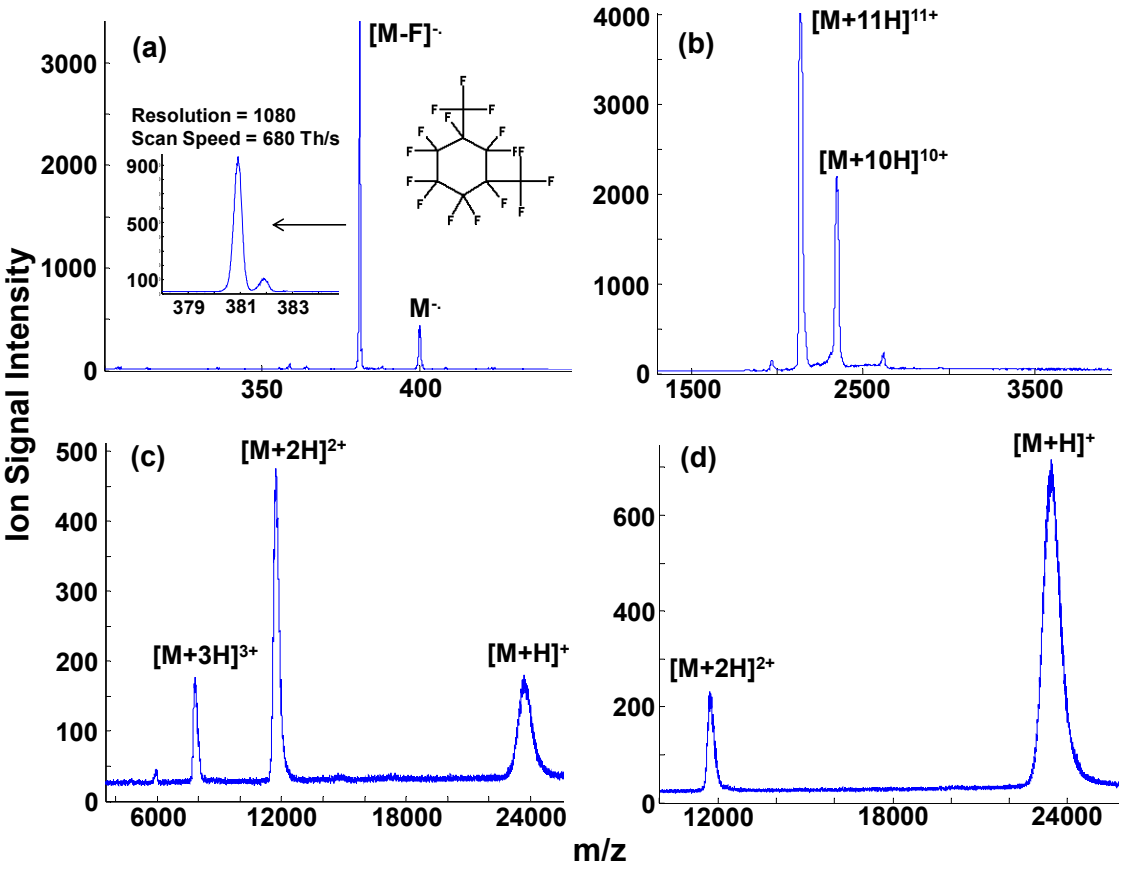

Figure 5. Mass spectra taken from dual polarity storage mode proton transfer ion/ion reactions of intact protein trypsin. (a) Negative ion mode spectrum of the proton transfer reagent ion, PDCH. (b) Pre-ion/ion reaction spectrum of trypsin ions generated directly from ESI. (c) Post-ion/ion reaction spectrum of ions shown in (a) and (b) with a 15 ms PDCH fill and 100 ms reaction. (d) Post-ion/ion reaction spectrum of ions shown in (a) and (b) with a 20 ms PDCH fill and 100 ms reaction.

www.manaraa.com

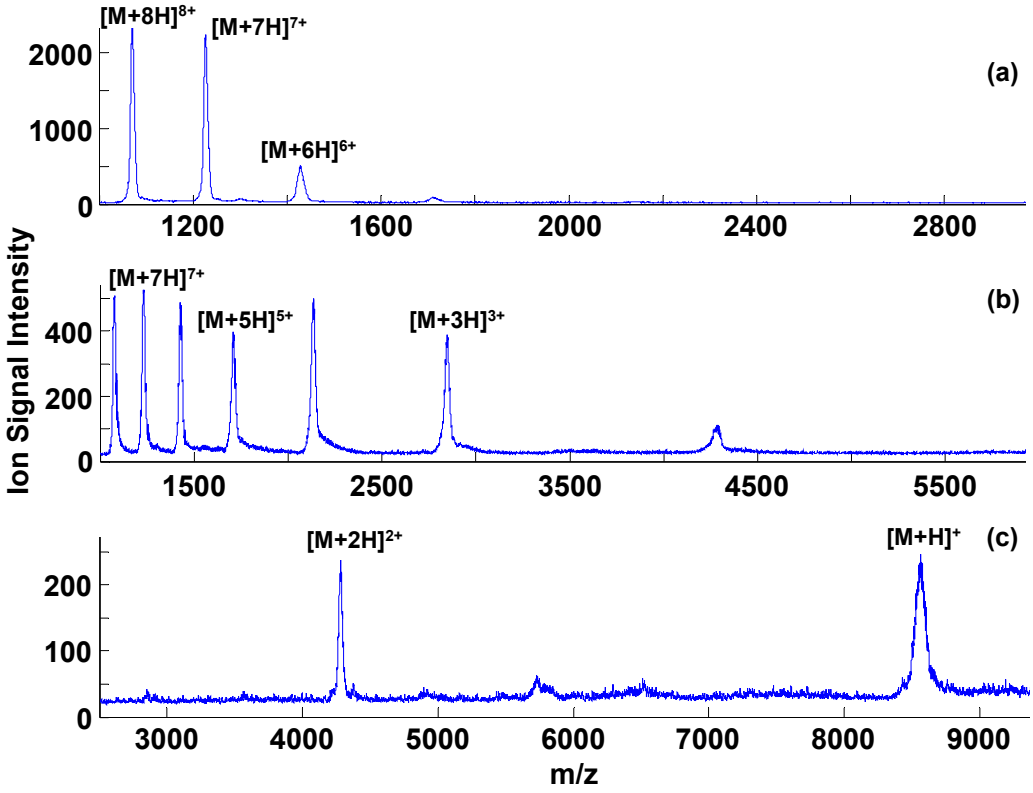

Figure 6. Mass spectra taken from transmission mode proton transfer ion/ion reactions of intact protein ubiquitin. (a) Pre-ion/ion reaction spectrum of ubiquitin ions generated directly from ESI. (b) Mass spectrum resulting from a transmission mode proton transfer ion/ion reaction enabled by passing PDCH anions through the population of trapped ubiquitin ions from (a) for 40 ms. (d) Mass spectrum resulting from a transmission mode proton transfer ion/ion reaction enabled by passing PDCH anions through the population of trapped ubiquitin ions from (a) for 70 ms.

www.manaraa.com

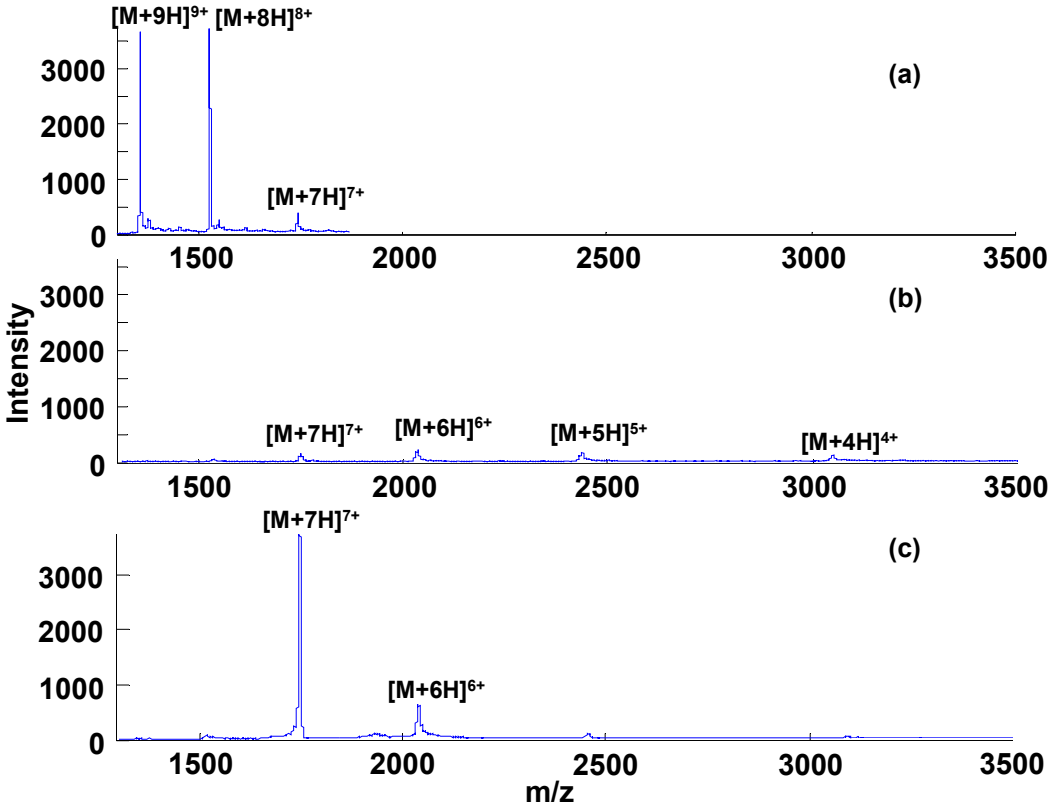

Figure 7. Mass spectra taken from an ion parking experiment during a transmission mode proton transfer ion/ion reaction. (a) Pre-ion/ion reaction spectrum of cytochrome *c* ions generated directly from ESI. (b) Mass spectrum resulting from a transmission mode proton transfer ion/ion reaction enabled by passing PDCH anions through the population of trapped cytochrome *c* from (a) for 20 ms. (c) Mass spectrum resulting from a transmission mode proton transfer ion/ion reaction enabled by passing PDCH anions through the population of trapped cytochrome *c* ion from (a) for 20 ms, during which a 1.8 $V_{0\text{-}p}$, 42 kHz sine wave was added to the x-rods of the LIT, enabling the $[M+7H]^{7+}$ ion to be "parked".

www.manaraa.com